Landau Theory of Causal Dynamical Triangulations

因果动态三角剖分的朗道理论

Dario Benedetti

达里奥·贝内代蒂

Contents

目录

Abstract

摘要

Understanding the continuum limit of a theory of discrete random geometries is a beautiful but difficult challenge. In this optic, we review here the insights that can be obtained for Causal dynamical triangulations (CDT) by employing the Landau approach to critical phenomena. In particular, concentrating on the cases of two and three dimensions, we will make the case that the configuration of the volume of spatial slices effectively plays the role of an order parameter, helping us understand the phase structure of CDT. Moreover, consistency with numerical simulations of CDT provides hints that the effective field theory of the model lives in the space of theories invariant under foliation-preserving diffeomorphisms. Among such theories, Hořava-Lifshitz gravity has the special status of being a perturbatively renormalizable theory, while general relativity sits in a subspace with enhanced symmetry. In order to reach either of them, one would likely need to fine-tune some of the parameters in the CDT action or additional ones from some generalization thereof.

理解离散随机几何理论的连续极限是一项美妙却艰巨的挑战。基于这一视角，本文我们综述了通过朗道临界现象方法研究因果动态三角剖分 (CDT) 得到的相关见解。我们尤其聚焦二维和三维的情形，论证空间切片体积构型可有效发挥序参量的作用，帮助我们理解 CDT 的相结构。此外，CDT 数值模拟的一致性提示，该模型的有效场论存在于保叶状结构微分同胚不变的理论空间中。在这类理论中，霍拉瓦-里夫希茨引力具有特殊地位，它是微扰可重整化的理论，而广义相对论则位于对称性增强的子空间中。想要得到其中任意一种理论，都很可能需要对 CDT 作用量中的部分参数，或是其推广形式中的额外参数进行精细调谐。

D. Benedetti ( )

D. 贝内代蒂 ( )

CPHT, CNRS, École polytechnique, Institut Polytechnique de Paris, Palaiseau, France e-mail: dario.benedetti@polytechnic

法国帕莱索巴黎综合理工学院 CNRS CPHT 研究所，e-mail: dario.benedetti@polytechnique.edu

---

Keywords

关键词

Quantum gravity - Random geometry - Lattice models - Phase diagrams . Causal dynamical triangulations - Hořava-Lifshitz gravity

量子引力——随机几何——格点模型——相图。因果动态三角剖分——霍拉瓦-利夫希茨引力

Introduction

引言

Lattice regularization is a common approach to taming in a nonperturbative way the ultraviolet divergences of a quantum field theory. For many quantum field theories, it is relatively straightforward to formulate a corresponding lattice field theory, but showing that a nontrivial continuum limit can be obtained is generally very difficult (For example, only recently has been it rigorously proven that the continuum limit of the ϕ^4 theory in four dimensions is trivial (i.e., non-interacting) [1].). The standard physical picture, based on the Wilsonian renormalization group, is that such a limit should exist if the lattice model has a second-order phase transition that requires the tuning of the interaction coupling in order to be reached. In such a scenario, one would construct the continuum limit as a scaling limit in which the coupling is tuned to the phase transition in a coordinated way with the tuning of the lattice spacing to zero. Lacking an exact solution for the given model, such a scaling limit is a challenging task, especially when the universality class of the phase transition is described by an interacting theory. Luckily, even simple calculations and approximations can often help in

establishing a correct physical picture. In particular, the Landau theory of critical phenomena provides very often a qualitatively (if not quantitatively) correct description of the phase transitions of a model.

格点正规化是非微扰处理量子场论紫外发散的常用方法。对许多量子场论而言，构造对应的格点场论相对直接，但证明存在非平庸连续极限一般都非常困难 (例如，四维下 ϕ^4 理论的连续极限是平庸的，也就是无相互作用，直到最近才得到严格证明 [1]。)。基于威尔逊重整化群的标准物理图像认为，如果格点模型存在需要微调相互作用耦合才能到达的二阶相变，那么该连续极限就应当存在。在此情形下，连续极限被构造为标度极限: 我们将耦合微调至相变点，同时将格点间距同步调至零。若给定模型不存在精确解，这种标度极限就是极具挑战的问题，尤其当相变的普适类由相互作用理论描述时更是如此。幸运的是，即使简单计算和近似也往往能帮助我们建立正确的物理图像。特别是，朗道临界现象理论在定性层面 (即使不是定量层面) 常常能给出模型相变的正确描述。

In gravity, even the first step of formulating a lattice theory is nontrivial (For the second step, that of the continuum limit, one hope would be to find a realization of Weinberg's asymptotic safety scenario [2-4].). Indeed, in general relativity, the gravitational force is described in terms of the geometry of spacetime, whose dynamics is governed by background independent laws, so we should not rely on a fixed lattice background. One proposal to construct a candidate lattice theory of Euclidean quantum gravity took shape in the 1980s in the context of noncritical bosonic string theory, and it is commonly known as dynamical triangulations (DT) [5]. It is based on Regge's coordinate-free approach to discrete gravity [6], in which continuous manifolds are replaced by piecewise flat manifolds (triangulations and their higher-dimensional generalizations, simplicial manifolds). However, unlike in

在引力领域，就连构造格点理论这第一步就并非平庸 (对于第二步，也就是连续极限，人们希望可以实现温伯格渐近安全场景 [2-4]。)。实际上，广义相对论中引力由时空几何描述，其动力学由背景无关的定律支配，因此我们不能依赖固定的格点背景。20 世纪 80 年代，非临界玻色弦理论框架下诞生了一个构造欧几里得量子引力候选格点理论的方案，它现在通常被称为动力学三角剖分 (DT)[5]。该方案基于里奇的无坐标离散引力方法 [6]: 该方法将连续流形替换为分段平坦流形，即三角剖分及其高维推广——单纯形流形。但它和

Regge calculus, in DT, one is prescribed to sum over all possible triangulations, with all edge-lengths fixed to the same value a , thus making DT also intrinsically background independent, in the sense that there is no fixed structure at all and no identifiable points. Originally DT was constructed for two-dimensional quantum gravity [7-9], in which case it is related to matrix models [10], and it had an exciting success in reproducing continuum results in the case of conformal charge $c < 1$, thus proving that this way of discretizing the functional integral over geometries makes sense (Even from a rigorous mathematical perspective, as reviewed in another chapter of the "Handbook of Quantum Gravity" [11].). Later, it was generalized to three and four dimensions, where however the results were more disappointing: no second-order phase transition could be found [12, 13]. Moreover, the two phases of the model, separated by a first-order transition, were characterized by very degenerate geometries that did not approach a classical limit at large scales [14] (DT were revived about a decade ago, on the analytical side by the discovery of the large- N limit of tensor models [15, 16] , prompting the hope that analytical control would show the way to improving DT, and on the numerical side by the exploration of some generalized models with hints of a new ("crinkled") phase [17] (see also [18] for a meeting point of the two developments). Unfortunately, so far, tensor models have not been able to solve the problem of escaping the branched polymer phase [19,20], while the crinckled phase of the generalized models turned out to be again rather unphysical, and still no second-order phase transition is in sight at finite

coupling [21-23].).

里奇微积分不同，在动力学三角剖分中，我们需要对所有可能的三角剖分求和，且所有边长都固定为同一值 a，这使得 DT 本身也是背景无关的，因为整个理论不存在任何固定结构，也没有可区分的点。DT 最初是为二维量子引力构造的 [7-9]，它在此情形下和矩阵模型相关 [10]，并且在共形荷为 $c < 1$ 的情形成功重现了连续谱结果，证明这种对几何泛函积分做离散化的方法是合理的 (即使从严格数学的角度来看也是如此，相关综述可见《量子引力手册》的另一章节 [11]。)。后来 DT 被推广到三维和四维，但结果却更令人失望: 人们始终没有找到二阶相变 [12, 13]。此外，被一级相变分开的模型两个相都存在高度简并几何，在大尺度下无法趋近经典极限 [14](大约十年前 DT 重新受到关注: 解析方面，人们发现了张量模型 [15, 16] 的大 N 极限，这让人们希望解析控制能为改进 DT 指明方向；数值方面，人们对一些推广模型进行探索，发现了存在新的“褶皱相”的线索 [17]，两种发展的汇合点可见文献 [18]。遗憾的是，到目前为止张量模型仍未能解决如何跳出支化聚合物相的问题 [19,20]，而推广模型的褶皱相也仍然相当非物理，在有限耦合下至今仍未发现二阶相变 [21-23]。)。

The state of affairs was significantly improved with the introduction of the model of causal dynamical triangulations (CDT) by Ambjorn and Loll (initially in two dimensions [24], and later in three and four dimensions, together with Jurkiewicz [25,26]). CDT modifies DT only by the requirement that the ensemble of triangulations be restricted with the requirement that each triangulation carries a non-singular foliation, i.e., a clear $(d + 1)$ -dimensional decomposition with d - dimensional slices (or leaves) of fixed topology, subsequent slices being always at fixed distance from each other (see [25] for the precise construction, or the two-dimensional example in Fig. 1 for an intuitive understanding). Notice in particular that the foliation induces a natural notion of time as the direction perpendicular to the foliation, and a natural choice of time coordinate t , such that all the vertices on a given slice are at the same value of t . With such a simple modification, originally motivated by the requirement of having always non-singular light cones in a Lorentzian version of the model (In this review we will only discuss models in Euclidean signature, as these are under better control, and in particular they are suitable for numerical simulations. The Lorentzian and Euclidean models can be easily Wick-rotated to each other at the discrete level. Given that Wick rotation is notoriously problematic in general relativity [27, 28] , the fact that in CDT (before any continuum limit) it poses instead no problems is a signal that perhaps the chosen ensemble of geometries is more restricted than one would have imagined.), the main problems of DT seemed to have been solved: a new phase of the model emerged with some classical behavior at large scales [26], separated from another phase by a second-order phase transition [29] (see the reviews [30,31] for a proper summary of results and a complete list of references).

安博恩和洛尔提出因果动态三角剖分 (CDT) 模型后，情况得到了显著改善 (该模型最初针对二维 [24]，随后与尤里基维茨合作拓展到三维和四维 [25,26])。CDT 仅对动态三角剖分 (DT) 做了一处修改: 要求三角剖分集合必须满足非奇异叶状结构条件，即存在清晰的 $(d+1)$ 维分解，该分解由拓扑固定的 d 维切片 (也称叶) 构成，相邻切片之间始终保持固定距离 (精确构造参见 [25]，二维实例可参见图 1，便于直观理解)。需要特别注意的是，叶状结构自然引出了垂直于切片方向的时间概念，也自然给出了时间坐标 t，因此同一切片上的所有顶点都对应相同的 t 值。这一简单修改最初的动机是: 在模型的洛伦兹版本中保证光锥始终非奇异 (本综述仅讨论欧几里得号差的模型, 因为这类模型更易控制，尤其适合数值模拟。在离散层面，洛伦兹模型和欧几里得模型可以很方便地通过威克转动互相转换。众所周知，广义相对论中的威克转动一直存在难题 [27, 28]，而在 CDT 中 (还未取任何连续极限时) 这一过程不存在任何问题，这暗示我们所选的几何集合的限制程度可能比原先预想的更严格)，修改后 DT 的核心问题似乎都得到了解决: 模型在大尺度下涌现出具有经典行为的新物相 [26]，该物相通过二级相变与另一物相隔开 [29](结果总结和完整参考文献可参见综述 [30,31])。

Fig. 1 Example of a triangulated portion of spacetime in the two-dimensional CDT model. The flattened picture captures the way triangles are glued together, but does not represent faithfully intrinsic distances, as edge lengths should be all equal

图 1 二维 CDT 模型中部分时空三角剖分的示例。扁平化示意图展示了三角形的粘合方式，但不能准确表示内禀距离，因为所有边的长度本应相等。

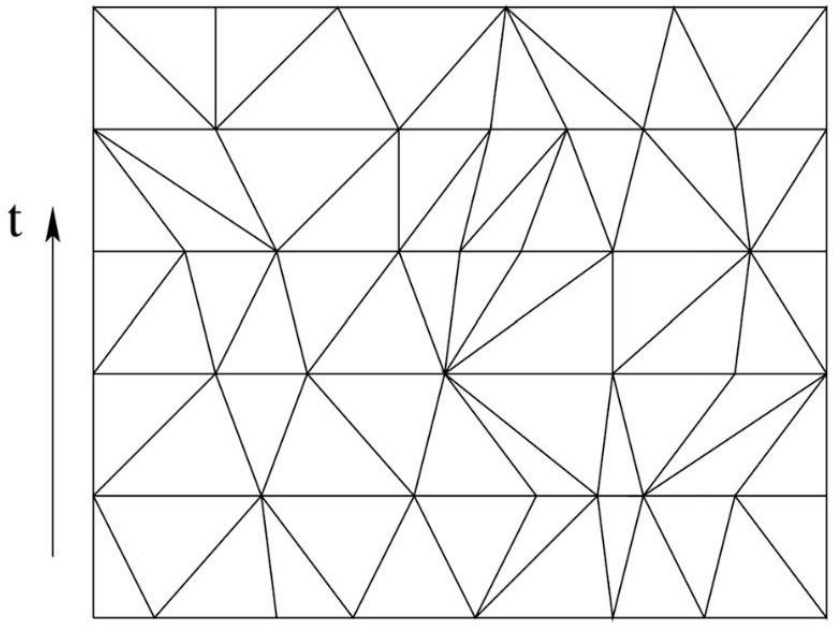

We should at this stage take a step back and reflect upon the way phase diagrams are found in these models, which are effectively statistical models of random geometry. As for any statistical model, the standard way to chart a phase diagram is to identify suitable order parameters taking different values in the different phases. Such order parameters should necessarily correspond to expectation values of observables, meaning quantities which are independent of (unobservable) gauge choices. Here one stumbles in the problem of observables in quantum gravity (e.g., [32,33]): as in any diffeomorphism invariant and background independent approach to quantum gravity, observables in DT are necessarily nonlocal. Luckily, this is not an immediate problem for the phase diagram, as order parameters are often nonlocal (e.g., the average magnetization in the Ising

model), at least for the identification of homogeneous phases, and indeed the two phases of DT can be distinguished by a global observable: the average linear size of the "universe." In particular, studying the scaling of it with the total volume of the universe, one can define an effective Hausdorff dimension d_H of the averaged universe. It turns out that for topological dimension $d = 3$ and 4, varying the lattice Newton constant, the effective dimension jumps from $d_H \sim 2$ (branched polymer phase) to $d_H \sim \infty$ (crumpled phase) [14]. Phases with the same Hausdorff dimensions were also found in CDT, but in addition a new phase was identified as well, with $d_H \sim d$ [26]. Clearly, this was a great advance, providing a zeroth order test of classical behavior being possible in these models, but much more is needed in order to reconstruct the possible continuum limit. For the latter, global observables are not very instructive, as, for example, it is hard to imagine how to construct and interpret an effective action for the Hausdorff dimension.

此时我们应当退一步，思考这类模型 (本质上是随机几何统计模型) 中相图的获取方式。和所有统计模型一样，绘制相图的标准方法是找到合适的序参量，它会在不同物相取不同值。这类序参量必须对应观测量的期望值，即观测量必须不依赖于不可观测的规范选择。这里我们遇到了量子引力中的观测量难题 (例如，参见 [32,33]): 和所有微分同胚不变、背景独立的量子引力研究方法一样，DT 中的观测量必然是非定域的。幸运的是，这对确定相图来说并非当务之急，因为序参量本身往往就是非定域的 (例如伊辛模型中的平均磁化强度)，至少在识别均匀物相时如此，而 DT 的两个物相确实可以通过一个整体观测量区分: 即“宇宙”的平均线性尺寸。具体来说，通过研究它与宇宙总体积的标度关系，我们可以定义平均宇宙的有效豪斯多夫维数 d_H 。研究发现，当拓扑维数为 $d = 3$ 和 4 时，改变格点牛顿常数，有效维数会从 $d_H \sim 2$ (支化聚合物相) 跃迁至 $d_H \sim \infty$ (褶皱相)[14]。CDT 中也找到了具有相同豪斯多夫维数的物相，但还额外识别出了一个新物相，其豪斯多夫维数为 $d_H \sim d$ [26]。显然这是一项重大进展，为这些模型中存在经典行为提供了零阶检验，但要重构可能的连续极限，我们还需要做更多工作。对于连续极限，整体观测量的指导意义有限，举例来说，我们很难想象如何构造并解释豪斯多夫维数的有效作用量。

In CDT, thanks to the foliation, more observables are available, of a slightly more local nature: observables that are local in time but nonlocal in space. The easiest observable of this type is the volume (In the two and three-dimensional cases, it would be more appropriate to call it length and area, respectively, but for simplicity, we stick to a general d -dimensional terminology.) of spatial slices $N_{d-1}(t)$, simply counting the number of $(d-1)$ -simplices in the spatial slice at time t . Armed with such observable, one can characterize the different phases of CDT in terms of volume profiles and even derive an effective action describing the dynamics of the spatial volume [34]. The latter will be our main focus in the following.

在因果动态三角剖分 (CDT) 中，得益于叶状结构，我们可以获得更多性质稍显局域的可观测量: 这类可观测量是时间局域、空间非局域的。该类最简单的可观测量是空间切片的体积 (二维和三维情形下，分别称之为长度和面积会更准确，但为简便起见，我们统一使用一般的 d 维术语。) $N_{d-1}(t)$ ，即直接统计时刻 t 处空间切片中 $(d-1)$ 单形的数量。有了这类可观测量，我们就可以通过体积轮廓表征 CDT 的不同相，甚至推导出描述空间体积动力学的有效作用量 [34]。后者将是我们下文讨论的核心。

Given the premises above, a natural question arises: are the foliation and its associated observables compatible with a fully diffeomorphism invariant and background independent continuum limit? Originally, the foliation was thought only as a way of selecting less pathological geometries in a partially gauge-fixed (proper time gauge) version of discrete quantum gravity (see [35] for a continuum point of view on this). However, the existence of observables that are local in time raises two problems: first, they would be just a gauge artifact, and should not be true observables of the theory; second, a coarse-grained effective action depending

on them would only be compatible with a gauge-fixed general-covariant action for very special values of the couplings. The last point is extremely important and, phrased differently, means that the most general and natural theory space in which a renormalization group flow of CDT should take place is that of theories invariant under foliation-preserving diffeomorphisms (FPD), and invariance under full (spacetime) diffeomorphisms would only be recovered on a submanifold of theory space (We are being cavalier about the fact that any classical theory can be written in a fully diffeomorphism-invariant way. What we mean here is a theory that can be written in such a way without introducing other fields than the metric.). FPD-invariant theories were introduced by Hořava [36, 37] in order to construct a gravitational theory that could be at the same time perturbatively renormalizable and unitary. This is achieved by introducing in the action higher derivatives in space, but not in time, which is possible thanks to the reduced diffeomorphism invariance. Such theories, of which several versions have been introduced and studied (see [38,39] for reviews), are commonly known as Hořava-Lifshitz (HL) gravity, as they are the gravitational analog of theories with a Lifshitz critical point. On the other hand, the space of FPD-invariant effective theories is more general and contains in particular also non-renormalizable ones.

基于上述前提，一个自然的问题随之而来: 叶状结构及其对应的可观测量，与完全微分同胚不变、背景无关的连续极限是否相容? 最初，叶状结构仅被视作在部分规范固定 (固有时规范) 的离散量子引力中筛选性质较好几何的一种方式 (连续视角的相关讨论见 [35])。然而，时间局域可观测量的存在引发了两个问题: 第一，它们可能只是规范伪影，不该成为理论真正的可观测量；第二，依赖这类可观测量的粗粒化有效作用量，仅在耦合取非常特殊的值时才与规范固定后的广义协变作用量相容。这一点极为重要，换而言之，CDT 的重整化群流所处的最一般、最自然的理论空间，是保叶状结构微分同胚 (FPD) 不变的理论空间，完整 (时空) 微分同胚不变性仅能在理论空间的一个子流形上恢复 (我们此处暂不讨论任何经典理论都可以写成完全微分同胚不变形式这一事实，我们这里指的是无需引入度规以外的其他场就能实现这种写法的理论)。FPD 不变理论由 Hořava 提出 [36,37]，目的是构造一个同时满足微扰可重整化和幺正性的引力理论。该理论通过在作用量中引入空间的高阶导数而非时间的高阶导数来实现这一点，这种引入之所以可行正是得益于微分同胚不变性的约化。这类理论已有多个版本被提出和研究 (综述见 [38,39])，通常被称为 Hořava-Lifshitz(HL) 引力，因为它是具有 Lifshitz 临界点理论的引力对应。另一方面，FPD 不变有效理论的空间更宽泛，尤其还包含不可重整化的理论。

First possible hints of a relation between CDT and HL-type gravity theories were discussed in [40-42], relying mostly on the presence of a foliation, on a qualitative resemblance between the phase diagram of CDT with the generic Lifshitz phase diagram, and on results concerning the spectral dimension (another useful notion of effective dimension). Other dynamical arguments have subsequently been added [43-46], and a longer list of arguments will be reviewed in section "Conclusions," but of course understanding the continuum limit of higher-dimensional background-independent statistical models like CDT is highly nontrivial, and therefore the precise relation is still open, in particular in four dimensions.

CDT 与 HL 型引力理论存在关联的初步线索在文献 [40-42] 中被讨论，这些线索主要基于: 两者都存在叶状结构、CDT 的相图与一般 Lifshitz 相图存在定性相似性，以及关于谱维 (另一个有用的有效维数概念) 的研究结果。后续又有研究者补充了其他动力学论证 [43-46]，我们会在“结论”章节回顾更多相关论证，但毋庸讳言，理解 CDT 这类高维背景无关统计模型的连续极限难度极大，因此两者的精确关系仍未有定论，四维情形尤其如此。

In any case, the fact that FPD-invariant effective theories are conceivable theories of dynamical geome-

try raises the following question: if CDT was describing a partially gauge-fixed but otherwise fully covariant theory, how would we construct a nonperturbative quantization of FPD-invariant theories in the spirit of dynamical triangulations, if not by introducing a foliation as in CDT? Most likely, the answer is that for FPD-invariant theories, we should indeed use the same ensemble of triangulations as in CDT, in general with a different action, with more parameters (as, e.g., in [47]). And if a fully diffeomorphism-invariant continuum limit could ever be reached from such generalized CDT models, this should be found within a subspace of their full theory space, i.e., by a careful fine-tuning of the couplings. Could we be so lucky that the standard CDT already sits in such a subspace? This might seem plausible, at least in two and three dimensions, where the CDT action is just a Regge discretization of the Einstein-Hilbert action, with cosmological and Newton constant (Less so in four dimensions, where the CDT action has a third coupling, not appearing in the Einstein-Hilbert action. However, this is a minor point with respect to what we want to stress here.). Consider the example of a scalar model on a regular lattice. Typically, an anisotropic action will lead to an anisotropic continuum limit, while discrete rotation symmetry will result in full rotation invariance in the continuum limit (see, e.g., [48]). That is, in this case, starting from an action which is a simple discretization of a rotation-invariant action leads to the expected result, or in other words, the fine-tuning is trivial. But rotation invariance is a global symmetry. Things are more complicated for gauge symmetries, as their breaking leads to new degrees of freedom: for example, HL gravity has a new scalar degree of freedom besides the massless spin-2 graviton. It is a well-known fact that in the case that the gauge invariance of a quantum field theory is broken by a lattice or by a momentum cutoff, in order to restore it in the continuum limit, and thus recover the desired target theory, one needs a nontrivial fine-tuning of all the possible breaking terms in the action, as, for example, extensively discussed in some lattice approach to chirality [49], or in constructive [50] and functional renormalization group [51,52] approaches to Yang-Mills theory. It seems reasonable to expect that recovering full diffeomorphism invariance in CDT would require some fine-tuning along those lines, although a luckier scenario (with no tuning of new couplings) cannot be ruled out as we still have a very limited understanding of the CDT measure and continuum limit in higher dimensions.

无论如何，保持 FPD 不变的有效理论是可行的动力学几何理论这一事实引出了下述问题: 如果 CDT 描述的是一个部分固定规范、但其余部分完全协变的理论，那我们该如何遵循动力学三角剖分的思想，构造 FPD 不变理论的非微扰量子化——难道不正是要像 CDT 中那样引入分层结构吗？最有可能的答案是: 对于 FPD 不变理论，我们通常确实应当采用和 CDT 相同的三角剖分系综，只不过作用量不同，包含更多参数 (例如文献 [47] 中的情况)。如果这类广义 CDT 模型真的能得到完全微分同胚不变的连续极限，那它也应当出现在完整理论空间的一个子空间内，即需要对耦合常数进行仔细精细调谐。那标准 CDT 会不会刚好就落在这样的子空间里？这看起来是合理的，至少在二维和三维中是如此: 这两种情况下 CDT 作用量就是爱因斯坦-希尔伯特作用量的里奇离散化，仅包含宇宙学常数和牛顿常数 (在四维中情况并非如此，CDT 作用量存在第三个不出现于爱因斯坦-希尔伯特作用量中的耦合。不过对于我们此处想要强调的内容而言，这只是一个次要问题。) 以规则格点上的标量模型为例: 一般来说，各向异性作用量会得到各向异性的连续极限，而离散旋转对称性会在连续极限下给出完整旋转不变性 (参见例如文献 [48])。也就是说，在这个例子里，从旋转不变作用量的简单离散化出发就能得到预期结果，换句话说，精细调谐是平凡的。但旋转不变性是整体对称性，规范对称的情况要复杂得多，因为规范对称破缺会产生新的自由度: 例如 Hořava-Lifshitz 引力除了无质量自旋 2 引力子外还存在一个新的标量自由度。众所周知，如果量子场论的规范不变性被格点或动量截断破坏，那么要想在连续极限中恢复规范不变性、从而得到我们想要的目标理论，就需要对作用量中所有可能的破缺项进行非平凡的精细调谐，例如格点手性理论的某些方法 [49]，以及杨-米尔斯理论的构造性方法 [50] 和泛函重整化群方法 [51,52] 中都对此有大量讨论。我们有合理的理由预期，要在 CDT 中恢复完整的微分同胚不变性，也需要沿着这类思路进行一定的精细调谐，不过由于我们对高维 CDT 测度和连续极限的理解仍然十分有限，也不能排除更幸运的情况——即不需要对新耦合进行调谐。

Let us recap the key elements of the discussion above. DT models provide a diffeomorphism invariant and background independent discretization of a quantum theory of dynamical geometry, but unfortunately they do not have a second-order phase transition, and they are dominated by very degenerate geometries. In order to solve these problems, in CDT, one reduces the ensemble of triangulations by introducing a built-in regular foliation. However, the foliation being a sort of background structure, this likely breaks part of the diffeomorphism invariance of the target theory (general relativity), and in order to restore that, one would presumably need to fine-tune the model, as well as add new counter-terms to the action. The latter part of this summary is so far conjectural, because, due to the complexity of the models, which are mostly studied by Monte Carlo simulations, we cannot rule out in all certainty that the standard CDT action would be a lucky choice leading to a full diffeomorphism invariant theory in the continuum.

让我们总结一下上述讨论的核心要点。DT 模型为动力学几何量子理论提供了微分同胚不变、背景独立的离散化，但遗憾的是它不存在二级相变，且系统被高度简并的几何主导。为了解决这些问题，CDT 通过引入内禀规则分层缩小了三角剖分系综的范围。然而，分层作为一类背景结构，很可能破坏了目标理论 (广义相对论) 的部分微分同胚不变性；要恢复这一不变性，我们大概需要对模型进行精细调谐，并在作用量中加入新的 counter 项。到目前为止，总结的后一部分仍是猜想，因为这类模型大多通过蒙特卡洛模拟研究，受复杂度所限，我们无法完全确定地排除标准 CDT 作用量就是那个幸运的选择、能在连续极限下给出完整微分同胚不变理论的可能性。

We will argue below that in two dimensions, it is quite clear that indeed in the continuum limit CDT is described by an FPD-invariant theory; that in three dimensions, there is some evidence supporting the same conclusion; and that even in four dimensions, there are some indications in the same direction. To that end, we will focus on the effective dynamics of the volume of the spatial slices, which can be seen as an

application of Landau theory to CDT. In particular, we will argue that by a deeper study of the effective action governing such observable, one can in principle distinguish between a gauge-fixed general-covariant action and an FPD-invariant one.

我们接下来将会论证: 在二维中，CDT 在连续极限下确实由 FPD 不变理论描述，这一点非常清晰; 在三维中，已有若干证据支持同样的结论；甚至在四维中，也存在一些指向同一方向的迹象。为此，我们将聚焦空间片体积的有效动力学，这可以看作朗道理论在 CDT 中的应用。我们尤其会论证，通过深入研究支配该可观测量的有效作用量，原则上可以区分固定规范的广义协变作用量和 FPD 不变作用量。

The rest of the review, mainly based on the results of [45,46], is organized as follows. In section "Landau Theory and CDT," we review the main ideas of the Landau theory of critical phenomena, the challenges of applying it to a background independent model, and how instead a Landau free energy is straightforwardly obtained for two-dimensional CDT, in a direct top-down approach. Armed with that, one recognizes in the continuum limit the two-dimensional version of HL gravity. In section "Spatial Volume Dynamics in Three-Dimensional CDT," we review the setup and numerical results for the dynamics of the spatial volumes in three-dimensional CDT. In section "Effective Models," we review a bottom-up proposal (based on numerical data and on the intuitions we tried to motivate in this introduction) for the Landau free energy associated with such spatial volumes, viewed as (time-dependent) order parameter of the model. We also review the numerical simulations of the coarse-grained model based on such Landau free energy, showing that qualitative features of the CDT phase diagram are reproduced. An extremization analysis of the continuum limit of the Landau free energy is reviewed in section "Analysis of the Model," providing in particular an analytical understanding of the condensation phenomenon observed in the semiclassical phase of CDT and one more indication that the correct effective action of the model sits in the space of FPD-invariant theories. Lastly, we conclude in section "Conclusions" with a short summary and a discussion of our current understanding of the relation between CDT and HL-like gravity theories.

本综述其余部分主要基于文献 [45,46] 的成果，结构安排如下: 在「朗道理论与因果动态三角剖分 (CDT)」一节中，我们回顾了临界现象朗道理论的核心思想、将其应用到背景无关模型面临的困难，以及如何通过直接自上而下方法，直接得到二维 CDT 的朗道自由能。以此为基础，我们可以在连续极限下识别出霍拉瓦-里夫希茨 (HL) 引力的二维形式。在「三维 CDT 中的空间体积动力学」一节中，我们回顾了三维 CDT 空间体积动力学的框架与数值结果。在「有效模型」一节中，我们回顾了一个自下而上的方案 (基于数值数据以及我们在本引言中尝试阐明的思路)，该方案给出了与上述空间体积对应的朗道自由能，空间体积在这里被视为模型的 (含时) 序参量。我们还回顾了基于该朗道自由能对粗粒化模型进行的数值模拟，结果表明该模型重现了 CDT 相图的定性特征。我们在「模型分析」一节回顾了对朗道自由能连续极限的极值分析，该分析尤其给出了对 CDT 半经典相观测到的凝聚现象的解析理解，还进一步证明了模型的正确有效作用量属于 FPD 不变理论空间。最后，我们在「结论」一节进行总结，简要讨论了目前我们对 CDT 与类 HL 引力理论之间关系的认识。

Landau Theory and CDT

朗道理论与因果动态三角剖分 (CDT)

The goal of Landau theory (e.g., [53]) is to provide a theoretical framework for understanding and pre-

dicting phase transitions in statistical systems. In this respect, it has represented an important landmark in statistical physics, successfully explaining many phenomena. It is also well-known to have strong limitations, predicting wrong scaling exponents below critical dimensions, and this led to the development of the renormalization group. However, in general, Landau theory remains a valid tool for a first analysis, at least at the qualitative level, for example, for understanding the structure of the phase diagram of a given model.

朗道理论 (例如文献 [53]) 的目标是为理解和预测统计系统的相变提供理论框架。它是统计物理学中一座重要里程碑，成功解释了诸多现象。但众所周知，朗道理论存在很大局限性，会在低于临界维度时预测出错误的标度指数，这也推动了重整化群理论的发展。不过总体而言，它仍是进行初步分析的有效工具，至少在定性层面成立，例如可以用来分析给定模型相图的结构。

The central aspect of Landau theory is that it postulates that phase diagrams can be explained in terms of order parameters and that these are effectively governed by a coarse-grained free energy functional, known as Landau free energy, which depends parametrically on the coupling constants of the system. The minima of the Landau free energy determine the thermodynamically favored configuration of the order parameters, and different favored configurations correspond to different phases. Typically, there will be a disordered phase, with vanishing order parameters and unbroken symmetries, and one or more ordered phases, with non-vanishing order parameters breaking some or all of the symmetries of the system. Therefore, given a statistical model, it is crucial to identify the order parameters and construct the corresponding Landau free energy.

朗道理论的核心是提出如下假设: 相图可以通过序参量解释, 序参量本质上由粗粒化自由能泛函 (即朗道自由能) 支配，该泛函参数依赖于系统的耦合常数。朗道自由能的极小值对应热力学上最有利的序参量构型，不同的有利构型对应不同的相。通常系统存在无序相: 此时序参量为零，对称性不破缺；还存在一个或多个有序相: 此时序参量非零，系统的部分或全部对称性发生破缺。因此，对于给定的统计模型，确定序参量并构造对应的朗道自由能是关键步骤。

There are two main approaches for constructing the Landau free energy: a phenomenological (bottom-up) approach, writing it as an expansion in the order parameters, constrained by the symmetries, as in effective field theories, and a top-down approach, deriving the Landau free energy by explicitly coarse-graining the microscopic model. The latter is of course seldomly applicable in practice, but it provides a very instructive way of thinking about the Landau theory, and it is hence worth of being briefly recalled (we essentially follow [53] for this).

构造朗道自由能主要有两种方法: 唯象 (自下而上) 方法将其写为序参量的展开式，由对称性约束，思路和有效场论一致；自上而下方法通过对微观模型做显式粗粒化推导得到朗道自由能。后者在实际中当然很少能用，但它为理解朗道理论提供了非常有启发性的思路，因此值得简要回顾 (本文此处基本遵循文献 [53] 的表述)。

Consider a spin system with Hamiltonian $H(\{s\})$, where $\{s\} = \{s_i \mid i \in \mathcal{L}\}$ is a configuration of spin variables s_i on the N sites of the lattice $\mathcal{L}$. The partition function is

考虑一个哈密顿量为 $H(\{s\})$ 的自旋系统，其中 $\{s\} = \{s_i \mid i \in \mathcal{L}\}$ 是晶格 $\mathcal{L}$ 的 N 格点上自旋变量 s_i 的一个构型。配分函数为

$$Z_{\text{spin}} = \sum_{\{s\}} e^{-\beta H(\{s\})}. \tag{1}$$

Next, partition the lattice into blocks $\mathcal{B}_r$, labeled by r , which can be thought of as a site of the coarse-grained lattice $\mathcal{L}'$. Each block contains $N(r)$ sites, such that $\sum_r N(r) = N$. We define the Landau free energy $L(\{m\})$, where $\{m\} = \{m(r) \mid r \in \mathcal{L}'\}$, as the Gibbs free energy for the system, constrained to be in a configuration compatible with a local magnetization configuration specified by $\{m\}$, i.e.:

接下来，将晶格划分为以 r 标记的块 $\mathcal{B}_r$ ，这些块可视为粗化晶格 $\mathcal{L}'$ 的格点。每个块包含 $N(r)$ 个格点，满足 $\sum_r N(r) = N$ 。我们将朗道自由能 $L(\{m\})$ (其中 $\{m\} = \{m(r) \mid r \in \mathcal{L}'\}$) 定义为满足以下条件的系统的吉布斯自由能: 系统被约束在与 $\{m\}$ 指定的局域磁化构型相容的构型中，即:

$$e^{-L(\{m\})} = \sum_{\left\{s_i | i \in \mathcal{L}, \frac{1}{N(r)} \sum_{j \in \mathcal{B}_r} s_j = m(r)\right\}} e^{-\beta H(\{s\})}. \tag{2}$$

From the definitions, it follows straightforwardly that the partition function can be expressed in terms of the Landau free energy as

根据定义可以直接推出，配分函数可以用朗道自由能表示为

$$Z_{\text{spin}} = \sum_{\{m\}} e^{-L(\{m\})} \tag{3}$$

It is clear that in this construction, $L(\{m\})$ can also be thought of as a Wilsonian effective Hamiltonian. This is in particular the case because the local magnetization $\{m\}$ is a similar (albeit coarse grained) type of variable as the original spin variables $\{s\}$, in the sense that we went from some spin variables to some other spin variables (perhaps with a different set of values, due to the averaging). The idea is however more general, and depending on the model and the relevant order parameter, one can define different coarse-graining procedures and end up with very different variables.

很明显，在该构造中，$L(\{m\})$ 也可被视作威尔逊有效哈密顿量。尤其如此是因为局部磁化强度 $\{m\}$ 与原自旋变量 $\{s\}$ 属于同类变量 (只不过是粗粒化后的): 我们是从一组自旋变量得到了另一组自旋变量，由于平均过程取值集合可能有所不同。不过这一思路更为通用，根据模型和相关序参量的不同，可以定义不同的粗粒化步骤，最终得到截然不同的变量。

Landau theory and quantum gravity Applying a similar construction to quantum gravity is of course marred with difficulties, in particular concerning the identification of order parameters, as observables are notoriously problematic in quantum gravity. Diffeomorphism invariance and background independence constrain observables to be nonlocal quantities, which are not very suitable for reconstructing a local effective action. Moreover, coarse graining presents several practical and conceptual obstacles, due to the absence of a background structure. Nevertheless, inventive approaches to the problem have been devised, with coarse graining procedures introduced for constructing a renormalization group flow in DT [54-58] and in spin foams [59-63]. More to the point of interest here, mean field models of DT have also been proposed [64,65]. The latter involved no coarse graining, and they were rather in the spirit of defining approximated Hamiltonians (or

actions, in the parlance of Euclidean QG) much like what is done when replacing the Ising model Hamiltonian with one in which spin interacts not just with its neighbor but with an average of all the other spins (the mean field). Again this procedure, which is straightforward in the Ising case, is not at all obvious in DT, and in fact the mean field models for DT were postulated, rather than derived from the model itself.

朗道理论与量子引力当然，将类似的构建方法应用于量子引力会面临诸多困难，特别是在序参量的识别方面，因为在量子引力中，可观测量一直以来都是个难题。微分同胚不变性和背景独立性将可观测量限制为非局域量，而这些量不太适合用于重构局域有效作用量。此外，由于缺乏背景结构，粗粒化过程存在一些实际和概念上的障碍。尽管如此，人们还是设计出了有创意的解决方法，在动态三角剖分 (DT)[54 - 58] 和自旋泡沫 [59 - 63] 中引入了粗粒化程序来构建重整化群流。更与这里的关注点相关的是，也有人提出了动态三角剖分的平均场模型 [64,65]。后者不涉及粗粒化，其思路更像是定义近似哈密顿量 (或者用欧几里得量子引力的术语来说，是作用量)，就像用一个自旋不仅与相邻自旋相互作用，还与所有其他自旋的平均值 (平均场) 相互作用的哈密顿量来取代伊辛模型的哈密顿量一样。同样，这个在伊辛模型中很直接的过程，在动态三角剖分中一点也不明显，实际上，动态三角剖分的平均场模型是假设出来的，而非从模型本身推导得出。

Once more, in CDT, things are (slightly) different, thanks to the foliation. Small-step blocking is still a very clumsy procedure, but we do have a natural partitioning of the lattice into large blocks: the leaves of the foliations. We can therefore define a Landau free energy by summing over all triangulations that on each slice lead to a prescribed value for a nonlocal slice observable. As anticipated, the choice of slice observable on which we will concentrate is the volume of the slice, which is essentially the only one studied so far, but it would be interesting to explore other options. As a way of clarifying this set of ideas and of introducing the more difficult higher-dimensional cases, we start by analyzing the two-dimensional CDT model in this perspective.

再说回 CDT，由于叶状结构的存在，情况 (略有) 不同。小步分块仍然是非常笨拙的处理，但我们确实拥有对晶格进行大块分划的自然方式: 叶状结构的叶层。我们可以通过对所有三角剖分求和来定义朗道自由能，这些三角剖分在每一个切片上都会给非局域切片观测量一个预设值。如之前所说，我们将重点研究的切片观测量是切片体积，它基本上是目前唯一被研究过的观测量，但探索其他选择会很有意义。为了厘清这套思路，并引出更困难的高维情况，我们首先从这个视角分析二维 CDT 模型。

CDT in a Nutshell

因果动态三角剖分简释

The CDT approach exactly parallels the usual lattice field theory with one fundamental difference: the fixed lattice is replaced by an ensemble of random triangulations. This is required by the fact that gravity is a theory of dynamical geometry, with no background spacetime fixed a priori.

CDT 方法与常规格点场论基本平行，仅存在一个核心差异: 固定格点被随机三角剖分的系综所取代。这一差异是必要的，因为引力是动态几何的理论，不存在先验固定的背景时空。

More concretely, one defines an ensemble of ”triangulations” to work with, a triangulation being defined by a simplicial manifold, i.e., a collection of d - dimensional flat simplices (the generalization of triangles

and tetrahedra) glued along their $(d-1)$ -dimensional faces and such that the neighborhood of any vertex is homeomorphic to a d -dimensional ball. A dynamical triangulation is one in which all the simplices are taken to be equilateral. In the simulations, we usually work with dynamical triangulations having a fixed number of d -simplices N , which we will denote $\mathcal{T}_N$. The ensemble of such triangulations $\{\mathcal{T}_N\}$ is obtained by gluing the N simplices in all possible ways allowed by the simplicial manifold condition and respecting a chosen topology. Furthermore, to avoid the sick behavior that was found in the old models of dynamical triangulations, CDT models have one further restriction on the ensemble: only triangulations with a global time foliation, with respect to which no spatial topology change occurs, are allowed. For more details on the geometrical meaning of this restriction and on its implementation see [25].

更具体地说，我们定义一个“三角剖分”系综来开展研究，三角剖分由单纯流形定义: 即一组 d 维平坦单形 (三角形与四面体的高维推广) 沿它们的 $(d-1)$ 维面粘合而成，且任意顶点的邻域同胚于一个 d 维球。动态三角剖分中所有单形均为等边单形。在模拟中，我们通常处理具有固定数量 d 维单形 N 的动态三角剖分，我们将其记为 $\mathcal{T}_N$ 。这类三角剖分的系综 $\{\mathcal{T}_N\}$ 通过以下方式得到: 在满足单纯流形条件、尊重选定拓扑的前提下，将 N 个单形以所有可能的方式粘合。此外，为避免旧动态三角剖分模型中出现的病态行为，CDT 模型对系综增设了一条限制: 仅允许存在整体时间叶状结构、且在该结构下不发生空间拓扑变化的三角剖分。关于该限制的几何意义及其实现的更多细节参见文献 [25]。

Once the ensemble is specified one can construct the partition function (Euclidean version of the path integral) as

确定系综后，我们可以构造配分函数 (路径积分的欧几里得版本) 如下

$$Z = \sum_N \sum_{\mathcal{T}_N} \frac{1}{C(\mathcal{T}_N)} e^{-S(\mathcal{T}_N)}, \tag{4}$$

where $S(\mathcal{T}_N)$ is the bare action and $C(\mathcal{T}_N)$ is the order of the automorphism group of $\mathcal{T}_N$, a symmetry factor naturally appearing when summing over unlabeled triangulations (e.g., [30]). Since we wish to recover general relativity in the classical limit, it is customary to use as a bare action the Einstein-Hilbert action adapted to a simplicial manifold, which is known as the Regge action. On a dynamical triangulation, the Regge action takes the very simple form

其中 $S(\mathcal{T}_N)$ 是裸作用量，$C(\mathcal{T}_N)$ 是 $\mathcal{T}_N$ 自同构群的阶，这是对无标记三角剖分求和时自然出现的对称因子 (例如参见文献 [30])。由于我们希望在经典极限下 recovered 广义相对论，通常将适配单纯流形的爱因斯坦-希尔伯特作用量作为裸作用量，即大家熟知的里奇作用量。在动态三角剖分上，里奇作用量形式非常简单，即

$$S(\mathcal{T}_N) = \kappa_d N - \kappa_{d-2} N_{d-2}, \tag{5}$$

where κ_d and κ_{d-2} are two coupling constants depending on the cosmological and Newton’ s constant appearing in the Regge action and N_{d-2} is the number of $(d-2)$ - dimensional sub-simplices (also called bones or hinges).

其中 κ_d 和 κ_{d-2} 是两个耦合常数，分别对应里奇作用量中的宇宙学常数和牛顿常数，N_{d-2} 是 $(d-2)$ 维子单形 (也称为骨或铰链) 的数量。

In principle, one could use a different action, with more parameters, but at this stage, this would only complicate the analysis of the results, and in a minimalist attitude, such a generalization of the CDT models is usually postponed till the moment (if ever) at which the model itself will ask for such an extension. For example, in 3 + 1 dimensions, a new parameter d has been introduced in the action, without which no physically interesting region would exist in the phase diagram [26]. Furthermore, we need to remember that, for fixed topology, only $d/2$ (for d even) or $(d+1)/2$ (for d odd) among the values $\{N_0, N_1, \ldots N_{d-1}, N_d = N\}$ are independent. Hence, for $d = 3$ and $d = 4$, only two of such variables are independent, and as a consequence, if we want to keep the action linear in N_j , we only have two coupling constants. The counting changes in CDT because we can distinguish sub-simplices whose vertices are all on one slice from those having vertices on two adjacent slices, and additional variables can be introduced in order to keep track of that. However, new topological relations are found too. The counting for CDT was carried out in [25], and one has that for $d = 4$, there are ten variables and seven constraints, leaving three independent variables, a fact that was used in [26] to introduce the new parameter. In $d = 3$, the situation is instead unchanged with respect to the DT case, as there are five constraints for seven variables and hence again only two independent variables. For this reason, it is not possible to introduce in three dimensions the analogue of the new parameter used in four dimensions.

原则上，我们可以使用带有更多参数的不同作用量，但在现阶段，这只会使结果分析复杂化，秉持极简主义的态度，CDT 模型的这类推广通常会推迟到模型本身确实需要这种扩展的时候 (如果真的需要的话)。例如，在 3+1 维中，作用量里已经引入了一个新参数 d，若没有该参数，相图中就不存在物理上有意义的区域 [26]。此外，我们需要记住，对于固定拓扑，在 $\{N_0, N_1, \ldots N_{d-1}, N_d = N\}$ 这些值中，只有 $d/2$ (当 d 为偶数时) 或 $(d+1)/2$ (当 d 为奇数时) 是独立的。因此，对于 $d = 3$ 和 $d = 4$ ，这类变量中只有两个是独立的，相应地，如果我们希望作用量对 N_j 保持线性，就只会有两个耦合常数。CDT 中的计数发生了变化，因为我们可以区分顶点全部落在一个切片上的子单形和顶点分布在两个相邻切片上的子单形，因此可以引入额外变量来记录这一区别。不过，我们也得到了新的拓扑关系。CDT 的计数已在文献 [25] 中完成，结果表明对于 $d = 4$ ，共有 10 个变量和 7 个约束，剩余 3 个独立变量，文献 [26] 就利用这一结论引入了那个新参数。而对于 $d = 3$ ，情况和 DT 情形相比没有变化，因为 7 个变量对应 5 个约束，因此仍然只有两个独立变量。因此，三维中无法引入四维所用新参数的对应项。

Typically, in CDT, one fixes also the number of time slices T , which in fact can be seen as a new free variable, appearing thanks to the foliation. We therefore often deal with the canonical partition function

通常，在 CDT 中，我们还会固定时间切片的数量 T ，它实际上可以看作一个新的自由变量，因叶状结构而存在。因此我们经常处理正则配分函数

$$Z(N,T) = \sum_{\mathcal{T}_{N,T}} \frac{1}{C\left(\mathcal{T}_{N,T}\right)} e^{-S(\mathcal{T}_{N,T})}, \tag{6}$$

where $\mathcal{T}_{N,T}$ now stands for a foliated d -dimensional simplicial manifold with a fixed number N of d -simplices and a fixed number T of spatial slices, plus some boundary conditions to be specified. Typically, one considers spatial slices with closed topology. In the time direction, the boundary conditions are either periodic

$(T+1 \sim 1)$ or open (slices at time 1 and T as boundaries). The latter case can be viewed as a propagator from an initial to a final geometry in $T-1$ steps.

其中 $\mathcal{T}_{N,T}$ 现在代表带叶状结构的 d 维单纯形流形，它固定了 d -单形的数量 N，固定了空间切片的数量 T，还带有一些待指定的边界条件。通常我们研究闭拓扑的空间切片。时间方向上的边界条件要么是周期边界条件 $(T+1 \sim 1)$，要么是开边界条件 (时间 1 和时间 T 的切片作为边界)。后者可以看作经过 $T-1$ 步从初始几何到末态几何的传播子。

Notice that thanks to the foliation, we can also introduce a transfer matrix W, given by the one-step propagator for the spatial slices, such that the grand canonical partition function for CDT with periodic boundary conditions in the time direction is $Z(T) = \mathrm{Tr}\left[W^T\right]$ (see, e.g.,[66]).

请注意，得益于叶状结构，我们还可以引入转移矩阵 W，它由空间切片的单步传播子给出，因此时间方向带周期边界条件的 CDT 巨正则配分函数为 $Z(T) = \mathrm{Tr}\left[W^T\right]$ (例如参见文献 [66])。

We are now ready to define more precisely the Landau free energy $L(\{m\})$ for spatial volume observable. In analogy with the definition (2) for the spin system, with the slices playing the role of the blocks that partition the lattice, we define

现在我们可以为空间体积可观测量更精确地定义朗道自由能 $L(\{m\})$ 了。类比自旋系统的定义 (2)，切片在这里起到了划分晶格的块的作用，我们定义:

$$e^{-L(\{m\};N,T)} = \sum_{\mathcal{T}_{N,T}} \frac{1}{C\left(\mathcal{T}_{N,T}\right)} e^{-S(\mathcal{T}_{N,T})} \prod_{i=1}^{T} \delta_{m_i, N_{d-1}(i)}, \tag{7}$$

where $N_{d-1}(i)$ denotes the number of $(d-1)$ -simplices at slice i in the simplicial manifold $\mathcal{T}_{N,T}$. Similarly, we can define a grand canonical Landau free energy $L(\{m\};T)$ by summing over simplicial manifolds $\mathcal{T}_T$ with unconstrained number of d -simplices.

其中 $N_{d-1}(i)$ 表示单纯形流形 $\mathcal{T}_{N,T}$ 的切片 i 上 $(d-1)$ -单形的数量。类似地，我们可以定义巨正则朗道自由能 $L(\{m\};T)$，对 d -单形数量无约束的单纯形流形 $\mathcal{T}_T$ 求和即可得到。

Assuming that, at least in some approximation, $L(\{m\};T)$ only contains nearest-neighbor interactions among the spatial volume variables, i.e., $L(\{m\};T) \approx \sum_{i=1}^{T} \tilde{L}(m_i, m_{i+1})$, then the grand canonical partition function will admit also a transfer matrix formulation with a transfer matrix $\widetilde{W} = e^{-\tilde{L}}$ for just the spatial volume variables:

假设至少在某种近似下，$L(\{m\};T)$ 仅包含空间体积变量之间的最近邻相互作用，即 $L(\{m\};T) \approx \sum_{i=1}^{T} \tilde{L}(m_i, m_{i+1})$，那么巨正则配分函数也可以对仅空间体积变量写成转移矩阵形式，对应的转移矩阵为 $\widetilde{W} = e^{-\tilde{L}}$:

$$Z(T) = \sum_{\{m\}} e^{-L(\{m\};T)} \approx \mathrm{Tr}\left[\widetilde{W}^T\right]. \tag{8}$$

It has been conjectured in [66] that, for $d > 2$, summing the geometry-to-geometry transfer matrix W over the boundary geometries, with fixed volumes taken to be large, a volume-to-volume transfer matrix is obtained, which then we could identify with $\widetilde{W}$. Such a conjecture seems closely related to the short-range assumption about $L(\{m\}; T)$, although it is probably stronger, in the sense that the former implies the latter, but not the other way round.

文献 [66] 中推测，对于 $d > 2$，将边界几何固定为大体积时，对几何间转移矩阵 W 按边界几何求和，即可得到体积间转移矩阵，我们可将其对应为 $\widetilde{W}$。该推测似乎与关于 $L(\{m\}; T)$ 的短程假设密切相关，不过该推测的条件更强: 前者蕴含后者，但反之不成立。

Balls-in-Boxes Models

盒中球模型

Before continuing our discussion of CDT, it is useful to introduce the so-called balls-in-boxes (BIB) models, which will play the role of effective models of CDT.

在继续讨论因果动力学三角剖分 (CDT) 之前，有必要先介绍所谓的盒中球 (BIB) 模型，这类模型将充当 CDT 的有效模型。

The statistical models known as balls-in-boxes (or zero-range process in the nonequilibrium version) are an interesting and versatile class of models which have been extensively studied in the statistical mechanics literature (see, e.g., [67]). They have also been used as mean field models of DT [65,68,69] and later also as effective models for the spatial volume dynamics of CDT in 3+1 dimensions [70]. We briefly review in this section their definition and some of their relevant properties.

这种名为盒中球的统计模型 (非平衡版本也称作零范围过程) 是一类有趣且用途广泛的模型，已在统计力学文献中被广泛研究 (参见例如文献 [67])。它们也被用作动力学三角剖分 (DT) 的平均场模型 [65,68,69]，之后还被用作 3+1 维 CDT 空间体积动力学的有效模型 [70]。本节我们将简要回顾这类模型的定义和部分相关性质。

A BIB model is defined as a one-dimensional lattice with T sites (boxes) to each of which is associated an integer number $m_i \geq m_{\min} \geq 0$ (the number of balls in box $i \in \{1, 2, \dots, T\}$). The total number of balls is fixed to be M. The canonical partition function of the statistical model is given as

BIB 模型定义为包含 T 个格点 (盒子) 的一维晶格，每个格点对应一个整数 $m_i \geq m_{\min} \geq 0$ (即盒子 $i \in \{1, 2, \dots, T\}$ 中的球数)。球的总数固定为 M。该统计模型的正则配分函数为:

$$
\begin{aligned}
Z_{\mathrm{BIB}}(T, M) &= \sum_{m_1=m_{\min}}^{M} \cdots \sum_{m_T=m_{\min}}^{M} \delta_{M,\sum_i m_i} \prod_{i=1}^{T} g(m_i, m_{i+1}) \\
&= \sum_{\{m_j\}} e^{-S(\{m_j\})} \delta_{M,\sum_i m_i},
\end{aligned}
\tag{9}
$$

with $m_{T+1} = m_1$. The last expression highlights the interpretation of such models as discretized one-dimensional path integrals with action $S\left(\{m_j\}\right)$. However, the fact that the configurations are subjected to the nonlocal constraint

满足 $m_{T+1} = m_1$ 。上式突出说明了这类模型可被解释为作用量为 $S\left(\{m_j\}\right)$ 的离散化一维路径积分。但构型需要满足非局域约束

$$\sum_{i=1}^{T} m_i = M \tag{10}$$

sets such models apart from standard (Euclidean) path integrals, thus justifying the use of a specific name such as balls-in-boxes. The weight function $g(m,n)$ (or the action $S\left(\{m_j\}\right)$) defines the particular model. In standard BIB models, there is no nearest-neighbor interaction, meaning that $g(m_i, m_{i+1}) = g(m_i)$; the model above is a generalization studied in [71, 72] .

这一点将这类模型与标准 (欧几里得) 路径积分区分开来，因此我们有必要为其赋予“盒中球”这个专门的名称。权重函数 $g(m,n)$ (或作用量 $S\left(\{m_j\}\right)$) 定义了具体的模型。标准 BIB 模型不存在最近邻相互作用，即满足 $g(m_i, m_{i+1}) = g(m_i)$ ； 上述模型是在 [71, 72] 中研究的广义形式。

Often, in particular for an analytical approach, it is useful to work in the grand canonical ensemble, for which the partition function reads

通常而言，对于解析处理，在巨正则系综下研究会更方便，巨正则系综的配分函数为:

$$\begin{aligned} Z_{\mathrm{BIB-gc}}(T,z) &= \sum_{M} Z_{\mathrm{BIB}}(T,M)\, z^M \\ &= \mathrm{Tr}\left[\widehat{W}^T\right], \end{aligned} \tag{11}$$

where we introduced the transfer matrix

其中我们引入了转移矩阵

$$\widehat{W}_{m,n} = z^{(m+n)/2} g(m,n)\,. \tag{12}$$

In the light of this relation, $g(m,n)$ is sometimes referred to as reduced transfer matrix.

根据该关系，$g(m,n)$ 有时也被称为约化转移矩阵。

One interesting feature of these models is that they can exhibit a condensation phenomenon. In the original BIB models, with $g(m_i, m_{i+1}) = g(m_i)$, this means that for certain values of the parameters, the model enters into a phase dominated by configurations completely localized at one (random) site. The mechanism behind such condensation remains similar in the more general models, but the nearest-neighbor interaction allows the condensate to spread over a region whose width scales with a power of the total volume M . As we

will see, it is this type of condensation which provides the basis for an explanation of the droplet configuration in CDT based on the much simpler BIB models.

这类模型的一个有趣特征是会发生凝聚现象。在原始 BIB 模型 (满足 $g(m_i, m_{i+1}) = g(m_i)$) 中，凝聚意味着在特定参数取值下，模型会进入一个由完全局域在单个 (随机) 格点上的构型主导的相。这种凝聚的机制在更广义的模型中基本相同，但最近邻相互作用会使凝聚态扩散在一个区域内，该区域的宽度随总体积 M 的幂次标度。正如我们将会看到的，正是这种凝聚现象为我们基于更简单的 BIB 模型解释 CDT 中的液滴构型提供了基础。

It should also be self-evident from the formulas above that the BIB models are straightforwardly interpretable as effective models of CDT in the Landau coarse grained picture of (7), in particular under the assumptions leading to (8). However, in principle, we do not need to conjecture any relation between the BIB transfer matrix and the full transfer matrix of CDT: the first equality in (8) is an exact rewriting, while for the second, we only need an assumption of short-range interaction between the slices.

从上述公式也能明显看出，BIB 模型可以直接被解释为朗道粗粒化图景 (7) 中 CDT 的有效模型，尤其是在推导得到式 (8) 的假设下。不过原则上我们不需要猜想 BIB 转移矩阵和 CDT 的完整转移矩阵之间存在任何关联: 式 (8) 的第一个等号是精确重写，而对于第二个等号，我们只需要假设切片之间存在短程相互作用即可。

Landau Theory of Two-Dimensional CDT

二维因果动态三角剖分 (CDT) 的朗道理论

In two dimensions, only one of the N_k variables is independent, e.g., the number of triangles N_2 . This is clear also from a continuum perspective, as the curvature term is topological; hence at fixed topology, the Einstein-Hilbert action reduces to a simple volume term. The two-dimensional CDT model [24] at fixed topology has thus only one coupling, the bare cosmological constant, while Newton's constant plays no role. The corresponding partition function has therefore the interpretation of generating function for the number of triangulations of the type in Fig. 1 with fixed number of triangles N and some given boundary conditions.

在二维空间中，N_k 个变量中仅有一个是独立变量，例如三角形的数量 N_2 。从连续统视角也能明确这一点，因为曲率项是拓扑性的；因此在固定拓扑下，爱因斯坦-希尔伯特作用量退化为简单的体积项。固定拓扑下的二维 CDT 模型 [24] 因此仅存在一个耦合常数，即裸宇宙学常数，而牛顿常数不起任何作用。相应的配分函数因此可被解释为生成函数，用于计数图 1 中固定三角形数量 N 、满足给定边界条件的此类三角剖分的数目。

The two-dimensional model of CDT can be solved exactly by various means [24, 73-75], so it would seem pointless to look for a Landau theory. However, the latter appears very naturally in the process of solving the model, and it is therefore a useful example of top-down approach to a Landau free energy in a quantum gravity model. In this case, the partition function for two-dimensional causal triangulations with fixed N and T (denoted $\left(\mathcal{T}_{N,T}\right)$ can be written as

二维 CDT 模型可以通过多种方法精确求解 [24, 73-75]，因此寻找朗道理论似乎毫无意义。但在求解该模型的过程中，朗道理论会非常自然地浮现，因此它是研究量子引力模型中朗道自由能自上而下方法的一个有用示例。在这种情况下，固定 N 和 T (记为 $\left(\mathcal{T}_{N,T}\right)$) 的二维因果三角剖分的配分函数可以写为:

$$
\begin{aligned}
Z_{2\,\mathrm{d-CDT}}(N,T) &= \sum_{\mathcal{T}_{N,T}} 1 \\
&= \sum_{l_1=1}^{N} \cdots \sum_{l_T=1}^{N} \delta_{N_2,2\sum_i l_i} \prod_{i=1}^{T} g(l_i, l_{i+1}) \\
&\equiv \sum_{\{l\}} e^{-L(\{l\};N,T)},
\end{aligned}
\tag{13}
$$

with $l_{T+1} = l_1$ (periodic boundary conditions in the time direction), and

其中 $l_{T+1} = l_1$ 满足时间方向周期性边界条件，且

$$
g(l_i, l_{i+1}) = \frac{(l_i + l_{i+1})!}{l_i! l_{i+1}!}, \tag{14}
$$

counting the number of triangulations of a strip with boundary lengths l_i and l_{i+1} , with open boundary conditions in the spacelike direction (It basically counts the number of ways we can place l_{i+1} balls in $l_i + 1$ boxes, so that in this case the reduced transfer matrix is itself a BIB model (with trivial reduced transfer matrix).).

用于计数边界长度为 l_i 和 l_{i+1} 、类空方向为开边界条件的带状三角剖分的数目 (它本质上是计数将 l_{i+1} 个球放入 $l_i + 1$ 个盒子的方法数，因此该情况下的约化转移矩阵本身就是一个 BIB 模型 (约化转移矩阵是平凡的)。)

In the second line of (13) we recognize a BIB model (compare to (9)), while in the last line we defined the function $L(\{l\}; N, T)$, which we interpret as a Landau free energy. Indeed, comparing to (2) and (3), we see that in the definition of $L(\{l\}; N, T)$ we are summing over triangulations with a block constraint, the blocks here being the spatial slices of each triangulation, and the constraint fixing the number of edges in each block (Such a nonlocal observable on a co-dimension-one slice is reminiscent of similar quantities considered in anisotropic systems, e.g., the Ising model with anisotropic competing next-to-nearest-neighbor interactions [76].).

在式 (13) 的第二行中我们可以识别出一个 BIB 模型 (与式 (9) 对比)，最后一行我们定义了函数 $L(\{l\}; N, T)$, 我们将其解释为朗道自由能。事实上, 对比式 (2) 和式 (3) 可以发现, 在 $L(\{l\}; N, T)$ 的定义中，我们对带块约束的三角剖分求和，此处的块就是每个三角剖分的空间切片，约束条件固定每个块中的边数 (这种余一维切片上的非定域观测让人联想到各向异性系统中研究的类似物理量，例如带有各向异性竞争次近邻相互作用的伊辛模型 [76]。)

Notice that the Landau free energy $L(\{l\}; N, T)$ contains a global constraint, but we can get rid of it by switching to the grand canonical ensemble. That is, by summing over N with a Boltzmann weight $e^{-\kappa_2 N}$, we obtain:

注意到朗道自由能 $L(\{l\};N,T)$ 包含一个全局约束，我们可以通过转换到大正则系综消除该约束。也就是说，对 N 按玻尔兹曼权重 $e^{-\kappa_2 N}$ 求和，我们得到:

$$L_{\mathrm{gc}}(\{l\};T,\kappa_2)=2\kappa_2\sum_i l_i-\sum_i \ln\left(g\left(l_i,l_{i+1}\right)\right). \tag{15}$$

It should be stressed that the second term is a purely entropic contribution, with no lattice coupling constant.

需要强调的是，第二项纯粹是熵贡献，不包含格点耦合常数。

Continuum limit The model is exactly solvable [24,73-75], and a continuum limit can be taken on the solution. It is however instructive to see what we can learn by first taking a continuum approximation and then minimizing the continuum Landau free energy. Using Stirling's formula, one finds that for large l_i and l_{i+1} and small $(l_{i+1}-l_i)/(l_i+l_{i+1})$,

连续极限: 该模型是精确可解的 [24,73-75]，可以在解上取连续极限。不过先做连续近似，再对连续朗道自由能最小化，以此探究我们能得到的结论是具有启发性的。利用斯特林公式可以发现，当 l_i 和 l_{i+1} 很大，而 $(l_{i+1}-l_i)/(l_i+l_{i+1})$，很小时，

$$g\left(l_i,l_{i+1}\right)\sim 2^{l_i+l_{i+1}}e^{-\frac{\left(l_{i+1}-l_i\right)^2}{l_i+l_{i+1}}}. \tag{16}$$

It is easy to take the continuum limit of the exponent in (16), thus obtaining

很容易对式 (16) 中的指数取连续极限，由此得到:

$$S_{2\,\mathrm{d-HL}}[\ell]=\int_{-\frac{\tau}{2}}^{\frac{\tau}{2}}dt\frac{\dot{\ell}(t)^2}{4\ell(t)}. \tag{17}$$

Such action (Here and in the following, we will generally refer to the continuum limit of the Landau free energy as an (effective) action.) can be interpreted as an action for the length $\ell(t)$ of the slices, describing two-dimensional HL gravity in proper-time gauge, as noticed in [44] (see also the dedicated chapter of the Handbook of Quantum Gravity [77]).

该作用量 (此处及下文中，我们一般将朗道自由能的连续极限称为 (有效) 作用量。) 可以被解释为切片长度 $\ell(t)$ 的作用量，正如文献 [44] 中指出的 (另见《量子引力手册》的专门章节 [77])，它描述了固有时间规范下的二维 HL 引力。

It is well known (see, e.g., [78] and references therein) that in a path integral quantization of gravity in the proper-time gauge, we lose the Hamiltonian constraint, unless we integrate over the total proper time. Such integration is not performed in CDT when computing finite-time propagators (by the definition of such observables) or when doing simulations with periodic boundary conditions in time, for obvious practical reasons. However, it should be stressed that in principle, this only means that the integral over time is postponed to a later stage. Indeed, in 1+1 dimensions, this integral can be carried out exactly, leading to a solution of the quantum Hamiltonian constraint or Wheeler-DeWitt equation [24]. What we want to stress here is that in

order to make contact between continuum models and CDT results with fixed total time, one should not try to impose the Hamiltonian constraint in the former. Bearing this in mind, we can try to see what a semiclassical analysis of (17) tells us.

众所周知 (例如参见文献 [78] 及其中引文)，在固有时规范下对引力做路径积分量子化时，除非我们对总固有时积分，否则会失去哈密顿约束。在 CDT 中计算有限时间传播子时 (根据这类可观测量的定义)，或是出于实际原因对时间周期性边界条件做模拟时，都不会进行这类积分。但需要强调的是，原则上这仅意味着对时间的积分被推迟到后续步骤。实际上，在 1+1 维中该积分可以精确完成，从而得到量子哈密顿约束即惠勒-德维特方程的解 [24]。我们在此想要强调的是，为了建立连续统模型与固定总时间的 CDT 结果之间的联系，不应尝试在连续统模型中强加哈密顿约束。牢记这一点，我们可以来看式 (17) 的半经典分析能给出什么结论。

Solving the equations of motion of (17) with the constraint $V_2 = \int_{-\frac{\tau}{2}}^{\frac{\tau}{2}} dt \ell(t)$, and with periodic boundary conditions in time, one finds either constant or oscillating solutions. The constant solution is in fact unique, due to the volume constraint: $\ell(t) = V_2/\tau$. The oscillating solutions form a discrete set, due to the periodicity condition. Plugging these solutions into the action (17), since $\ell(t) \geq 0$ and $\dot{\ell}(t) \neq 0$ (except at isolated points) for the oscillating solution, it is obvious that the constant solution has the least action (it evaluates to zero), and therefore it must dominate the path integral. Note that the Hamiltonian constraint would fix the amplitude independently of the total time τ, and therefore we would have periodic solutions only for special values of τ. We could consider also droplet configurations of the kind that we will introduce in higher dimensions, but the constant solution would still dominate over them, as the action (17) is non-negative, and equal to zero if and only if $\dot{\ell}(t) = 0$ for all t.

在约束 $V_2 = \int_{-\frac{\tau}{2}}^{\frac{\tau}{2}} dt \ell(t)$ 和时间周期性边界条件下求解式 (17) 的运动方程，我们会得到常数解或振荡解。由于体积约束 $\ell(t) = V_2/\tau$，常数解实际上是唯一的。由于周期性条件，振荡解构成一个离散集合。将这些解代入作用量 (17)，对于振荡解，由于 $\ell(t) \geq 0$ 且 $\dot{\ell}(t) \neq 0$ (孤立点除外)，显然常数解的作用量最小 (其作用量为零)，因此它一定会主导路径积分。注意，哈密顿约束会固定振幅，且与总时间 τ 无关，因此仅当 τ 取特殊值时我们才能得到周期解。我们也可以考虑后续介绍高维情况时会引入的液滴构型，但常数解仍然比它们更占主导，因为作用量 (17) 是非负的，且当且仅当对所有 t 都满足 $\dot{\ell}(t) = 0$ 时作用量才为零。

The dominance of the constant solution is in complete agreement with the Monte Carlo snapshots from numerical simulations [79], which, unlike the higher-dimensional models, show no sign of translational symmetry breaking and average to a constant profile. This can also be seen from the analytical solution [24], which gives a constant $\langle \ell(t) \rangle \propto 1/\sqrt{\Lambda}$, where Λ is the continuum cosmological constant in the grand canonical ensemble (One might worry that in the case of periodic boundary conditions, a simple average will always lead to a translational-invariant result. The usual way to deal to avoid blurring a broken phase with an average over vacua is to introduce an explicit symmetry breaking term in the model and check if the symmetry breaking persists when this is continuously removed. For example, one could break explicitly the translational symmetry by introducing initial and final boundaries of fixed length and check that for large τ, the bulk is approximately constant, but this would be a long and unnecessary parentheses here. As we will discuss later, in numerical simulations, there is a more practical way to effectively select a single vacuum.). In any case, one should also remember that in $1+1$ dimensions, $\sqrt{\langle \ell^2 \rangle - \langle \ell \rangle^2} \propto 1/\sqrt{\Lambda}$, i.e., fluctuations have the same magnitude as the average configuration, thus hiding any possible classical behavior of the latter.

常数解的主导性与数值模拟得到的蒙特卡罗快照 [79] 完全一致，和高维模型不同，这些快照没有显示出平移对称性破缺的迹象，平均后得到均匀剖面。这也可以从解析解 [24] 中看出，该解析解给出常数 $\langle \ell\,(t)\rangle \propto 1/\sqrt{\Lambda}$，其中 Λ 是巨正则系综中的连续宇宙学常数 (有人可能会担心，在周期性边界条件下，简单平均总会得到平移不变结果。为了避免因对真空平均模糊破缺相，通常的处理方法是在模型中引入显式对称性破缺项，再检查当该项被连续移除后对称性破缺是否仍存在。例如，可以通过引入固定长度的初始和最终边界来显式破缺平移对称性，再检查当 τ 很大时本体是否近似为常数，但在此展开说明会冗长且不必要。正如我们后续会讨论的，在数值模拟中有一种更实用的方法来有效选取单个真空)。无论如何，我们还应当记住，在 $1+1$ 维中，$\sqrt{\langle \ell^2\rangle - \langle \ell\rangle^2} \propto 1/\sqrt{\Lambda}$，即涨落的幅度和平均构型的幅度相同，因此掩盖了平均构型任何可能的经典行为。

The role of higher-order terms in the Stirling approximation has been studied in [80], where it was shown that including enough matter fields the leading order correction (a logarithmic potential term in the exponent of (16)) becomes important and leads to a phase transition to a droplet phase, similar to the one we will describe below.

斯特林近似中高阶项的作用已在文献 [80] 中研究，该文表明，当包含足够多物质场时，领头阶修正 (即式 (16) 指数中的对数势项) 会变得重要，并会导致相变进入液滴相，和我们下文将要描述的相类似。

Effective theory vs minisuperspace models

有效理论 vs 极小超空间模型

We should stress once more that (17) is not a minisuperspace approximation for the quantization of the bare theory. In fact, the bare action in two-dimensional CDT is trivial. Equation (17) is instead obtained nonperturbatively as a purely entropic contribution from the sum over all triangulations. This also shows as a proof of principle that even if we start with a bare action of general relativity, the structure of triangulations of our ensemble can determine a more general universality class. Of course, such a phenomenon should not come as a surprise: while it is easy to define a diffeomorphism-invariant action (in the continuum), it is highly nontrivial to define a regularized diffeomorphism-invariant measure for the path integral, and therefore, it is precisely there that a possible breaking of gauge symmetries might occur.

我们需要再次强调，方程 (17) 并非裸理论量子化的极小超空间近似。事实上，二维因果动态三角剖分 (CDT) 中的裸作用量是平凡的。方程 (17) 实际上是对所有三角剖分求和得到的纯熵贡献，是非微扰结果。这也从原理上证明，即使我们从广义相对论的裸作用量出发，我们系综的三角剖分结构也可以决定更普适的普适类。当然，这种现象并不出人意料: 虽然在连续体中很容易定义微分同胚不变作用量，但要为路径积分定义正则化的微分同胚不变测度却高度非平凡，因此恰恰是在这里可能发生规范对称性的破缺。

Spatial Volume Dynamics in Three-Dimensional CDT

三维 CDT 中的空间体积动力学

In this section, we concentrate on the case $d = 3$, for which very few analytical results are known (e.g., [66,81,82]) because of the difficulty in solving statistical models in dimensions higher than two. Therefore, most of the current understanding of this case derives from Monte Carlo simulations.

在本节中，我们聚焦于 $d = 3$ 的情形，由于求解二维以上的统计模型存在难度，目前已知的解析结果极少 (例如文献 [66,81,82])，因此当前对该情形的认知大多来源于蒙特卡洛模拟。

In the simulations, one typically uses the topological constraints in order to trade the variable N_1 for N_0 , which is easier to keep track of, and thus replace (5) by

在模拟中，人们通常利用拓扑约束将变量 N_1 换为更便于追踪的 N_0 ，从而用下式替换 (5):

$$S(\mathcal{T}_N) = \kappa_3 N - \kappa_0 N_0. \tag{18}$$

Furthermore, as we mentioned, in the computer simulations, we work at a fixed volume, and hence we replace (4) by the partition function for the canonical ensemble,

此外，正如前文所述，在计算机模拟中我们在固定体积下开展计算，因此用正则系综的配分函数替换 (4):

$$Z_N = \sum_{\mathcal{T}_N} \frac{1}{C(\mathcal{T}_N)} e^{\kappa_0 N_0}, \tag{19}$$

where we have made use of the simple form of the action (18). Note that the grand canonical partition function Z is the discrete Laplace transform of Z_N with respect to N .

其中我们利用了作用量 (18) 的简单形式。注意巨正则配分函数 Z 是 Z_N 相对于 N 的离散拉普拉斯变换。

The expectation value of an observable O is calculated as

可观测量 O 的期望值计算如下:

$$\langle O \rangle_N = \frac{1}{Z_N} \sum_{\mathcal{T}_N} \frac{1}{C(\mathcal{T}_N)} e^{\kappa_0 N_0} O(\mathcal{T}_N), \tag{20}$$

which is related to the grand canonical expectation value as a function of κ_3 via

它作为 κ_3 的函数，通过下式与巨正则期望值关联:

$$\langle O \rangle = \frac{1}{Z} \sum_N e^{-\kappa_3 N} Z_N \langle O \rangle_N. \tag{21}$$

Simulations Simulations were performed in [41, 45] using the Markov-chain Monte Carlo technique. An adaptation of some previously existing code for the Monte Carlo simulations (used in [83]) was used for this purpose. The code generates a finite set of sample configurations $\{\mathcal{T}^{(1)}, \ldots, \mathcal{T}^{(M)}\}$ according to the probability

distribution $\mathcal{P}(\mathcal{T}) = \frac{1}{Z} e^{-S(\mathcal{T})}$. One then approximates the expectation value of an observable by its arithmetic mean across these samples:

模拟文献 [41, 45] 利用马尔可夫链蒙特卡洛技术完成了模拟。为此，我们改编了此前已有的蒙特卡洛模拟代码 (曾用于文献 [83])。该代码根据概率分布 $\mathcal{P}(\mathcal{T}) = \frac{1}{Z} e^{-S(\mathcal{T})}$ 生成有限的样本构型集合 $\left\{\mathcal{T}^{(1)}, \ldots, \mathcal{T}^{(M)}\right\}$，随后通过可观测量在所有样本中的算术均值对其期望值做近似:

$$\langle O \rangle \approx \frac{1}{M} \sum_{j=1}^{M} O\left(\mathcal{T}^{(j)}\right). \tag{22}$$

As usual in three-dimensional CDT simulations, the spacetime topology was fixed to $S^2 \times S^1$, i.e., spherical spatial sections and cyclical time (Simulations with different boundary conditions in the time or spatial directions have been performed in [84] and [85], respectively, and the results are consistent with those reviewed here.). Values of N up to a maximum of 200k $\equiv 2 \times 10^5$ were studied, although some errors for the larger values of N are greater since less configurations could be generated to be averaged over, within practical time constraints. All simulations were carried out with coupling constant $\kappa_0 = 5$, in the phase where previous evidence points to the emergence of a well-behaved (three-dimensional) geometry. The total number of time-steps was set to $T = 96$.

和常规的三维 CDT 模拟一样，时空拓扑固定为 $S^2 \times S^1$，即空间截面为球面、时间方向为周期 (分别在文献 [84] 和 [85] 中完成了时间方向和空间方向带不同边界条件的模拟，所得结果与本文综述的结论一致)。本次研究涵盖了直至最大值 200k $\equiv 2 \times 10^5$ 的 N 取值，不过由于在实际时间限制内能够生成并用于平均的构型更少，较大 N 对应的误差更大。所有模拟都在耦合常数 $\kappa_0 = 5$ 下开展，对应已有证据表明存在良好 (三维) 几何涌现的相。时间步总数设定为 $T = 96$。

The Volume Data

体积数据

The observable we study here is the volume of the spatial slices, which in the three-dimensional CDT model corresponds to the number of spatial triangles $N_2(i)$ as a function of discrete time i. Because the triangulation is connected, we always have $N_2(i) > 0$. Furthermore, because we restrict to simplicial manifolds, the smallest triangulation of a two-sphere has four triangles, giving

我们在此研究的可观测量是空间切片的体积，在三维 CDT 模型中，它对应空间三角形的数量 $N_2(i)$，是离散时间 i 的函数。由于三角剖分是连通的，我们始终有 $N_2(i) > 0$。此外，由于我们限制为单纯流形，二维球面的最小三角剖分包含四个三角形，因此有

$$N_2(i) \geq n_{\min} = 4 \tag{23}$$

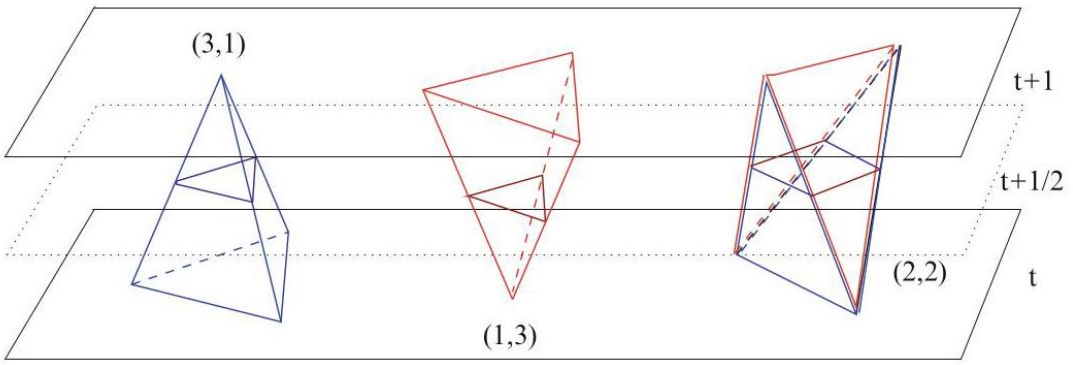

Fig. 2 The three types of tetrahedral building blocks in three-dimensional CDT and their intersections with the $t + 1/2$ plane

图 2 三维 CDT 中三类四面体构造块及其与 $t + 1/2$ 平面的交点

Another possible observable is the volume of the spatial slices at half-integer values of time, which amounts to a weighted sum of the number of (3,1) and of (2,2) tetrahedra (see Fig. 2) between slices i and $i + 1$. We expect that in the phase of extended geometry (where $N_{(3,1)} \sim 2N_{(2,2)}$), any such differences in definitions of volume as a function of time should be irrelevant in the continuum limit.

另一种可能的可观测量是半整数时间点处空间切片的体积，相当于切片 i 和 $i + 1$ 之间 (3,1) 型与 (2,2) 型四面体数量的加权和 (参见图 2) 我们预期，在扩展几何相 (其中 $N_{(3,1)} \sim 2N_{(2,2)}$) 中，任何这类关于体积随时间定义的差异在连续极限下都无关紧要。

Note that a triangle is always shared by two tetrahedra, so that, for the number $N_2^{(s)}$ of spatial triangles, we have

注意一个三角形始终被两个四面体共用，因此对于空间三角形的数量 $N_2^{(s)}$ ，我们有

$$N_2^{(s)} = \sum_{i=1}^{T} N_2(i) = \frac{1}{2} N_{(3,1)}, \tag{24}$$

which in the extended phase we expect to be roughly one third of the total volume N_3 . For the value of κ_0 we used, the distribution of $N_2^{(s)}$ is very peaked (for $N_3 = 100\text{k}$, the relative standard deviation is only 0.2% ; see Fig. 3), and we find that $N_{(2,2)}$ is just slightly smaller than a third of the total volume.

我们预期在扩展相中，它约为总体积 N_3 的三分之一。对于我们所用的 κ_0 值，$N_2^{(s)}$ 的分布峰度非常高 (对于 $N_3 = 100\text{k}$ ，相对标准差仅为 0.2% ；参见图 3)，我们发现 $N_{(2,2)}$ 仅比总体积的三分之一略小一点。

In Fig. 4 we show the volume profile $N_2(i)$ from a snapshot of a Monte Carlo simulation. One notices immediately a phenomenon of spontaneous (translational) symmetry breaking: the Monte Carlo configuration shows a condensation of the volume around a specific time. Averaging over Monte Carlo configurations, the translational symmetry gets restored, but this is because a blind average amounts to summing over the degenerate vacua of the broken phase. As usual, in order to see spontaneous symmetry breaking, we should

select only one vacuum. For example, in a spin system, this is done by first coupling the spins to an external magnetic field, which is then switched off. In the CDT simulations, we select one vacuum by performing a recentering of the Monte Carlo configurations. In practice, we have to find the center of volume $t_{CV}(j)$ for each Monte Carlo configuration j, and we have to shift time so that $t'_{CV}(j) = T/2$ for every configuration in the new time variable. We performed this operation following the method given in [86,87]. Once the data are centered in this way, it makes sense to study the average of $N_2(i)$. A plot of $\langle N_2(i)\rangle$, together with fluctuations, is displayed in Fig. 5.

在图 4 中，我们展示了蒙特卡洛模拟快照得到的体积剖面 $N_2(i)$。可以立刻观察到自发 (平移) 对称性破缺现象: 蒙特卡洛构型显示体积在特定时间附近凝聚。对蒙特卡洛构型取平均后，平移对称性得以恢复，但这是因为盲平均相当于对破缺相的简并真空求和。和通常情况一样，要观察自发对称性破缺，我们应当只选取一个真空。例如在自旋系统中，这一步是通过先让自旋耦合外磁场，再关闭外磁场实现的。在 CDT 模拟中，我们通过对蒙特卡洛构型重新中心化来选取一个真空。实际操作中，我们需要对每个蒙特卡洛构型 j 找到体积中心 $t_{CV}(j)$，然后平移时间，使得在新的时间变量中对每个构型都满足 $t'_{CV}(j) = T/2$。我们按照文献 [86,87] 给出的方法执行了该操作。数据以这种方式中心化后，研究 $N_2(i)$ 的平均值就有意义了。图 5 展示了 $\langle N_2(i)\rangle$ 的图及涨落情况。

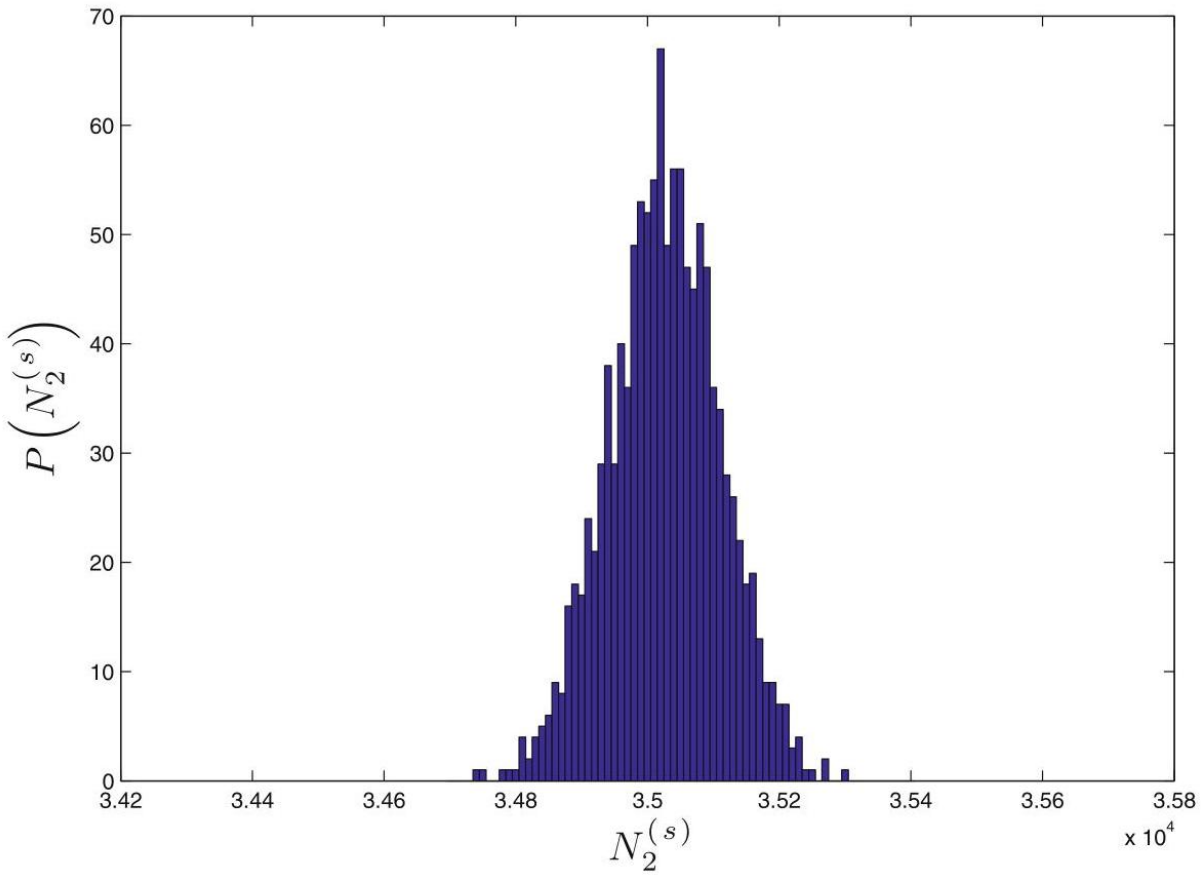

Fig. 3 The distribution of the total number of spatial triangles $N_2^{(s)}$ (grouped in bins of size 10), for $N_3 =$ 100k . The expectation value is $\left\langle N_2^{(s)}\right\rangle = 35026$, with standard deviation $\sigma = 85$

图 3 空间三角形总数 $N_2^{(s)}$ 的分布 (分组为大小 10 的区间), 对应 $N_3 = 100\text{k}$ 。期望值为 $\left\langle N_2^{(s)} \right\rangle = 35026$ ，标准差为 $\sigma = 85$

The volume profile has a characteristic extended part (typically referred to as the blob or droplet) and a long flat tail (referred to as the stalk). Within the latter, the spatial volume is very close to its kinematical minimum, $\frac{1}{m} \sum_{i=1\ldots m}^{i\in \text{ stalk}} \langle N_2(i) \rangle \equiv n_s \sim 10$, and it is independent of the total volume. Most of the total volume is therefore concentrated in the blob. We will discuss in the following sections how to explain this condensation phenomenon and which function best describes the volume profile.

体积分布具有特征性的延展部分 (通常称为团块或液滴)，以及一条长而平缓的尾部 (称为茎部)。在尾部区域，空间体积非常接近其运动学最小值 $\frac{1}{m} \sum_{i=1\ldots m}^{i\in \text{ stalk}} \langle N_2(i) \rangle \equiv n_s \sim 10$ ，且与总体积无关。因此总体积大多集中在团块中。我们将在后续章节中解释这种凝聚现象，并说明哪种函数最适合描述该体积分布。

The Continuum Limit

连续极限

We conclude this section by discussing how the continuum limit $a \to 0$ is investigated on the basis of the simulation data. All observables and couplings in the simulations are given as dimensionless numbers, as such are also all the quantities appearing in (18) and the definition of the model. Length dimensions are introduced by multiplying the quantity of interest by the appropriate power of the cutoff a , the length of spacelike edges (Despite the Euclidean signature, we use the words spacelike and timelike to distinguish the orientation of edges with respect to the foliation.). For example, we can write $\tau = a\alpha T$ for the time interval, where we have introduced a parameter $\alpha > 0$ to allow a different length of the timelike edges. Next, we can write $V_2 = \frac{\sqrt{3}}{4} a^2 N_2$ for the volume of a slice (the numerical prefactor being the area of an equilateral triangle of unit side), $V_3 = v_{(3,1)}(\alpha)\, a^3 N_{(3,1)} + v_{(2,2)}(\alpha)\, a^3 N_{(2,2)}$ for the total volume, etc. Here, $v_{(3,1)}(\alpha)$ and $v_{(2,2)}(\alpha)$ stand for the volume of the $(3,1)$ and $(2,2)$ simplices with spatial edges of length one and time edges of length α (they both coincide with the equilateral tetrahedron for $\alpha = 1$, with volume $v_3 = 1/6\sqrt{2}$; see [30]).

我们在本节最后讨论如何基于模拟数据研究连续极限 $a \to 0$ 。模拟中所有可观测量和耦合均以无量纲数给出，因此出现在式 (18) 和模型定义中的所有物理量也都是无量纲的。长度量纲可通过将目标物理量乘上截断 a 的对应幂次得到，a 是类空边的长度 (尽管使用欧几里得号差，我们仍用类空、类时区分边相对于叶化的方向)。例如，我们可以将时间间隔写为 $\tau = a\alpha T$ ，这里我们引入参数 $\alpha > 0$ 来表示类时边可以具有不同长度。接下来我们可以将一个切片的体积写为 $V_2 = \frac{\sqrt{3}}{4} a^2 N_2$ (数值前置因子是单位边长等边三角形的面积)，总体积写为 $V_3 = v_{(3,1)}(\alpha)\, a^3 N_{(3,1)} + v_{(2,2)}(\alpha)\, a^3 N_{(2,2)}$ ，以此类推。此处，$v_{(3,1)}(\alpha)$ 和 $v_{(2,2)}(\alpha)$ 分别代表空间边长为 1、时间边长为 α 的 $(3,1)$ 和 $(2,2)$ 单形的体积 (当 $\alpha = 1$ 时二者均等同于等边四面体，体积为 $v_3 = 1/6\sqrt{2}$ ；参见文献 [30])。

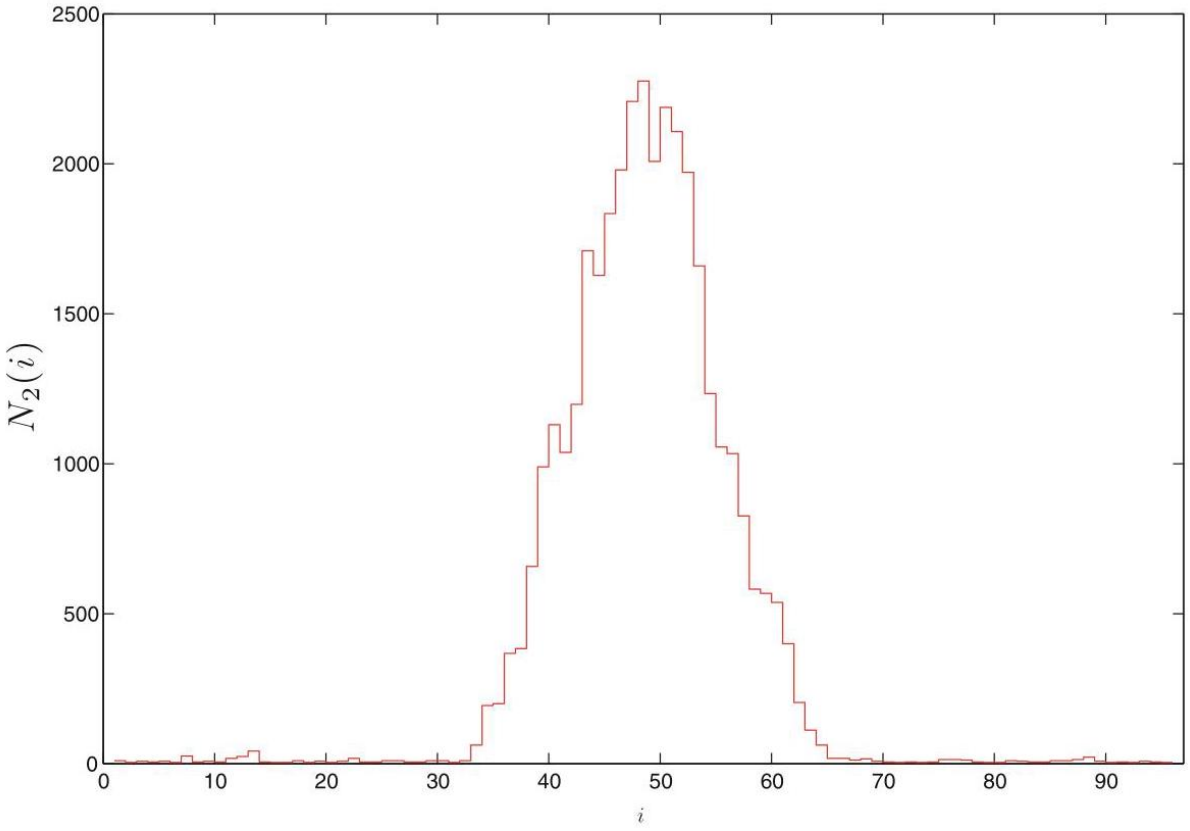

Fig. 4 The spatial area $N_2(i)$ as a function of time, from a single configuration taken at random in the data set of Monte Carlo simulations for $N_3 = 100$k

图 4 蒙特卡罗模拟数据集对 $N_3 = 100$k 随机抽取的一个构型中，空间面积 $N_2(i)$ 作为时间的函数

An essential part of the continuum limit procedure is to have $N \to \infty$ and $a \to 0$ in such a way that the physical volume

连续极限步骤的核心要求是，调节 $N \to \infty$ 和 $a \to 0$ 使得物理体积

$$V \sim a^d N \tag{25}$$

remains finite. This implies that when we multiply a dimensionless quantity by a^n , in order to switch to its dimensional counterpart, in practice, we multiply it by $N^{-n/d}$. For example, in CDT, we also demand that $\tau \sim N^{-1/d} T$ stays finite.

保持有限。这意味着当我们将一个无量纲量乘上 a^n 得到其对应有量纲形式时，实际操作中我们是将它乘上 $N^{-n/d}$ 。例如，在 CDT 中我们同样要求 $\tau \sim N^{-1/d} T$ 保持有限。

In the thermodynamic limit, we expect that, besides the total volume (25), also other dimensional large-scale observables will become independent of the cutoff a. Therefore, we expect to see scaling behavior when working with simulations at sufficiently large N , i.e., we expect that an observable $\langle \mathcal{O}(i) \rangle_N$, depending on the discrete time variable $i = 1, \ldots, T$, will satisfy for some fixed (continuum time) t :

在热力学极限下，我们预期除了总体积 (25) 之外，其他有量纲大尺度可观测量也会变得与截断 a 无关。因此我们预期，在足够大的 N 下进行模拟会出现标度行为，也就是说，依赖于离散时间变量 $i = 1, \dots, T$ 的可观测量 $\langle \mathcal{O}(i) \rangle_N$ 会对某个固定的 (连续时间) t 满足:

$$N^{-n/d} \left\langle \mathcal{O}\left(N^{1/d} t\right) \right\rangle_N = N'^{-n/d} \left\langle \mathcal{O}\left(N'^{1/d} t\right) \right\rangle_{N'}, \tag{26}$$

where the value of the observable at non-integer time is to be intended from an interpolating fit. The natural expectation would be that (25) and (26) hold with n given by the expected dimension of the observable, but this is not guaranteed a priori, and it is instead used as a check of the good classical properties of the model, as we do in the following. Moreover, not all quantities will show scaling: the dimensionless version of some quantity might remain independent of N . The typical example is the correlation length l_c , from $\langle \mathcal{O}(i)\, \mathcal{O}(j) \rangle_N - \langle \mathcal{O}(i) \rangle_N \langle \mathcal{O}(j) \rangle_N \sim e^{-|i-j|/l_c}$ (at large $|i-j|$); in order to obtain a finite dimensionful correlation length $\ell_c = a l_c \sim N^{-1/d} l_c$, one needs to tune the couplings toward a critical point where l_c diverges. We will not be concerned with correlation lengths here, but we will see another example of quantity that stays at the cutoff scale, i.e., the volume of the stalk in the droplet phase.

其中非整数时间处的可观测量值需通过插值拟合得到。自然的预期是，(25) 和 (26) 成立，其中 n 由可观测量的预期维度给出，但这一点无法先验保证，因此反而可将其作为检验模型良好经典性质的标准，我们下文也会这么做。此外，并非所有量都满足标度律: 部分量的无量纲形式可能始终与 N 无关。典型例子是关联长度 l_c ，来自 $\langle \mathcal{O}(i)\, \mathcal{O}(j) \rangle_N - \langle \mathcal{O}(i) \rangle_N \langle \mathcal{O}(j) \rangle_N \sim e^{-|i-j|/l_c}$ (大 $|i-j|$ 情况下); 为得到有限的量纲关联长度 $\ell_c = a l_c \sim N^{-1/d} l_c$ ，需要将耦合调至临界点，此时 l_c 发散。本文不讨论关联长度，但我们会看到另一个停留在截断尺度上的量的例子，即液滴相茎结构的体积。

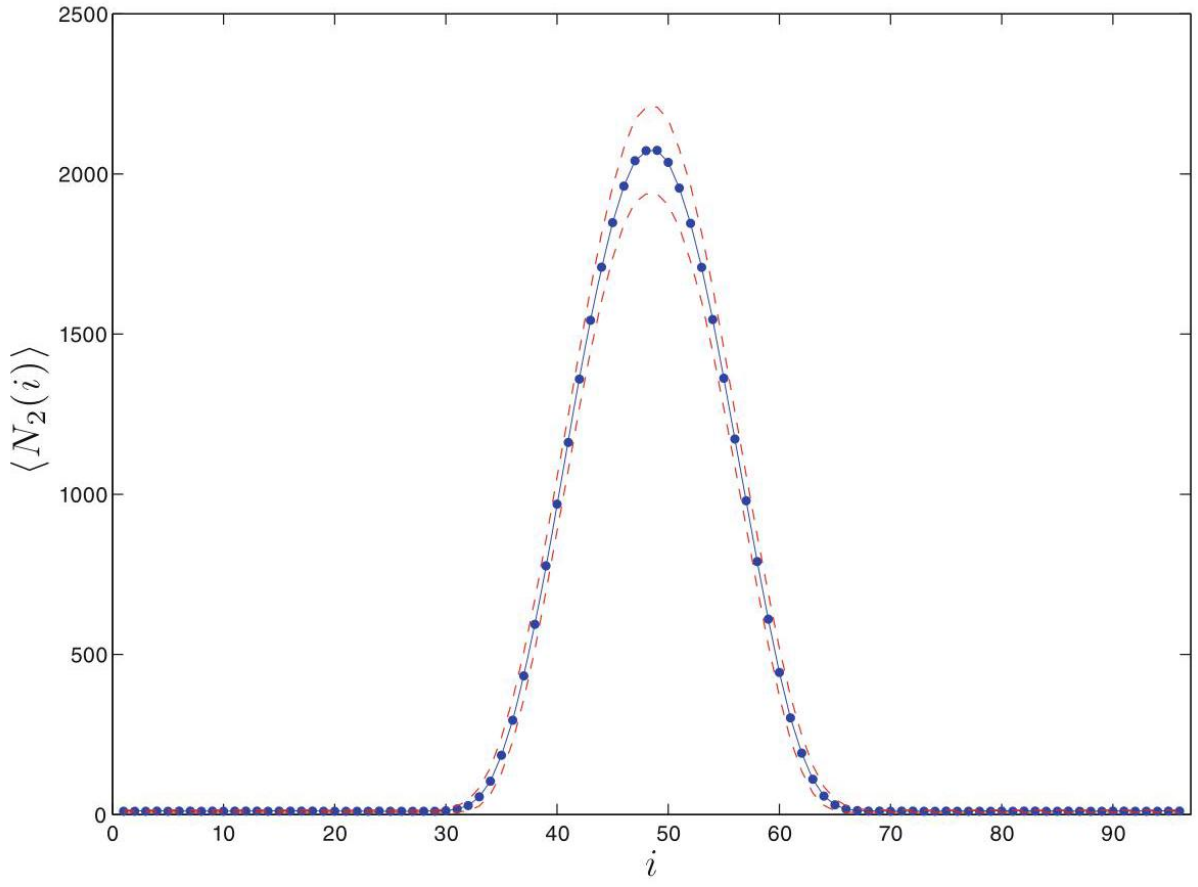

Fig. 5 The mean spatial area as a function of discrete time, for $N_3 = 100\text{k}$. The blue dots represent the mean area $\langle N_2(i)\rangle$ of the volume data at time i , while the blue line is just an interpolation curve. Error bars (estimated, e.g., by the jackknife method) are roughly of the size of the dot radii, or smaller, and thus we chose to omit them for clarity (this is done throughout the paper). The dashed red lines are interpolating curves for $\langle N_2(i)\rangle \pm \sigma/2$, where $\sigma = \sqrt{\left\langle (N_2(i))^2 \right\rangle - \langle N_2(i)\rangle^2}$ is the size of the fluctuations

图 5 平均空间面积随离散时间的变化，对应 $N_3 = 100\text{k}$ 。蓝色点表示时间 i 处体积数据的平均面积 $\langle N_2(i)\rangle$ ，蓝色线仅为插值曲线。误差棒 (例如通过刀切法估计) 大小约等于或小于点的半径，因此为清晰起见我们选择将其省略 (全文均采用此处理)。红色虚线是对应 $\langle N_2(i)\rangle \pm \sigma/2$ 的插值曲线，其中 $\sigma = \sqrt{\left\langle (N_2(i))^2 \right\rangle - \langle N_2(i)\rangle^2}$ 为涨落幅度

Figure 6 shows a scaling of the type (26). Here we have plotted $\langle N_2(i)\rangle^{1/2} / \left\langle \widetilde{N}_2^{(s)} \right\rangle^{1/3}$ as a function of $i/\left\langle \widetilde{N}_2^{(s)} \right\rangle^{1/3}$, for different data sets corresponding to different total volumes N . Following the procedure used in [26], we used $\left\langle \widetilde{N}_2^{(s)} \right\rangle = \left\langle N_2^{(s)} \right\rangle - n_s T$, instead of $\left\langle N_2^{(s)} \right\rangle$ (or N_3 , which as we saw, is proportional to it) in the rescaling because we know that the volume in the stalk does not scale. The plot clearly shows that the superposition is extremely good inside the droplet, while in the stalk, the rescaled volume goes to zero for growing N_3 .

图 6 展示了 (26) 类型的标度。此处我们绘制了 $\langle N_2(i)\rangle^{1/2} / \left\langle \widetilde{N}_2^{(s)} \right\rangle^{1/3}$ 随 $i/\left\langle \widetilde{N}_2^{(s)} \right\rangle^{1/3}$ 的变化，对应不同总容积 N 的多个数据集。遵循文献 [26] 的方法，我们在重标度中使用 $\left\langle \widetilde{N}_2^{(s)} \right\rangle = \left\langle N_2^{(s)} \right\rangle - n_s T$ 而非 $\left\langle N_2^{(s)} \right\rangle$ (或 N_3 ，正如我们所见，二者成正比)，因为我们已知茎结构的体积不满足标度。该图清晰表明，液滴内部的叠加效果极佳，而在茎结构中，重标度体积随 N_3 增大趋于零。

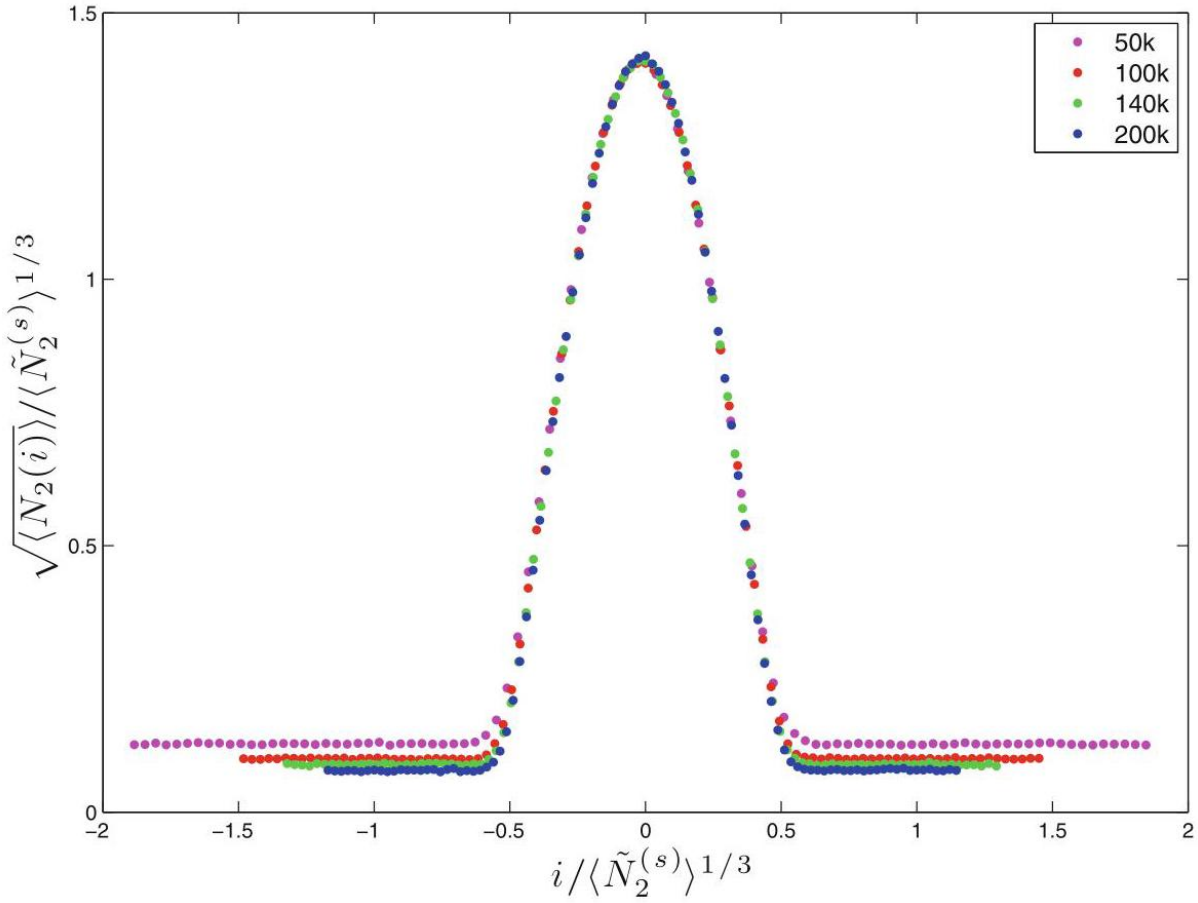

Fig. 6 The square root of the mean spatial area as a function of discrete time (shifted so that the peak is at the origin). Both the mean area and the time variable are rescaled with the appropriate power of the average total volume $\widetilde{N}_2^{(s)} = N_2^{(s)} - n_s T$, in order to display scaling

图 6 平均空间面积的平方根随离散时间的变化 (平移后峰值位于原点)。为展示标度性质，平均面积和时间变量都用平均总体积 $\widetilde{N}_2^{(s)} = N_2^{(s)} - n_s T$ 的适当次幂做了重标度

Another dynamical quantity that goes to zero in the continuum is the size of the fluctuations around the average, which we expect to be controlled by Newton's constant. Indeed, without any fine-tuning of the dimensionless couplings, all the couplings having positive (negative) length dimension will go to zero (infinity) as $a \to 0$. As Newton' s constant has the dimension of length for $d = 3$, it is expected to go to zero in the naive continuum limit (in four spacetime dimensions, where Newton's constant has dimension of length to the second power, this has been observed in [86]). A finite coupling in the continuum could perhaps be attained by fine-tuning the bare coupling to a second-order phase transition.

在连续极限中趋于零的另一个动力学量是平均值附近涨落的大小，我们预期该涨落由牛顿常数控制。事实上，不对无量纲耦合做任何精细调节，所有具有正 (负) 长度量纲的耦合都会随 $a \to 0$ 趋于零 (无穷大)。由于对 $d = 3$ 而言牛顿常数具有长度量纲，因此它在朴素连续极限中预期会趋于零 (在四维时空当中，牛顿常数具有长度平方量纲，这一现象已在文献 [86] 中被观测到)。或许可以通过将裸耦合精细调节到二级相变来在连续极限中得到有限的耦合。

Effective Models

有效模型

In this section, we review how in four and (in more detail) three dimensions the dynamics of spatial volumes in CDT can be effectively described by BIB models.

本节我们将介绍，四维与 (更详细讨论的) 三维 CDT 中的空间体积动力学，如何通过 BIB 模型得到有效描述。

Minimization of the BIB model action, in accordance with its interpretation as a Landau free energy, leads to a good qualitative description of the full CDT phase diagram.

根据 BIB 模型作为朗道自由能的解释，对其作用量进行最小化后，可得到完整 CDT 相图的良好定性描述。

Four-Dimensional CDT

四维 CDT

In [70], Bogacz et al. studied a BIB model, which is roughly a discretized version of a minisuperspace model corresponding to four-dimensional general relativity and which was originally considered in [34] to explain the data from the simulations. It was found that this very simple model can account for many of the observed features of CDT in four dimensions, including its rich phase diagram. In particular, a droplet phase was found, which has remarkable similarities to the extended phase of CDT, although of course the comparison is limited to the behavior of the spatial volume against time.

在文献 [70] 中，Bogacz 等人研究了一个 BIB 模型，它大致是对应四维广义相对论的迷你超空间模型的离散版本，最初在文献 [34] 中被提出用于解释模拟数据。研究发现，这个极为简单的模型可以解释四维 CDT 的许多观测特征，包括其丰富的相图。尤其值得注意的是，该模型得到了一个滴相，它与 CDT 的延展相具有显著的相似性，当然这种对比仅限于空间体积随时间变化的行为。

The model is defined by the following reduced transfer matrix,

该模型由下述约化转移矩阵定义:

$$g\left(m_i, m_{i+1}\right) = \exp\left(-c_1 \frac{2\left(m_{i+1} - m_i\right)^2}{m_i + m_{i+1}} - c_2 \frac{m_i^{1/3} + m_{i+1}^{1/3}}{2}\right). \tag{27}$$

In the continuum, this corresponds to the following action for the volume $V_3(t)$ of the 3-dimensional spatial slices,

在连续极限下，它对应三维空间切片体积 $V_3(t)$ 的下述作用量:

$$S_{4\,\mathrm{d-mini}}[V_3] = \frac{1}{2G}\int_{-\frac{\tau}{2}}^{\frac{\tau}{2}} dt\left(c_1\frac{\dot{V}_3^2(t)}{V_3(t)} + c_2 V_3^{1/3}(t)\right), \tag{28}$$

which is precisely of the type obtained from a minisuperspace reduction of general relativity (where $c_1 = 1/\mathcal{N}$, and $c_2 = 9\left(2\pi^2\right)^{2/3}\mathcal{N}, \mathcal{N}$ being the lapse function). This is the action that was conjectured from the very beginning by Ambjorn et al. as an effective description for the extended part of the universe (or blob) in their simulations [34], a conjecture which was further corroborated over the years [26,86,88-90]. The novelty in [70] was the suggestion that the same effective action can explain much more than just the dynamics inside the blob. Effectively, we can reinterpret the insight from [70] as the observation that the BIB model with reduced transfer matrix (27) provides a good guess for a Landau free energy, i.e., in a bottom-up approach.

其形式恰好是广义相对论迷你超空间约化得到的形式 (其中 $c_1 = 1/\mathcal{N}$ ， $c_2 = 9\left(2\pi^2\right)^{2/3}\mathcal{N}, \mathcal{N}$ 是迟缩函数)。Ambjorn 等人最初就推测该作用量可以有效描述他们模拟中宇宙 (即团块) 的延展部分 [34]，多年来的研究进一步证实了这一猜想 [26,86,88-90]。文献 [70] 的创新点在于提出，同一个有效作用量能解释的内容远不止团块内部的动力学。实际上，我们可以将文献 [70] 的见解重新解读为: 带有约化转移矩阵 (27) 的 BIB 模型给出了朗道自由能的一个合理猜测，这属于自下而上的研究思路。

Notice that in the minisuperspace action that one would derive from the Einstein-Hilbert action the constant c_1 would be negative, while for a meaningful use of (28) as an effective action, and from comparison to the numerical data [34], we must take it to be positive (The choice looks of course irrelevant if all we have is this action, as we can just change its overall sign, but this is not so if in the full Einstein-Hilbert action we want also the spin-two modes to have the good sign.). It would thus seem that in CDT, the conformal factor problem [91] affecting Euclidean quantum gravity is solved, perhaps cured by nonperturbative contributions from the functional measure, as suggested in [35], effectively recovering the rotated minisuperspace model of [92]. We will comment further on this below, arguing that in fact a simpler explanation is possible.

注意，从爱因斯坦-希尔伯特作用量推导得到的迷你超空间作用量中，常数项 c_1 为负，但要将 (28) 用作有效作用量，并且结合数值模拟数据 [34]，我们必须取其为正 (如果我们只有这个作用量，这个选择当然无关紧要，只需改变整体符号即可，但如果我们希望完整爱因斯坦-希尔伯特作用量中的自旋-2 模式也具有正确符号，情况就不同了)。由此看来，CDT 似乎解决了影响欧几里得量子引力的共形因子问题 [91]，正如文献 [35] 提出的，泛函测度的非微扰贡献或许解决了该问题，最终得到了文献 [92] 中转动后的迷你超空间模型。我们下文会进一步讨论这一点，并提出实际上存在更简单的解释。

Another important difference between the usual minisuperspace model of general relativity and the BIB model is that in the latter, there is no analogue of the lapse to be integrated in the partition function and neither there is a summation/integration over T . As a consequence, there is no Hamiltonian constraint to be imposed in the semiclassical analysis. Above, we emphasized that the same situation should be expected in CDT, where the distance between one spatial slice and the next is constant and the total time extension of the universe is fixed in all simulations to date. This is also supported by the strong evidence from numerical simulations that the BIB model is a good effective description for CDT.

广义相对论常规迷你超空间模型与 BIB 模型的另一个重要区别是，后者中没有对应迟缩函数的项需要在配分函数中积分，也不需要对 T 求和/积分。因此，在半经典分析中不需要施加哈密顿约束。上文我们已经强调，CDT 中也会出现同样的情况:CDT 中相邻两个空间切片的间距是常数，迄今为止所有模拟都固定了宇宙的总时间延展。数值模拟也有充分证据表明 BIB 模型是 CDT 的良好有效描述，这也支持了上述结论。

The equations of motion derived by varying (28) with respect to $V_3(t)$ are

对 (28) 关于 $V_3(t)$ 变分得到的运动方程为

$$c_1\left(\left(\frac{\dot{V}_3}{V_3}\right)^2-2\frac{\ddot{V}_3}{V_3}\right)+\frac{c_2}{3}\frac{1}{V_3^{2/3}}-\Lambda=0, \tag{29}$$

where the cosmological constant Λ is introduced as a Lagrange multiplier, to be fixed by imposing the volume constraint. If we were to impose also the Hamiltonian constraint $H\equiv c_1\dot{V}_3^2(t)/V_3(t)-c_2V_3^{1/3}(t)+\Lambda V_3(t)=0$, the combined system of equations would reduce to a first-order differential equation (by deriving the Hamiltonian constraint with respect to time and eliminating $\ddot{V}_3(t)$ between the two equations). As such, its solutions would have only one free integration constant, which could be fixed, for example, by demanding that the maximum of $V_3(t)$ be at $t=0$. The solution would then be the "cos3" solution discussed by Ambjorn et al. in [86,88]. However, without the Hamiltonian constraint, the equation remains second order, and thus there is one more free parameter, which allows us to perform a minimization of the on-shell action.

其中宇宙学常数 Λ 作为拉格朗日乘数引入，需通过施加体积约束确定。如果我们还要施加哈密顿约束 $H\equiv c_1\dot{V}_3^2(t)/V_3(t)-c_2V_3^{1/3}(t)+\Lambda V_3(t)=0$，联立方程组将约化为一阶微分方程 (通过对哈密顿约束求时间导数，消去两个方程中的 $\ddot{V}_3(t)$ 得到)。如此一来，其解仅含一个自由积分常数，例如可通过要求 $V_3(t)$ 的最大值位于 $t=0$ 处来确定。该解就是安伯恩等人在文献 [86,88] 中讨论的“cos3”解。但如果没有哈密顿约束，方程仍为二阶，因此多一个自由参数，这让我们可以对壳上作用量进行最小化。

For such a minimization, one does not need to restrict to class $C^2\left(S^1\right)$ functions, since for a well-defined action (28), it is sufficient that $V_3(t)\in C^1\left(S^1\right)$. This allows the authors of [70] to consider droplet configurations that are not classical solutions but that are expected on the basis of simulations and heuristic arguments (One should bear in mind that this sort of analysis is not aimed at reproducing the detailed profile of CDT at the junction between blob and stalk. In the junction region of the droplet, we expect the effect of subleading terms in the action to be non-negligible. Furthermore, the time-interval mesh in the CDT simulations is not fine enough to reveal much about the smoothness of the average profile at such junction.). Using $V_4=\int_{-\frac{\tau}{2}}^{\frac{\tau}{2}}dtV_3(t)$ for the total volume in the continuum, they obtain the following expression for the dominant contribution to the path integral in a particular region of the phase diagram(As we will see in more detail for the three-dimensional case, a number of parametric conditions must be satisfied for such configuration to dominate.):

进行这种最小化时，不需要限制在类 $C^2\left(S^1\right)$ 函数中，因为对于定义良好的作用量 (28)，只要满足 $V_3(t) \in C^1\left(S^1\right)$ 就足够了。这使得文献 [70] 的作者能够研究并非经典解的滴状构型，而这类构型是从模拟和启发式论证中得到预期的 (需要注意的是，这类分析的目的并不是重现团块与柄连接处 CDT 的详细轮廓。在滴状的连接区域，我们预期作用量中亚领先项的效应不可忽略。此外，CDT 模拟中的时间间隔网格不够精细，无法揭示该连接处平均轮廓光滑度的太多信息)。利用 $V_4 = \int_{-\frac{\tau}{2}}^{\frac{\tau}{2}} dt V_3(t)$ 表示连续体中的总体积，他们得到了相图特定区域中路径积分主导贡献的下述表达式 (正如我们在讨论三维情况时会更详细看到的，这类构型要占据主导必须满足若干参数条件):

$$\bar{V}_3(t) = \begin{cases} \frac{3\omega V_4}{4}\cos^3(\omega t), & \text{for } t \in \left[-\frac{\pi}{2\omega}, +\frac{\pi}{2\omega}\right], \\ 0, & \text{for } t \in \left[-\frac{\tau}{2}, -\frac{\pi}{2\omega}\right) \cup \left(+\frac{\pi}{2\omega}, +\frac{\tau}{2}\right], \end{cases} \tag{30}$$

where

其中

$$\omega = \frac{\sqrt{2}}{3V_4^{1/4}}\left(\frac{c_2}{c_1}\right)^{3/8}. \tag{31}$$

Notice that $V_3(t) = 0$ obviously minimizes the action (28) for positive c_1 and c_2. However, alone, it would fail to satisfy the volume constraint, while a balance between the zero and the "cos3" solutions wins the energy balance, resulting in a condensation. Interestingly, the blob part of (30), together with (31), corresponds to the solution obtained by imposing also the Hamiltonian constraint, but this seems a mere coincidence.

显然，对于正的 c_1 和 c_2，$V_3(t) = 0$ 会最小化作用量 (28)。但仅靠它无法满足体积约束，而零解与“cos3”解之间的平衡能在能量竞争中胜出，最终产生凝聚。有趣的是，(30) 的团块部分结合 (31)，对应了同时施加哈密顿约束得到的解，但这似乎只是巧合。

The crucial point to be made here is that the presence of a potential term in (28) allows non-constant configurations such as (30) to dominate the path integral. Thus, the conclusions derived in this case are qualitatively different from those derived from (17) in the two-dimensional case.

此处需要指出的关键点是，(28) 中势项的存在，使得 (30) 这类非恒定构型能够主导路径积分。因此，这种情况下得到的结论，与二维情况中从 (17) 得到的结论在定性上完全不同。

The result is very interesting because it shows how the reduced model in four dimensions reproduces not only the extended part of the universe but also its stalk, and it gives a prediction for their relative time extension. The same model also predicts other phases [70] that resemble the so-called phases A and B of CDT [26]. However, it should be stressed that it fails to capture the more recently discovered "bifurcation" phase of CDT [93, 94], for which the spatial volume is not sufficient and another order parameter is required.

这个结果非常有意思，因为它表明四维约化模型不仅重现了宇宙的延展部分，也重现了它的柄状结构，还对它们的相对时间延展给出了预言。同一个模型还预言了其他类似于 CDT 中所谓 A 相和 B 相的相 [70,26]。但需要强调的是，它无法描述最近才发现的 CDT“分岔”相 [93,94]，描述该相仅用空间体积是不够的，还需要另一个序参量。

It is also worth noticing that from the Einstein-Hilbert action, the ratio c_2/c_1 would be fixed, thus leaving us with no parameters for a fit to the CDT simulations. Since the width of the universe (for fixed V_4) depends on the bare coupling κ_0 [86], this is another indication that the effective action describing the volume dynamics is different from what would be expected from general relativity. In other words, the (Δ, κ_0) space of CDT coupling constants translates into a (c_1, c_2) plane of effective coupling constants in the BIB model, while we would expect only one in the GR minisuperspace model. On the other hand, such argument is not conclusive, as the additional parameter could turn out to be irrelevant (in the renormalization group sense) in the continuum limit and thus amount just to an innocuous lattice artefact.

同样值得注意的是，从爱因斯坦-希尔伯特作用量来看，比率 c_2/c_1 会是固定值，因此我们没有可用于拟合 CDT 模拟的参数。由于宇宙的宽度 (固定 V_4 时) 依赖于裸耦合 κ_0 [86]，这进一步表明描述体积动力学的有效作用量与广义相对论的预期不同。换言之，CDT 耦合常数的 (Δ, κ_0) 空间对应 BIB 模型中有效耦合常数的 (c_1, c_2) 平面，而我们在 GR 微超空间模型中仅预期得到一个耦合常数。另一方面，该论证并不具有确定性，因为这个额外参数在连续极限中 (按重整化群的含义) 可能本来就是无关参数，因此它仅仅是一种无害的格点伪影。

We will now argue that in three dimensions, a stronger case can be made for a departure of the effective BIB model from a GR minisuperspace model.

我们接下来将要说明，在三维情形下，有更充分的证据表明 BIB 有效模型偏离了 GR 微超空间模型。

Three-Dimensional CDT

三维 CDT

In three dimensions, the minisuperspace reduction of the Einstein-Hilbert action contains no potential term, i.e., the action for the spatial areas in the proper-time gauge is exactly of the same form as (17), but with the length $L(t)$ replaced by the area of the spatial slices $V_2(t)$. As in the two-dimensional case, in the presence of a volume constraint $V_3 = \int dt V_2(t)$, one finds oscillating solutions of the equations of motion, with a volume profile $V_2(t) \sim \cos^2(\omega t)$, which is compatible with the one observed inside the blob of Fig. 5. For this reason, such action has been suggested as an effective action for CDT [83,95] (see also [84]). However, as pointed out in [45], in light of the results on BIB models for two- and four-dimensional CDT, the similarity of the general relativistic minisuperspace action in three dimensions to (17) immediately raises the question of how such an effective action could ever explain the important differences between two- and three-dimensional CDT. Given that the two-dimensional case reduces exactly to a BIB model and the four-dimensional case is well described (in its spatial volume dynamics) by a BIB model, we would expect a similar model to give also a good approximation for the three-dimensional model.

三维下，爱因斯坦-希尔伯特作用量的超空间约化不含势能项，即固有时规范下空间面积的作用量形式恰好与式 (17) 相同，只是将长度 $L(t)$ 替换为空间切片的面积 $V_2(t)$。与二维情形类似，在存在体积约束 $V_3 = \int dt V_2(t)$ 时，可得到运动方程的振荡解，其体积轮廓 $V_2(t) \sim \cos^2(\omega t)$ 与图 5 团块中观测到的轮廓一致。因此，该作用量已被提议作为 CDT 的有效作用量 [83,95](另见 [84])。然而，正如文献 [45] 指出，结合二维和四维 CDT 的 BIB 模型研究结果，三维广义相对论超空间作用量与式 (17) 的相似性立刻引出一个问题: 这样的有效作用量如何解释二维和三维 CDT 之间的显著差异? 鉴于二维情形恰好退化为 BIB 模型，四维情形的空间体积动力学也能被 BIB 模型很好描述，我们可以预期同类模型也能为三维模型提供良好近似。

Of course, an important difference between two and three dimensions is in the scaling of dimensionful quantities. Most importantly, Newton's constant is dimensionless for $d = 2$, while it has dimension of length for $d = 3$. As a consequence, in the (naive, not fine-tuned) continuum limit, Newton's constant (and with it the fluctuations around the average volume of the slices) scales to zero in the latter case, while it stays constant in the former. In two dimensions, as there are no other scales besides the cosmological one, the size of the fluctuations in the continuum limit is as large as the expectation value, thus blurring any classical behavior. On the contrary, in three dimensions, the fluctuations go to zero, and the classical (mean field) behavior should dominate.

当然，二维和三维的一个重要区别是量纲缩放。最关键的是，牛顿常数对 $d = 2$ 而言是无量纲的，对 $d = 3$ 则具有长度量纲。因此，在 (朴素、未精细调节的) 连续极限下，三维情形中牛顿常数 (以及切片平均体积的涨落) 会缩放至零，而二维情形中牛顿常数保持不变。二维中除了宇宙学尺度外不存在其他尺度，因此连续极限下涨落的幅度和期望值一样大，模糊了所有经典行为。反之，三维中涨落会趋近于零，经典 (平均场) 行为应当占据主导。

Regardless of how the fluctuations behave, it turns out that the action derived from the Einstein-Hilbert action fails in reproducing the CDT results in an important way. Repeating the analysis of Bogacz et al. for three dimensions, we simply have to set $c_2 = 0$ in the previous subsection or just recall what we have said about the two-dimensional case. From (31), we then find that $\omega = 0$ and the width of the droplet diverges. However, (31) does not hold in this case, as it would violate the condition $\pi/\omega < \tau$, which is to be assumed in (30). On the other hand, we have already explained what happens in the two-dimensional case, and going to three dimensions, we simply have to replace $V_2 \to V_3$ and $\ell(t) \to V_2(t)$. The droplet solution which minimizes the action is obtained for $\omega = \pi/\tau$. However, it is easily checked that in such a case, the action is strictly positive, while for $V_2(t) = V_3/\tau$, the action vanishes. We conclude that a BIB model derived from the three-dimensional Einstein-Hilbert action would predict a constant average profile for the two-dimensional volumes. This is also supported by the numerical simulation of [70], as for $c_2 = 0$ and $c_1 > 0$, the model defined by (27) lies in the correlated fluid phase, not the droplet phase.

无论涨落行为如何，事实证明由爱因斯坦-希尔伯特作用量导出的作用量在一个重要方面无法重现 CDT 的结果。我们重复 Bogacz 等人对三维的分析，只需在上一小节中设置 $c_2 = 0$，或直接回顾我们对二维情形的讨论。接着从式 (31) 可得 $\omega = 0$ 和液滴宽度发散。但式 (31) 在此情形不成立，因为它会违反式 (30) 中需要假定的条件 $\pi/\omega < \tau$。另一方面，我们已经解释过二维情形会发生什么，推广到三维只需替换 $V_2 \to V_3$ 和 $\ell(t) \to V_2(t)$。使作用量最小化的液滴解在 $\omega = \pi/\tau$ 条件下得到。但不难验证，该情形下作用量严格为正，而 $V_2(t) = V_3/\tau$ 时作用量为零。我们的结论是，从三维爱因斯坦-希尔伯特作用量导出的 BIB 模型会预测二维体积存在恒定平均轮廓。这也得到文献 [70] 数值模拟的支持: 对于 $c_2 = 0$ 和 $c_1 > 0$，式 (27) 定义的模型处于关联流体相，而非液滴相。

We are left with the challenge of explaining the droplet condensation of three-dimensional CDT as a condensation of a BIB model. This also provides us with an extraordinary opportunity to test corrections to the effective action of [83, 95]. In higher dimensions, such corrections are expected to be subdominant with respect to the linear spatial curvature term coming from the Einstein-Hilbert action (the one multiplied by c_2 in (28)). Fortunately, however, the $d = 3$ case is an exception to this, because this linear curvature term results in an irrelevant constant term for the potential and hence drops out of the story, making higher-order corrections relevant.

我们目前面临的挑战是如何将三维 CDT 的液滴凝聚解释为 BIB 模型的凝聚。这也为我们提供了一个绝佳的机会来检验 [83, 95] 中有效作用量的修正。在更高维度中，这类修正相对于爱因斯坦-希尔伯特作用量给出的线性空间曲率项 (即式 (28) 中乘在 c_2 上的项) 而言是次要的。但幸运的是，$d = 3$ 情形是个例外: 这个线性曲率项对势只贡献一个无关的常数项，因此会从推导中消去，使得高阶修正变得重要。

In view of that, and inspired by the reasonings outlined in the introduction, as well as by the fact that there is presently no evidence for the presence of higher-order time derivatives in the effective action [89], in [45], we proposed an alternative effective theory for the spatial areas, one derived from HL gravity.

鉴于此，受引言中所述推论的启发，同时也考虑到目前没有证据表明有效作用量中存在高阶时间导数 [89]，我们在 [45] 中针对空间面积提出了一种源自 HL 引力的替代有效理论。

Starting point One sets off with the most generic, projectable, $z = 2$ action for Hořava-Lifshitz gravity in three dimensions [36]:

出发点我们从三维霍拉瓦-利夫希茨引力最一般的可投影 $z = 2$ 作用量出发 [36]:

$$S_{3\,\mathrm{d-HL}} = \frac{1}{16\pi G}\int \mathrm{d}t\, \mathrm{d}^2x \mathcal{N}\sqrt{g}\left\{\left(K_{ij}K^{ij} - \lambda K^2\right) + 2\Lambda - bR - \gamma R^2\right\}.$$

(32)

As discussed in the introduction, HL gravity describes a class of metric theories supporting a preferred foliation. Thus, the space-time diffeomorphism symmetry is broken down to foliation-preserving diffeomorphisms (Such foliation-preserving diffeomorphisms are described by time-reparameterizations and spatial diffeomor-phisms of the form:

正如引言中讨论的，HL 引力描述了一类支持优先叶状结构的度规理论。因此，时空微分同胚对称性破缺为保持叶状结构的微分同胚 (这类保持叶状结构的微分同胚由如下形式的时间重参数化和空间微分同胚描述:

$$t \to t + \xi^0(t) \quad \text{and} \quad x^i \to x^i + \xi^i(t, x), \tag{33}$$

where (t, x^i) are coordinates in an atlas of charts adapted to the foliation.).

其中 (t, x^i) 是适配该叶状结构的图集中的坐标。)。

In (32), the action is presented in terms of ADM variables: $\mathcal{N}$ is the lapse function, g is the determinant of the spatial metric, R is its Ricci scalar, K_{ij} is the extrinsic curvature associated to the leaves of the foliation, and K is its trace.

式 (32) 中的作用量用 ADM 变量表示: $\mathcal{N}$ 是时移函数，g 是空间度规的行列式，R 是空间度规的里奇标量，K_{ij} 是与叶状结构叶片关联的外曲率，K 是外曲率的迹。

The action contains the familiar parameter pair (G, Λ) , corresponding to Newton’ s constant and the cosmological constant, respectively. The parameter $\sigma = \pm 1$ neatly encapsulates some metric signature information. Meanwhile λ, b , and γ characterize the deviation from full diffeomorphism invariance. Indeed, for $\lambda = b = 1$ and $\gamma = 0$, one recovers the Einstein-Hilbert Lagrangian in Euclidean signature: $2\Lambda - \mathcal{R}$, where $\mathcal{R}$ is the spacetime Ricci tensor (Notice that we have changed the overall sign of the action with respect to [45, 46] , because in retrospective, we find the present choice more clear. Ultimately the two ways of presenting this motivational steps are equivalent as they lead to the same effective action (thanks also to the freedom we have in choosing λ in HL gravity).).

作用量包含我们熟悉的参数对 (G, Λ) ，分别对应牛顿常数和宇宙学常数。参数 $\sigma = \pm 1$ 清晰概括了度规符号的相关信息，而 λ, b 和 γ 则刻画了理论对完整微分同胚不变性的偏离。事实上，当 $\lambda = b = =1$ 且 $\gamma = 0$ 时，我们可以得到欧几里得符号下的爱因斯坦-希尔伯特拉格朗日量: $2\Lambda - \mathcal{R}$ ，其中 $\mathcal{R}$ 是时空里奇张量 (请注意，相对于 [45, 46] 我们改变了作用量的整体符号，因为我们现在认为当前的选择更清晰。最终两种表述这些动机步骤的方式是等价的，因为它们会得到相同的有效作用量——这也得益于我们在 HL 引力中选择 λ 的自由度)。

The theory is said to be projectable if one imposes at the outset that the lapse function is spatially constant: $\mathcal{N} = \mathcal{N}(t)$.

如果我们从一开始就要求时移函数在空间上是常数，即满足 $\mathcal{N} = \mathcal{N}(t)$ ，则该理论是可投影的。

The z -exponent refers to half the maximal order of spatial derivatives appearing in the action. Thus for $z = 2$, it may contain at most four spatial derivatives, permitting the inclusion of the R^2 term.

z 指数对应作用量中空间导数最大阶数的一半。因此对于 $z = 2$ ，作用量最多包含四阶空间导数，允许包含 R^2 项。

We consider spacetimes with topology $S^2 \times S^1$, that is, spherical spatial slices and a compactified time. To implement this, we impose periodic boundary conditions in time, with period τ .

我们考虑拓扑为 $S^2 \times S^1$ 的时空，也就是空间切片为球面、时间是紧致化的时空。为了实现这一点，我们对时间施加周期为 τ 的周期性边界条件。

Mini-superspace reduction We perform a minisuperspace reduction to constant lapse, vanishing shift vector (hidden so far in the extrinsic curvature) and spatial metric $g_{ij} = \phi^2(t)\,\hat{g}_{ij}$, where $\hat{g}_{ij}$ is the standard metric on the unit sphere. And in order to compare to CDT in the canonical ensemble, we replace the cosmological term as:

超空间约化我们进行超空间约化，假设时移为常数、移位矢量为零 (外曲率中至今未显式写出的部分), 空间度规取 $g_{ij} = \phi^2(t)\,\hat{g}_{ij}$ 形式，其中 $\hat{g}_{ij}$ 是单位球面上的标准度规。为了和正则系综下的 CDT 比较，我们将宇宙学项替换为:

$$\frac{2\Lambda}{16\pi G}\int \mathrm{d}t\ \mathrm{d}^2x\mathcal{N}\sqrt{g} \to \frac{2\Lambda}{16\pi G}\left(V_3 - \int \mathrm{d}t\ \mathrm{d}^2x\mathcal{N}\sqrt{g}\right), \tag{34}$$

and treat Λ as a Lagrange multiplier.

并将 Λ 当作拉格朗日乘子处理。

With a redefinition of parameters (We define:

经过参数重新定义 (我们定义:

$$\kappa^2 = \frac{NG}{1-2\lambda},\ \omega^2 = \frac{N^2\Lambda}{1-2\lambda},\ b' = -\frac{\mathcal{N}^2 b}{1-2\lambda},\ \xi = \frac{2\mathcal{N}^2\gamma}{1-2\lambda}. \tag{35}$$

the action becomes:

作用量变为:

$$S_{3\text{ d}-\text{HL}-\text{ mini}}[\phi] = \frac{1}{2\kappa^2}\int_{-\frac{\tau}{2}}^{\frac{\tau}{2}} \mathrm{d}t\left\{\dot{\phi}^2 - \omega^2\phi^2 + b' - \frac{\xi}{\phi^2}\right\}. \tag{36}$$

The remaining field $\phi(t)$ is a time-dependent scale factor determining the area of the spatial slice at time t : $V_2(t) = 4\pi\phi^2(t)$. The constant b' term is clearly irrelevant for the problem of minimization of the action, and this can be traced back to the topological nature of the R term in (32) for the projectable case.

剩余场 $\phi(t)$ 是一个依赖时间的标度因子，决定了时刻 t : $V_2(t) = 4\pi\phi^2(t)$ 空间切片的面积。常数 b' 项显然对作用量的极小化问题没有影响，这一点可以追溯到可投影情形下式 (32) 中 R 项的拓扑性质。

The good sign of the action (a positive definite kinetic term) corresponds to $\kappa^2 > 0$, i.e., $\lambda < 1/2$. However, in order to satisfy the periodic boundary conditions and to get real oscillating solutions, it turns out that one needs to take $\omega^2 > 0$ and $\xi > 0$ (i.e., an R^2 term with the bad sign), thus leading to a potential, which

is unbounded from below. Both sources of unboundedness are cured by (again CDT-inspired) constraints on the configuration space:

作用量的良好符号 (正定动能项) 对应 $\kappa^2 > 0$，即 $\lambda < 1/2$。然而，为了满足周期性边界条件并得到实振荡解，结果表明需要取 $\omega^2 > 0$ 和 $\xi > 0$ (即带有不良符号的 R^2 项)，从而得到一个下无界的势。两种无界问题都可以通过构型空间上 (同样受 CDT 启发得到) 的约束解决:

1. The unbounded ϕ^2 term is tamed by the fact that we are at fixed total volume, i.e., in the canonical ensemble. As the original Λ above, ω^2 should be treated as a Lagrange multiplier. The Euler-Lagrange equations for ϕ are unchanged, while variation with respect to the Lagrange multiplier imposes the constraint:

1. 无界的 ϕ^2 项因我们处于固定总体积即正则系综而得到约束。和上文原本的 Λ 一样，ω^2 应当被处理为拉格朗日乘子。ϕ 的欧拉-拉格朗日方程保持不变，而对拉格朗日乘子做变分会施加如下约束:

$$\mathcal{V} \equiv 4\pi N \int_{-\frac{\tau}{2}}^{\frac{\tau}{2}} \mathrm{d}t \phi^2(t) - V_3 = 0, \tag{37}$$

that is, it fixes the 3-volume, and thus there is no unboundedness problem from the sign of the ω^2 term.

也就是说，它固定了 3 维体积，因此 ω^2 项的符号不会带来无界问题。

2. The potential unboundedness stemming from the $1/\phi^2$ term is instead avoided by imposing a minimal spatial volume constraint at the outset, such as (Note that the compatibility of (37) with (38) requires $\varepsilon < \sqrt{V_3/(4\pi N\tau)}$.):

2. 源于 $1/\phi^2$ 项的势能无界问题可以通过在一开始就施加最小空间体积约束来避免，例如 (注意式 (37) 和式 (38) 相容要求 $\varepsilon < \sqrt{V_3/(4\pi N\tau)}$。):

$$\phi(t) > \varepsilon, \ \forall t. \tag{38}$$

This can be thought as a regularization of the theory, and as discussed in [45], there are possible scaling limits to safely let $\varepsilon \to 0$.

这可以被看作该理论的正则化，正如文献 [45] 中讨论的，存在能安全令 $\varepsilon \to 0$ 的标度极限。

Alternatively, we could think of the $1/\phi^2$ term in (36) as a truncation of the large- ϕ expansion of a potential that is not singular at $\phi = 0$, e.g., $1/\left(\varepsilon^2 + \phi^2\right)$.

或者，我们可以将式 (36) 中的 $1/\phi^2$ 项看作在 $\phi = 0$ 处非奇异的势的大 ϕ 展开截断，例如 $1/\left(\varepsilon^2 + \phi^2\right)$。

Note that the constant lapse $\mathcal{N}$ has been neatly hidden away in (36). This is rather innocuous in a classical setting. But in principle, it is a degree of freedom that should be integrated over in a quantum regime leading to the imposition of a Hamiltonian constraint. Following [45], we shall not consider this scenario, rather setting $\mathcal{N} = 1$ from here on. As we discussed above, that is appropriate when wishing to compare to CDT with fixed total time.

请注意，常数时移 $\mathcal{N}$ 已经被整齐地隐藏在式 (36) 中。这在经典框架中并无大碍。但原则上它是量子区域需要被积分的自由度，积分后会得到哈密顿约束。按照文献 [45]，我们不讨论这种情况，从现在开始直接设 $\mathcal{N}=1$ 。正如我们前文讨论的，当需要和固定总时间的 CDT 比较时，这种处理是合适的。

In order to rewrite, in analogy to the two- and four-dimensional cases, the effective action in terms of area of the slices, we can simply change variables to:

为了和二维、四维情形类比，用切片面积重新表述有效作用量，我们只需做变量替换得到:

$$V_2 = 4\pi\phi^2, \tag{39}$$

which comes from having assumed the slices to be 2-spheres of radius ϕ . Leaving aside the constant term and the harmonic term, which is part of the volume constraint, one can rewrite (36) as:

它源于我们假设切片是半径为 ϕ 的二维球面。撇开常数项和属于体积约束一部分的调和项不谈，我们可以将式 (36) 重写为:

$$\tilde{S}_{3\text{ d}-\text{HL}-\text{mini}}[\phi] \equiv \frac{1}{2\kappa^2}\int_{-\frac{\tau}{2}}^{\frac{\tau}{2}} \mathrm{d}t \left\{\dot{\phi}^2 - \frac{\xi}{\phi^2}\right\} = \frac{1}{2\kappa^2}\int_{-\frac{\tau}{2}}^{\frac{\tau}{2}} \mathrm{d}t \left\{\frac{1}{16\pi}\frac{\dot{V_2}^2}{V_2} - \frac{4\pi\xi}{V_2}\right\}. \tag{40}$$

BIB model and its phases The action (40) is the form of the action that can most naturally be translated into a discrete BIB model of the type (9). The obvious discretization amounts to choosing the following reduced transfer matrix:

BIB 模型及其相作用量 (40) 是最自然地转化为式 (9) 类型的离散 BIB 模型的作用量形式。直接离散化就是选取如下约化转移矩阵:

$$g\left(m_j, m_{j+1}\right) = \exp\left\{-\frac{2\left(m_{j+1}-m_j\right)^2}{m_{j+1}+m_j}b_1 + \frac{2}{m_{j+1}+m_j}b_2\right\}, \tag{41}$$

where b_1 and b_2 are parameters that can be related to the continuous ones and the factors 2 remind us that we have chosen to write in the denominators the arithmetic mean of m_j and m_{j+1} (other choices, even non-symmetric, are possible but are expected to be irrelevant in the continuum limit [70]).

其中 b_1 和 b_2 是可以和连续参数关联的参数, 因子 2 提醒我们, 我们选择在分母中写入 m_j 和 m_{j+1} 的算术平均 (其他选择，哪怕是非对称的选择也是可以的，但在连续极限中被认为是无关紧要的 [70])。

We performed Monte Carlo simulations of this BIB model in [46], and we found evidence for five phases, whose location in the (b_1, b_2) plane is illustrated in Fig. 7. Typical configurations for each phase are presented in Fig. 8, and they are characterized as follows (see [46] for more details):

我们在文献 [46] 中对该 BIB 模型做了蒙特卡洛模拟，找到了存在五个相的证据，它们在 (b_1, b_2) 平面上的位置如图 7 所示。每个相的典型构型如图 8 所示，特征如下 (更多细节参见 [46]):

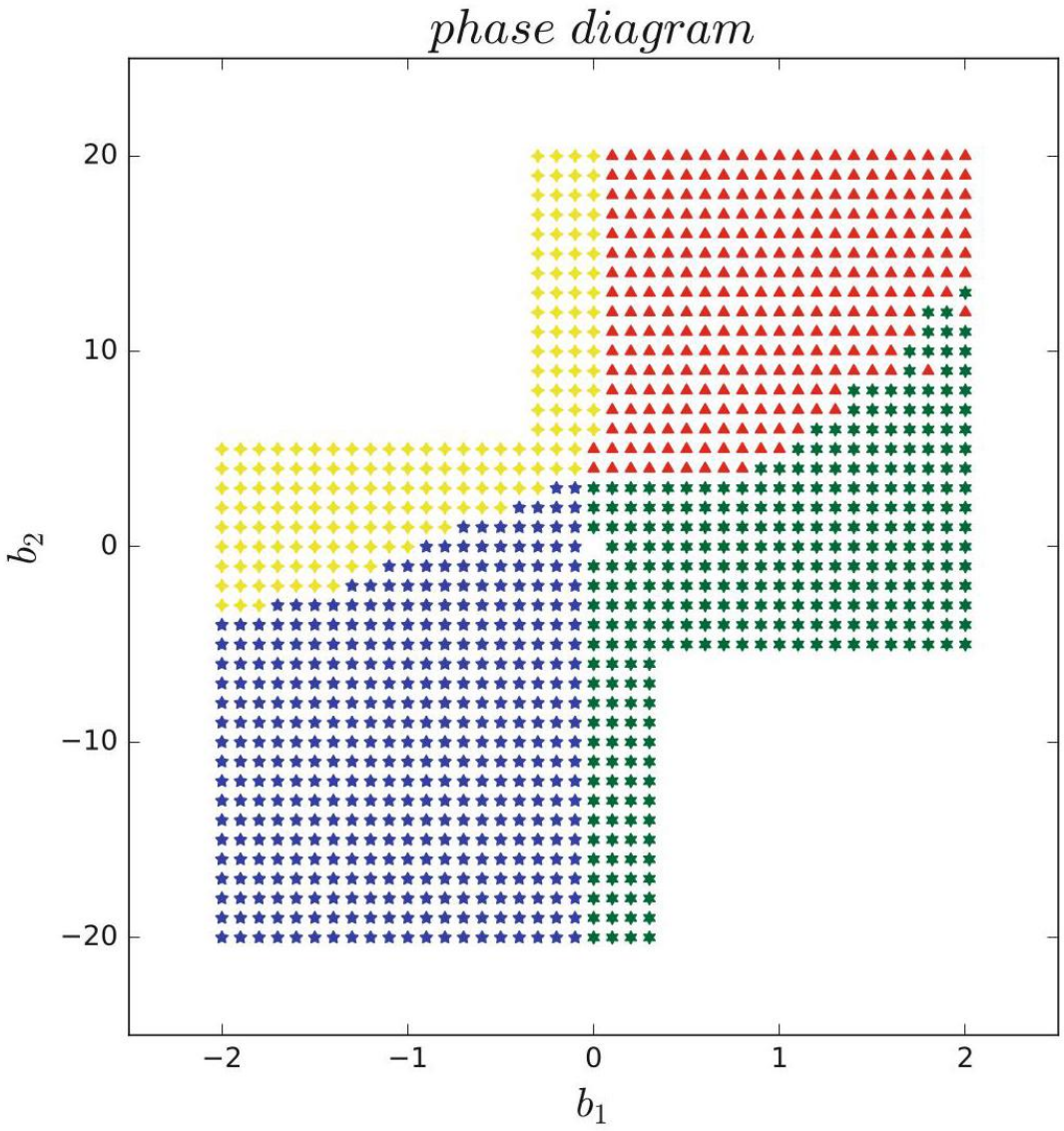

Fig. 7 Phase diagram for the BIB model with reduced transfer matrix (41), with $T = 80$ and $M = 4000$: droplet (red triangles), localized (yellow squares), antiferromagnetic (blue pentagons), correlated fluid (green hexagons), and uncorrelated fluid (origin)

图 7 采用约化传递矩阵 (41) 的 BIB 模型相图，其中 $T = 80$ 和 $M = 4000$: 液滴相 (红色三角形)、定域相 (黄色正方形)、反铁磁相 (蓝色五边形)、关联流体相 (绿色六边形)、非关联流体相 (原点)

- Droplet phase: This phase occurs for $b_1 > 0, b_2 > b_{2,\,\mathrm{crit}}\,(b_1)$. For a typical configuration, the majority of volume condenses onto a contiguous subset of time slices of width greater than one. The remainder of the volume forms a stalk with each constituent time slice possessing minimal volume.

- 液滴相: 该相出现在 $b_1 > 0, b_2 > b_{2,\,\mathrm{crit}}\,(b_1)$ 处。典型构型中，大部分体积凝聚在宽度大于 1 的连续时间切片子集上，剩余体积形成一个柄，每个组成时间切片仅拥有最小体积。

- Localized phase: This phase exists for $b_1 < 0, b_2 > b_{2,\,\mathrm{crit}}\,(b_1)$. For a typical configuration, all volume resides on one time slice, while all other times possess minimal volume.

- 定域相: 该相存在于 $b_1 < 0, b_2 > b_{2,\,\mathrm{crit}}\,(b_1)$ 处。典型构型中，所有体积都集中在一个时间切片上，其余所有时间切片仅拥有最小体积。

- Antiferromagnetic fluid phase: This phase exists for $b_1 < 0, b_2 < b_{2,\,\mathrm{crit}}\,(b_1)$. A typical configuration consists of alternating peaks and troughs, where the troughs possess minimal volume.

- 反铁磁流体相: 该相存在于 $b_1 < 0, b_2 < b_{2,\,\mathrm{crit}}\,(b_1)$ 处。典型构型由交替的峰和谷构成，其中谷仅拥有最小体积。

- Correlated fluid phase: This phase exists for $b_1 > 0, b_2 < b_{2,\,\mathrm{crit}}\,(b_1)$. A typical configuration consists of the volume approximately evenly allotted to the time slices, with relatively small fluctuations about the mean volume.

- 关联流体相: 该相存在于 $b_1 > 0, b_2 < b_{2,\,\mathrm{crit}}\,(b_1)$ 处。典型构型中体积近似均匀分配给所有时间切片，相对于平均体积的涨落相对较小。

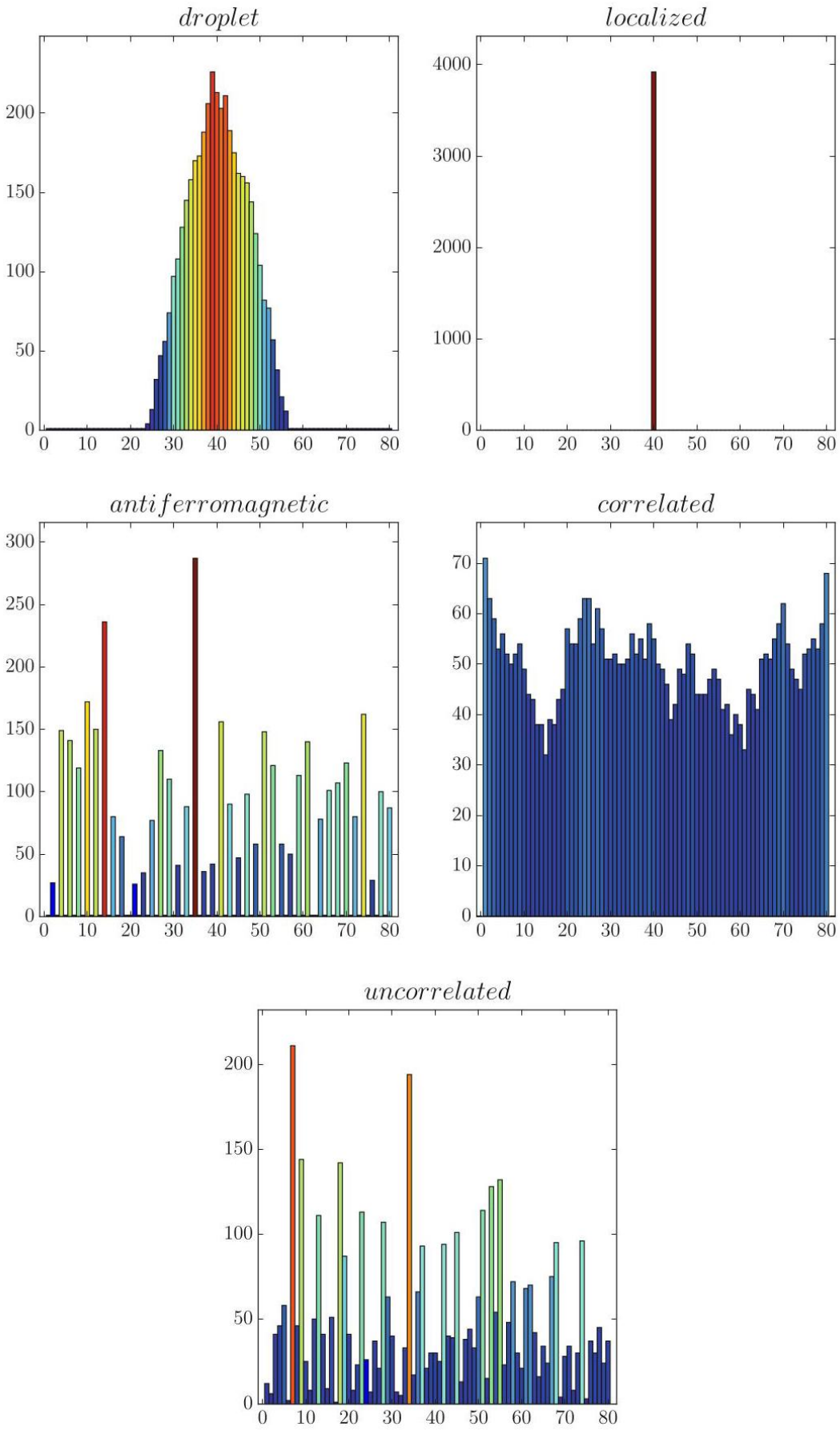
droplet
localized
antiferromagnetic
correlated
uncorrelated

Fig. 8 Typical configurations for the various phases (left-to-right): droplet, localized, antiferromagnetic, correlated fluid, uncorrelated fluid

图 8 各相的典型构型 (从左到右): 液滴相、定域相、反铁磁相、关联流体相、非关联流体相

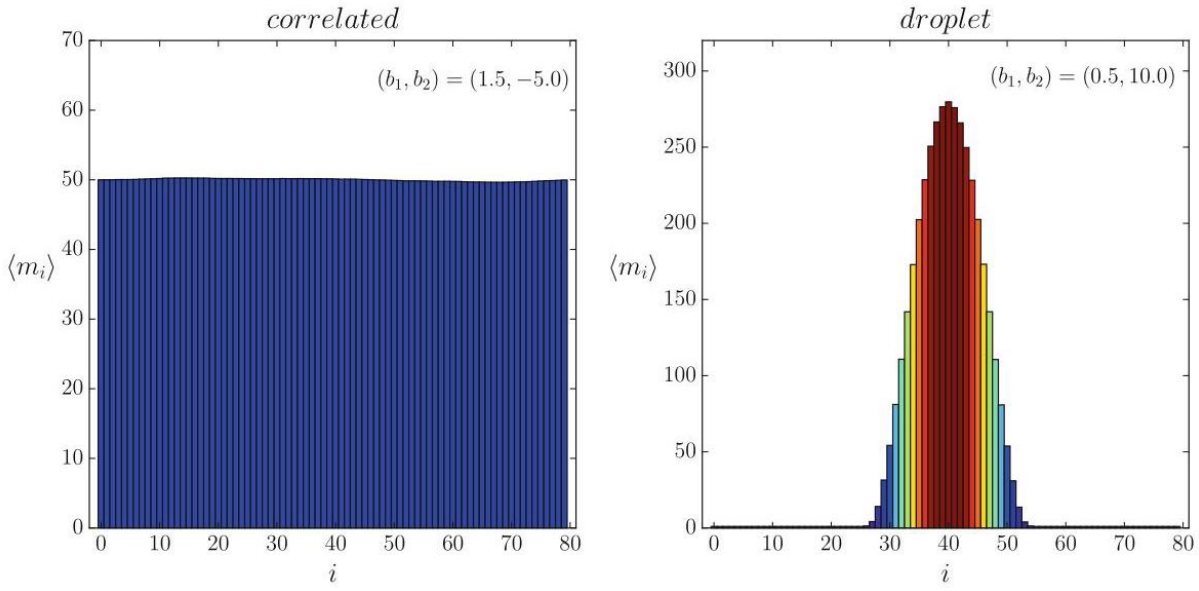

Fig. 9 Mean value $\langle m_i \rangle$ as a function of i , for non-centered samples in the correlated phase and centered samples in the droplet phase

图 9 $\langle m_i \rangle$ 的平均值随 i 变化的函数，关联相中的非中心样本与液滴相中的中心样本

- Uncorrelated fluid phase: This phase exists near the origin, i.e., for $b_1 \sim b_2 \sim 0$, and probably only at the origin in the thermodynamic limit. It is a phase dominated by the entropy of configurations rather than by the action, which indeed vanishes at the origin, where the model is easily solved [70].

- 非关联流体相: 该相存在于原点附近，即对应 $b_1 \sim b_2 \sim 0$ ，在热力学极限下可能仅存在于原点处。该相由构型熵而非作用量主导，作用量在原点处确实为零，该模型在此处可轻松求解 [70]。

Two of the phases above are akin to the two phases appearing in three-dimensional CDT, namely, the droplet and the correlated phase. Clearly the former (see its averaged profile in Fig. 9) should correspond to the droplet configuration of Fig. 5, and we will get back to their comparison below. Notice also that although the typical configuration in the correlated phase shows relatively large fluctuation at our value of M , the ensemble average in Fig. 9 shows that they neatly average to a constant configuration. The antiferromagnetic and localized phases appear at negative kinetic term, and for this reason, we will not discuss them further.

上述相中有两个与三维 CDT 中出现的两个相类似，即液滴相和关联相。显然前者 (其平均轮廓见图 9) 应当对应图 5 的液滴构型，我们将在下文回到二者的比较。另需注意，尽管在我们取的 M 值下关联相的典型构型涨落相对较大，但图 9 中的系综平均表明，这些涨落平均后恰好得到常数构型。反铁磁相和定域相出现在负动能项处，因此我们不再进一步讨论。

Analysis of the Model

模型分析

We can reverse the derivation of the BIB model and go back to the continuum, in order to look for the configurations that minimize the Landau free energy. First off, we notice that a three-dimensional interpretation of the BIB model is justified by the scaling observed in the droplet phase (see Fig. 10), which is of the same type as the scaling in the three-dimensional CDT model (see Fig. 6).

我们可以逆推 BIB 模型，回到连续统情形，寻找朗道自由能极小的构型。首先我们注意到，液滴相观测到的标度行为 (见图 10) 证明对 BIB 模型的三维诠释是合理的，该标度行为与三维 CDT 模型中的标度行为类型相同 (见图 6)。

Let us introduce a lattice spacing a and define a continuous time variable $t = aj$, with period $\tau = aT$. Furthermore, we define a continuous volume variable $V_3 = v_3 a^3 M$, as well as interpret the number of balls in a given box j as the two-dimensional volume of a slice at time t : $V_2 = v_2 a^2 m$. Here, v_2 and v_3 are two arbitrary constants, which could be related to the details of the three-dimensional building blocks of CDT.

我们引入晶格间距 a ，定义具有周期 $\tau = aT$ 的连续时间变量 $t = aj$ 。此外，我们定义连续体积变量 $V_3 = v_3 a^3 M$ ，并将给定盒子 j 中的球数诠释为时刻 t ：$V_2 = v_2 a^2 m$ 处切片的二维体积。此处 v_2 和 v_3 是两个任意常数，可能与 CDT 三维结构单元的细节有关。

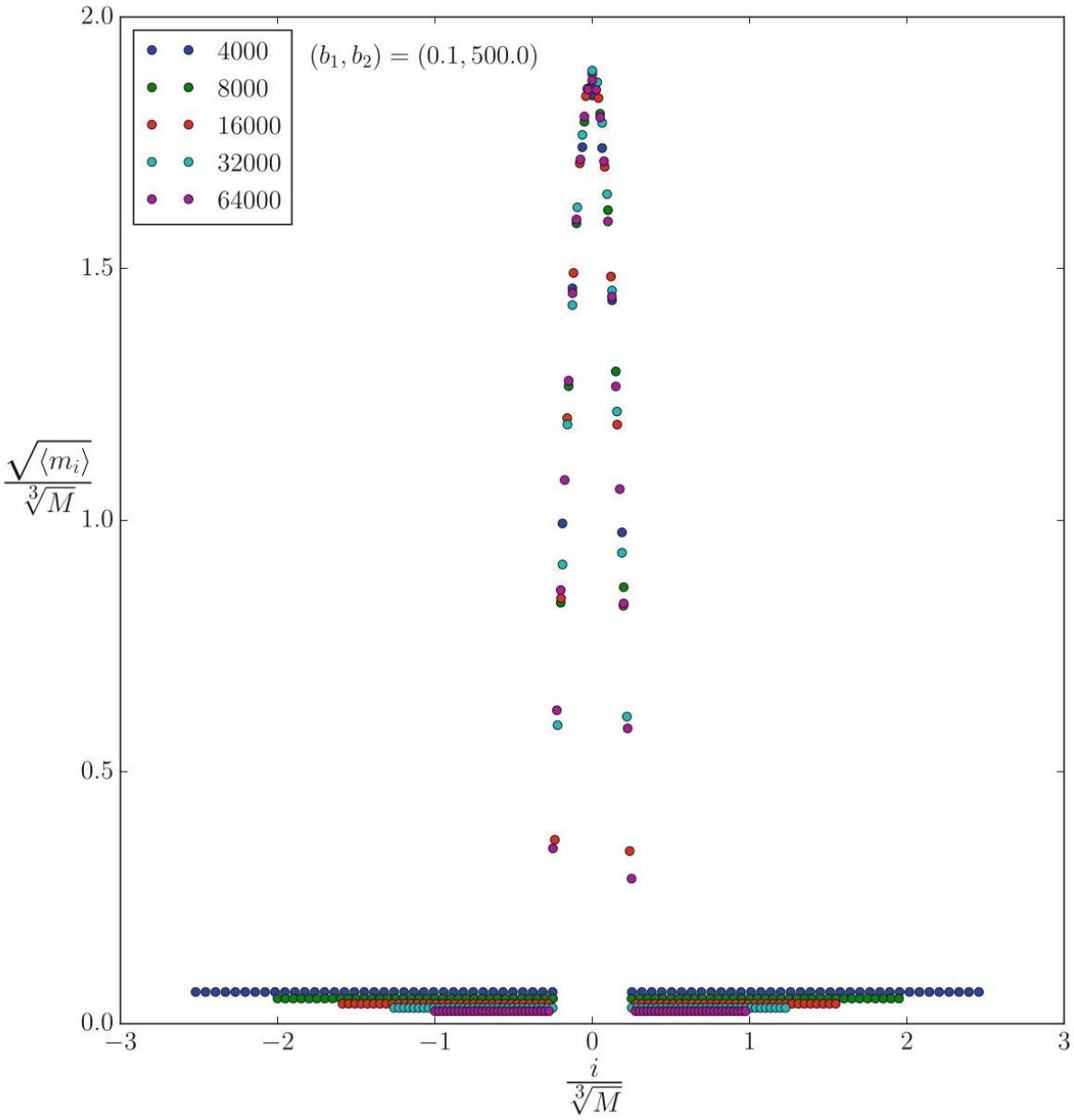

Fig. 10 Scaling of averaged droplet with respect to volume M (between 4k and 64k) at fixed $T = 80$. We notice that rescaling both $\sqrt{\langle m_i \rangle}$ and i with $\sqrt[3]{M}$, we obtain a droplet whose shape is essentially independent of M

图 10 固定 $T = 80$ 时，平均液滴相对于体积 M (介于 4k 和 64k 之间) 的标度。我们注意到，将 $\sqrt{\langle m_i \rangle}$ 和 i 都按 $\sqrt[3]{M}$ 重标度后，得到的液滴形状基本不依赖 M

In the limit $a \to 0$, with τ and V_3 fixed, the exponent in (41) becomes the action

在 $a \to 0$ 极限下，固定 τ 和 V_3 ，式 (41) 中的指数变为作用量

$$S[V_2] = \frac{1}{a} \int_0^\tau dt \left\{ \frac{b_1}{\upsilon_2} \frac{\dot{V_2}^2}{V_2} - a^2 b_2 \upsilon_2 \frac{1}{V_2} \right\}, \tag{42}$$

while the constraint on the total number of balls becomes the following volume constraint:

而总球数约束则变为如下体积约束:

$$\int_0^\tau dt V_2 = \frac{v_2}{v_3} V_3 \tag{43}$$

It is then natural to take $v_2 = v_3 \equiv v$.

此时自然可以取 $v_2 = v_3 \equiv v$ 。

The presence of the $1/a$ factor in front of the action (42) suggests that in the continuum limit, the minimization of the action should provide a trustable approach to understanding the phase diagram of the BIB model. Note that it would be wrong to discard the potential term because of the a^2 multiplying it, because V_2 itself can be of order a^2 .

作用量 (42) 前存在 $1/a$ 因子表明，在连续统极限下，作用量极小化应当是理解 BIB 模型相图的可靠方法。注意，不能因为势能项乘了 a^2 就将其舍弃，因为 V_2 本身可以是 a^2 量级。

A comparison of the actions (40) and (42) leads to the identifications:

对比作用量 (40) 和 (42)，可得到对应关系:

$$\frac{1}{32\pi\kappa^2} = \frac{b_1}{av}, \ \frac{2\pi\xi}{\kappa^2} = ab_2 v, \tag{44}$$

or:

$$\frac{b_2}{b_1} = \frac{64\pi^2\xi}{v^2 a^2}. \tag{45}$$

One can eliminate any reference to the cutoff scale a by looking only at dimensionless ratios of the parameters of the model. For example, using $va^2 m_{\min} = 4\pi\varepsilon^2$, one can write:

我们可以仅通过模型参数的无量纲比值消除所有对截断标度 a 的依赖。例如，利用 $va^2 m_{\min} = 4\pi\varepsilon^2$ ，我们可以写出:

$$\frac{v b_2}{b_1 m_{\min}} = \frac{16\pi\xi}{\varepsilon^2}. \tag{46}$$

In this way, we can translate predictions from the continuum to the discrete.

通过这种方式，我们可以将连续统的预言转换到离散情形。

For the continuum analysis, we will stick to the action in the ϕ parametrization, written as in (36) for deriving the equations of motion and as in (40) for evaluating it on-shell (the ω^2 term being part of the constraint does not contribute to the on-shell action). The equations of motion derived from (36) are of Ermakov-Pinney type, i.e.:

对于连续统分析，我们将坚持使用 ϕ 参数化的作用量: 推导运动方程时采用式 (36) 的形式，在壳计算作用量时采用式 (40) 的形式 (ω^2 项属于约束的一部分，对在壳作用量没有贡献)。由式 (36) 推导出的运动方程是埃马科夫-平尼型，即:

$$\ddot{\phi} + \omega^2 \phi - \frac{\xi}{\phi^3} = 0, \tag{47}$$

and their solution is:

其解为:

$$\phi_0(t) = \frac{1}{\omega A}\sqrt{(\omega^2 A^4 - \xi)\cos^2(\omega t + \psi) + \xi}, \tag{48}$$

where A and ψ are integration constants. Shifting the maximum of the curve to $t = 0$ fixes $\psi = 0$, and the maximal value $\phi_0(0) = A$ is then fixed by initial conditions. Meanwhile, the constraint $\mathcal{V}$ suffices to determine ω in terms of $\{V_3, A, \xi\}$. However, notice that these solutions oscillate with period $\frac{\pi}{\omega}$, and therefore in order to satisfy periodic boundary conditions at $t = \pm\tau/2, \omega$ must also satisfy $\frac{\pi}{\omega} = \frac{\tau}{n}$ for some positive integer n . As a consequence, the space of solutions forms a discrete set.

其中 A 和 ψ 是积分常数。将曲线的最大值移到 $t = 0$ 即可确定 $\psi = 0$ ，最大取值 $\phi_0(0) = A$ 则由初始条件确定。同时，利用约束 $\mathcal{V}$ 足以由 $\{V_3, A, \xi\}$ 确定 ω 。但需要注意，这些解的振荡周期为 $\frac{\pi}{\omega}$ ，因此为了满足 $t = \pm\tau/2, \omega$ 处的周期性边界条件，还必须满足 $\frac{\pi}{\omega} = \frac{\tau}{n}$ ，其中 n 为某个正整数，因此解空间构成一个离散集合。

These solutions never reach zero for $\xi > 0$. This has ramifications for the spacetime topology. In particular, it indicates the non-occurrence of potential conical singularities; rather there is a minimal throat, at which the space-time bounces.

对于 $\xi > 0$ ，这些解永远不会取零。这对时空拓扑有重要影响: 它表明不会出现潜在的锥形奇点，反而存在一个极小喉道，时空会在此处反弹。

Besides the oscillating solutions, there is also a constant solution:

除振荡解外，还存在常数解:

$$\overline{\phi}_0(t) = \sqrt{\frac{V_3}{4\pi\tau}}, \tag{49}$$

which is a special case of equation (48) with $A = \xi^{1/4}/\sqrt{\omega}$, and $\omega = 4\pi\tau\sqrt{\xi}/V_3$ fixed by the volume constraint. This solution has special significance, since in comparison to the other local extrema, it has least action (The on-shell action evaluates to:

这是方程 (48) 的特殊情况，其中 $A = \xi^{1/4}/\sqrt{\omega}$ 和 $\omega = 4\pi\tau\sqrt{\xi}/V_3$ 由体积约束固定。该解具有特殊意义，因为与其他局部极值相比，它的作用量最小 (在壳作用量的计算结果为:

$$\tilde{S}_{3\,\mathrm{d-HL-\,mini}}\left[\phi_0\right]=\frac{n\pi}{8\kappa^2}\left(\frac{nV_3}{N\tau^2}-8\sqrt{\xi}\right),$$

(50)

$$\tilde{S}_{3\,\mathrm{d-HL-mini}}\left[\overline{\phi}_0\right]=-\frac{2\pi N\tau^2\xi}{\kappa^2 V_3}.$$

$$\tilde{S}_{3\,\mathrm{d-HL-mini}}\left[\overline{\phi}_0\right]\leq\tilde{S}_{3\,\mathrm{d-HL-mini}}\left[\phi_0\right]. \tag{51}$$

However, a standard second derivative test for constrained local extrema reveals that even the constant solution might not be a stable minimum for $\xi>0$ sufficiently large. Indeed the Hessian of (36) reads

然而，对约束局部极值的标准二阶导数检验表明，当 $\xi>0$ 足够大时，即使是常数解也可能不是稳定极小值。的确，(36) 式的黑塞矩阵可写为

$$\mathcal{H}\left(t,t'\right)=\left(-\partial_t^2-\omega^2-\frac{3\xi}{\phi(t)^4}\right)\delta\left(t-t'\right), \tag{52}$$

and on the constant configuration, it is diagonalized by the Fourier basis; as the tangent space to the constraint surface (37) at the constant solution is spanned by all the non-constant Fourier modes, we simply find that the condition for such a solution to be a minimum is

且在常数构型上，它可通过傅里叶基对角化；由于常数解处约束曲面 (37) 的切空间由所有非恒定傅里叶模式张成，我们直接得到该解成为极小值的条件是

$$\left(\frac{2\pi n}{\tau}\right)^2-\omega^2-\frac{3\xi}{\overline{\phi}_0^4}=\left(\frac{2\pi n}{\tau}\right)^2-\frac{4\xi(4\pi\tau)^2}{{V_3}^2}>0, \tag{53}$$

which is violated (at least by the $n=1$ mode) as soon as $\xi>{V_3}^2/\left(16\tau^4\right)$.

只要 $\xi>{V_3}^2/\left(16\tau^4\right)$，该条件就 (至少对 $n=1$ 模式而言) 不成立。

Keeping in mind that droplet-stalk configurations are of interest to us, we notice that the solutions (48) and (49) above capture fairly well the bulk of the droplet and the stalk, respectively. Therefore, with a touch of naiveté, let us graft the two together and construct a configuration of the form:

考虑到液滴-茎构型是我们的研究兴趣，我们注意到上述解 (48) 和 (49) 分别能相当好地描述液滴主体和茎的特征。因此，我们不妨略带天真地将二者拼接起来，构造出如下形式的构型:

$$\widetilde{\phi}(t)=\begin{cases}\frac{1}{\omega A}\sqrt{\left(\omega^2A^4-\xi\right)\cos^2\left(\omega t\right)+\xi} & \text{for } t\in\left[-\frac{\pi}{2\omega},+\frac{\pi}{2\omega}\right],\\ \frac{\sqrt{\xi}}{\omega A} & \text{for } t\in\left[-\frac{\tau}{2},-\frac{\pi}{2\omega}\right)\cup\left(+\frac{\pi}{2\omega},+\frac{\tau}{2}\right],\end{cases} \tag{54}$$

where one period of a configuration of the form (48) is confined to a subinterval of length $\pi/\omega<\tau$, while a constant configuration is attached in the remainder.

其中形式为 (48) 的构型的一个周期被限制在长度为 $\pi/\omega<\tau$ 的子区间内，剩余区间连接一个常数构型。

Such configurations are unusual for at least two reasons. First, they do not in general correspond to solutions of the Euler-Lagrange equations, except in the degenerate cases $A^2 = \left(V_3 + \sqrt{V_3^2 - 16\tau^4\xi}\right)/(4\pi\tau)$, for which $\omega = \pi/\tau$, i.e., there is no stalk, and $A^2 = \xi^{1/2}/\omega = V_3/(4\pi\tau)$, for which $\widetilde{\phi} = \overline{\phi}_0$, i.e., there is no droplet. Second, they are only $C^1([-\tau/2, \tau/2])$, the second derivative being discontinuous at $t = \pm\frac{\pi}{2\omega}$. Nevertheless, we will now argue that they are relevant for the analysis of the model.

这类构型的特殊之处至少有两点。第一, 除退化情况外, 它们一般不满足欧拉-拉格朗 ange 方程: 退化情况包括 $A^2 = \left(V_3 + \sqrt{V_3^2 - 16\tau^4\xi}\right)/(4\pi\tau)$, 对应 $\omega = \pi/\tau$, 即不存在茎; 以及 $A^2 = \xi^{1/2}/\omega = V_3/(4\pi\tau)$ ，对应 $\widetilde{\phi} = \overline{\phi}_0$ ，即不存在液滴。第二，它们仅为 $C^1([-\tau/2, \tau/2])$ ，二阶导数在 $t = \pm\frac{\pi}{2\omega}$ 处不连续。尽管如此，我们接下来将论证它们对模型分析是有意义的。

Local extrema vs absolute minima The partition function of the system, in the continuum, reads:

局部极值与绝对极小值该系统在连续介质下的配分函数可写为:

$$Z_{3\text{ d}-\text{HL}-\text{ mini}} = \int_{\phi(t)>\varepsilon} \mathcal{D}\phi\,(t)\,\delta\,(\mathcal{V}) \exp\left\{-\frac{1}{2\kappa^2}\int_{-\frac{\tau}{2}}^{\frac{\tau}{2}} \mathrm{d}t\left[\dot{\phi}^2 - \frac{\xi}{\phi^2}\right]\right\}. \tag{55}$$

In the limit $\kappa \to 0$, we expect the partition function (and the observables) to be dominated by those configurations that minimize the action. Under the assumption that the space of field configurations is such that the action is at least differentiable (in the functional sense), there are two possible ways minima can arise: local extrema (i.e., solutions of the equations of motion) or minima lying on the boundary of configuration space. In the case that local extrema provide the dominant configurations for the path integral, this would imply dominance of the constant solution, because as we have seen, this has the least action among all the solutions. On the other hand, if a configuration lying on the boundary of configuration space provides an absolute minimum, then we can have a nonconstant profile. Such a possibility arises quite naturally in situations where an action unbounded from below is tamed by constraints. In our case, as we have already pointed out, the unboundedness of the action (40) at $\xi > 0$ is tamed by the constraint (38), which introduces a boundary in configuration space. Therefore, absolute minima that are not local extrema can be expected. Indeed, it was argued in [45] that this is precisely what gives rise to the droplet phase, with a profile of the form (54) dominating the partition function.

在 $\kappa \to 0$ 极限下，我们预期配分函数 (以及观测量) 由使作用量最小的构型主导。假设场构型空间满足作用量至少 (在泛函意义上) 可微，极小值的存在有两种可能情况: 局部极值 (即运动方程的解), 或位于构型空间边界上的极小值。如果局部极值是路径积分的主导构型，那么常数解将占主导，因为正如我们所见，它在所有解中作用量最小。反之，如果位于构型空间边界的构型给出绝对极小值，那么我们就能得到非恒定轮廓。当下方无界的作用量被约束限制时，这种可能性会自然出现。在我们的问题中，正如我们已经指出的，作用量 (40) 在 $\xi > 0$ 处的下方无界被约束 (38) 限制，该约束在构型空间中引入了一个边界。因此，我们可以预期存在不是局部极值的绝对极小值。的确，文献 [45] 中已经指出，这正是液滴相产生的原因，形式为 (54) 的轮廓主导了配分函数。

The rationale behind (54) is based on a balance between kinetic and potential terms in the action (created by their relative sign difference). If one looks at the kinetic term alone (at positive b_1 , i.e., κ^2), then it is obvious that the minimizing configuration is a constant one, $\dot{\phi}\,(t) = 0$. The volume constraint then fixes the value of $\phi\,(t)$ to (49). On the other hand, if one looks only at the potential term, then minimization would

seem to push to a configuration with $\phi(t) = 0$, leading to a singular value of the action, which would clearly dominate over any other configuration (as long as $\dot{\phi}(t)$ stays finite). This is of course the instability caused by the unboundedness of the action, and as already repeatedly stressed, it is cured by the constraint (38), as a consequence of which the potential actually favors the configuration $\phi(t) = \varepsilon$. In fact, the volume constraint forbids a solution with $\phi(t) = \varepsilon$ everywhere, but clearly if it were just for the potential term, a delta-function configuration $V_2(t) = \left(V_3 - 4\pi\varepsilon^2\tau\right)\delta(t - t_0) + 4\pi\varepsilon^2$ would do the job (Our choice of working with the variable ϕ rather than V_2 would not be the best in this case due to the need of taking the square root of the delta function.), i.e., a localized configuration as seen in the top right of Fig. 8, which indeed is found in particular at $b_2 > 0$ and $b_1 = 0$.

(54) 的基本原理基于作用量中动能项与势能项的平衡 (由二者的相对符号差产生)。若仅考察动能项 (当 b_1 为正，即 κ^2)，显然使作用量最小的构型是常数构型 $\dot{\phi}(t) = 0$ 。体积约束由此将 $\phi(t)$ 的值固定为 (49)。另一方面，若仅考察势能项，最小化似乎会趋向 $\phi(t) = 0$ 的构型，导致作用量出现奇异值，该奇异值显然会主导所有其他构型 (只要 $\dot{\phi}(t)$ 保持有限)。这当然是作用量无界导致的不稳定性，且正如我们反复强调的，该不稳定性由约束 (38) 解决: 在此约束下，势能实际上更偏好构型 $\phi(t) = \varepsilon$ 。事实上，体积约束禁止处处为 $\phi(t) = \varepsilon$ 的解，但显然如果只考虑势能项，δ 函数构型 $V_2(t) = \left(V_3 - 4\pi\varepsilon^2\tau\right)\delta(t - t_0) + 4\pi\varepsilon^2$ 就满足要求 (我们选择使用变量 ϕ 而非 V_2 在这种情况下不是最优选择，因为需要对 δ 函数开平方)，即如图 8 右上角所示的局域构型，这一构型确实在 $b_2 > 0$ 和 $b_1 = 0$ 处被明确观测到。

Therefore, for ε small enough, one sees a competition between the kinetic term, which favors the constant configuration, and the potential, which favors the delta-function configuration. What (54) envisages is a situation where the latter essentially wins, with the constant part being fixed at the minimal slice volume for the optimal choice of A , but with the kinetic term smoothing out the delta function, to a shape determined by local minimization of the action (Notice that for negative b_1 the kinetic term loses its smoothing effect, and we might expect the delta function configuration to dominate. This is indeed what we find in the simulations.).

因此，当 ε 足够小时，偏好常数构型的动能项与偏好 δ 函数构型的势能项之间存在竞争。(54) 所描述的场景是后者基本占据主导，常数部分固定在最小切片体积以对应 A 的最优选择，但动能项会将 δ 函数平滑化为由作用量局部极小化确定的形状 (注意当 b_1 为负时，动能项会失去平滑效果，我们可以预期 δ 函数构型将占据主导，这也确实是我们在模拟中观测到的结果。)

Phase transition The discussion above was intended to provide a simple intuition of why a configuration such as (54) might dominate the path integral, but of course one has to explicitly check whether that is the case. The presence of several parameters and the fact that (37) leads to a cubic equation for ω complicate things, and in [45], only a perturbative analysis for small ε and ξ was presented.

相变上述讨论旨在为“(54) 这类构型为何会主导路径积分”提供简单直观的解释，但显然必须对此进行明确检验。多个参数的存在以及 (37) 会导出关于 ω 的三次方程的事实让问题变得复杂，在文献 [45] 中，仅给出了小 ε 和小 ξ 下的微扰分析。

Indeed plugging (54) into (37), we find:

将 (54) 代入 (37)，我们确实得到:

$$V_3 = 4\pi\left(\frac{\pi\left(\xi + A^4\omega^2\right)}{2A^2\omega^3} + \frac{\xi}{A^2\omega^2}\left(\tau - \frac{\pi}{\omega}\right)\right), \tag{56}$$

which, multiplied by ω^3 (nonzero; otherwise we would have the constant solution again), gives us a cubic equation for ω. It is convenient to rewrite the latter in terms of ε rather than A, taking $A = \sqrt{\xi}/(\varepsilon\omega)$, because we expect the constant part to reach its minimal allowed value (from the considerations above and from the perturbative analysis of [45]). We arrive at:

将该式乘以 ω^3（ω^3 非零，否则我们又会得到常数解），即可得到关于 ω 的三次方程。在取 $A = \sqrt{\xi}/(\varepsilon\omega)$ 的条件下，用 ε 而非 A 重写该方程会更方便，因为根据前文的讨论和文献 [45] 的微扰分析，我们预期常数部分会达到其允许的最小值。由此我们得到：

$$\left(4\pi\tau\varepsilon^4 - V_3\varepsilon^2\right)\omega^3 - 2\pi^2\varepsilon^4\omega^2 + 2\pi^2\xi = 0. \tag{57}$$

Although solvable, the general solution to such an equation is not very enlightening due to the presence of several parameters. We can gain some insight with some further assumptions on the nature of the roots. The discriminant of the cubic equation is:

尽管该方程可解，但由于存在多个参数，方程的通解并不具有多少启发性。我们可以通过对根的性质做进一步假设来获得一些洞见。三次方程的判别式为：

$$-108\pi^4\xi^2\varepsilon^4\left(V_3 - 4\pi\tau\varepsilon^2\right)^2 + 64\pi^8\xi\varepsilon^{12}, \tag{58}$$

and it has the following two roots when viewed as a function of ξ:

将其视为关于 ξ 的函数时，它有如下两个根：

$$\xi_1 = 0, \text{ and } \xi_2 = \frac{16\pi^4\varepsilon^8}{27(V_3 - 4\pi\tau\varepsilon^2)^2} > 0. \tag{59}$$

For small ε and large V_3, the positive root takes a very small value, and therefore we concentrate on the case $\xi > \xi_2$. In such case, the discriminant is negative, and therefore the cubic equation has only one real root. Then we can use the representation of the real root in terms of hyperbolic functions, writing:

对于小 ε 和大 V_3，正根的取值非常小，因此我们聚焦于 $\xi > \xi_2$ 的情况。在该情况下判别式为负，因此三次方程仅有一个实根。随后我们可以用双曲函数表示这个实根，写作：

$$\omega_0 = 2\sqrt{\frac{-p}{3}}\cosh\left(\frac{1}{3}\operatorname{arcosh}\left(\frac{3q}{2p}\sqrt{-\frac{3}{p}}\right)\right) - \frac{a_2}{3a_3}, \tag{60}$$

where:

其中：

$$p = \frac{3a_3a_1 - a_2^2}{3a_3^2} = -\frac{4\pi^4\varepsilon^4}{3(V_3 - 4\pi\tau\varepsilon^2)^2}, \tag{61}$$

$$q = \frac{27a_3^2a_0 - 9a_3a_2a_1 + 2a_2^3}{27a_3^3} = \frac{16\pi^6\varepsilon^8 - 54\pi^2\xi\left(V_3 - 4\pi\tau\varepsilon^2\right)^2}{27\varepsilon^2\left(V_3 - 4\pi\tau\varepsilon^2\right)^3}, \tag{62}$$

and a_n is the coefficient of ω^n in the cubic equation (57). Furthermore, in (60), we have assumed $p < 0, q < 0$, and $4p^3 + 27q^2 > 0$, which are all valid for large enough V_3 .

且 a_n 是三次方程 (57) 中 ω^n 的系数。此外，在 (60) 中我们已假设 $p < 0, q < 0$ 和 $4p^3 + 27q^2 > 0$ ，这些假设对于足够大的 V_3 均成立。

Lastly, we take (54) with $A = \sqrt{\xi}/(\varepsilon\omega)$ and replace ω by the solution (60), to obtain a profile which is a function of ξ, V_3, τ , and ε . Denoting such configuration as $\widehat{\phi}_0(t)$, we are interested in studying:

最后，我们取含 $A = \sqrt{\xi}/(\varepsilon\omega)$ 的 (54) 式，将 ω 替换为解 (60)，得到一个关于 ξ, V_3, τ 和 ε 的轮廓。将该构型记为 $\widehat{\phi}_0(t)$ ，我们重点研究:

$$\mathcal{S} \equiv \tilde{S}_{3\,\mathrm{d-HL-mini}}\left[\overline{\phi}_0\right] - \tilde{S}_{3\,\mathrm{d-HL-mini}}\left[\widehat{\phi}_0\right] \tag{63}$$

as a function of ξ , at fixed κ^2, V_3, τ , and ε , in order to check if and when the droplet configuration (54) dominates (i.e., $\mathcal{S} > 0$).

它是固定 κ^2, V_3, τ 和 ε 下 ξ 的函数，用于检验滴构型 (54) 是否以及何时占主导 (即 $\mathcal{S} > 0$)。

More conveniently, we can re-express $\mathcal{S}$ in terms of the discrete BIB dimensionless parameters, eliminating ξ, V_3 , and τ by means of the relations:

更方便的是，我们可以利用离散 BIB 无量纲参数重新表示 $\mathcal{S}$ ，通过以下关系消去 ξ, V_3 和 τ :

$$\frac{16\pi\xi}{\varepsilon^2} = \frac{vb_2}{b_1 m_{\min}}, \tag{64}$$

$$\frac{V_3}{(4\pi\varepsilon^2)^{3/2}} = \frac{M}{m_{\min}^{3/2}v^{1/2}}, \tag{65}$$

$$\frac{\tau}{(4\pi\varepsilon^2)^{1/2}} = \frac{T}{(m_{\min}v)^{1/2}}. \tag{66}$$

One then finds that both ε and $\sqrt{v}$ factor out, so that $\mathcal{S}' \equiv \kappa^2\mathcal{S}/\left(\varepsilon\sqrt{v}\right)$ depends only on the remaining discrete parameters. In particular, for $m_{\min} = 1, \mathcal{S}'$ depends only on M, T , and the ratio b_2/b_1 .

不难发现 ε 和 $\sqrt{v}$ 均可被分离出来，因此 $\mathcal{S}' \equiv \kappa^2\mathcal{S}/\left(\varepsilon\sqrt{v}\right)$ 仅依赖于剩余的离散参数。特别地，对于 $m_{\min} = 1, \mathcal{S}'$ 而言，它仅取决于 M, T 和比率 b_2/b_1 。

We thus come to our main conclusion: for fixed M and T , the reasoning based on the minimization of the action predicts that there is a phase transition between a droplet ($\mathcal{S} > 0$) and a correlated fluid phase ($\mathcal{S} < 0$) , with the boundary between the two phases being given by a straight line in the (b_1, b_2) plane. In fact, for fixed M and $T, \mathcal{S}'$ is only a function of the ratio $\alpha \equiv b_2/b_1$, and the point at which $\mathcal{S}'(\alpha_c) = 0$ corresponds to the phase transition. Unfortunately, such an equation cannot be solved in a closed form, and we are limited to a

numerical evaluation of α_c . For example, at $M = 4000$ and $T = 80$, we find $\alpha_c = 1.5$, while at $M = 16000$ and $T = 80$, we find $\alpha_c = 7.1$. We can also check numerically that at large volume, $\alpha_c \propto M/T^3$. However, the quantitative predictions about the location of the phase transition should not be taken too seriously, because near the phase transition, we expect the fluctuations to become important and affect the transition point.

由此我们得出主要结论: 在固定 M 和 T 时, 基于作用量最小化的推导预测, 滴相 ($\mathcal{S} > 0$) 和关联流体相 ($\mathcal{S} < 0$) 之间存在相变, 两相的边界在 (b_1, b_2) 平面上为一条直线。实际上, 固定 M 时 $T, \mathcal{S}'$ 仅是比率 $\alpha \equiv b_2/b_1$ 的函数, 满足 $\mathcal{S}'(\alpha_c) = 0$ 的点对应相变点。遗憾的是, 该方程无法得到闭式解, 我们只能对 α_c 进行数值计算。例如, 在 $M = 4000$ 和 $T = 80$ 条件下, 我们得到 $\alpha_c = 1.5$; 而在 $M = 16000$ 和 $T = 80$ 条件下, 我们得到 $\alpha_c = 7.1$ 。我们还可以通过数值验证大体积下满足 $\alpha_c \propto M/T^3$ 。但我们不应过度采信关于相变位置的定量预测, 因为在相变点附近, 我们预期涨落会变得显著并影响转变点的位置。

The above results show that the droplet configuration (54) wins over the constant one in a certain range of parameters. What we have not shown is that there are no other solutions that win over both in that same range of parameters. In fact it is plausible that the actual dominant configuration is a smooth version of (54), i.e., one in which bulk and stalk are joined smoothly. However, we believe that the mechanism described above for our ansatz correctly captures the essential physical features of the problem, and this feeling is corroborated by the numerical simulations that have confirmed the existence of a droplet phase in the BIB model (9) with reduced transfer matrix (41).

上述结果表明, 在一定参数范围内, 滴构型 (54) 优于恒定构型。但我们尚未证明, 在同一参数范围内不存在比这两种构型都更优的其他解。实际上, 实际占主导地位的构型很可能是 (54) 的光滑版本, 即本体和茎秆平滑连接的构型。但我们认为, 我们上述假设所描述的机制正确抓住了该问题的核心物理特征, 这一判断也得到数值模拟的支持: 数值模拟已证实, 带有约化转移矩阵 (41) 的 BIB 模型 (9) 中确实存在滴相。

Conclusions

结论

In this chapter, we have argued that the spatial volume profile in CDT can be interpreted as a sort of coarse-grained order parameter and that its associated Landau free energy can help us understand the CDT phased diagram and the dynamics leading to it. At the same time, it can also teach us something about the continuum limit, thanks to the partially local nature of such observable. Armed with such observable, and with the Landau theory point of view in mind, we have made the case that the continuum limit of CDT is most likely described by an FPD-invariant effective field theory, as in HL-type theories.

在本章中, 我们提出 CDT 中的空间体积分布可被解释为一种粗晶化序参量, 其对应的朗道自由能可帮助我们理解 CDT 相图以及形成该相图的动力学。同时, 由于这种可观测量具有部分局域性, 它还能帮助我们研究连续极限情况。借助这一可观测量, 并结合朗道理论视角, 我们论证了 CDT 的连续极限极有可能由如 HL 型理论那样的 FPD 不变有效场论描述。

In particular, we have first reviewed the fact that in two-dimensional CDT, the Landau free energy for the spatial length is obtained exactly, and in the continuum limit, it coincides with the two-dimensional HL

gravity model. We have then argued that in order to explain the spacetime condensation phenomenon of three-dimensional CDT, reviewed in section "The Volume Data," a Landau free energy obtained as the discretization of a minisuperspace reduction of the Einstein-Hilbert action is not sufficient, as it would instead predict the dominance of a constant profile. By studying instead a Landau free energy inspired by HL gravity, proposed in [45], we have shown that a continuum semiclassical analysis leads to a condensation, captured by the dominant profile (54), compatible with the one observed in CDT. Such a semiclassical analysis is corroborated by the Monte Carlo simulations [46] of the effective BIB model, whose main results are summarized by Figs. 7 and 11. The former shows the rich phase diagram of the BIB model proposed in [45]. In particular, note the presence of a droplet phase, which however would be absent were one to set $b_2 = 0$, as in the BIB model related to minisuperspace reduction of general relativity. Figure 11 shows instead the excellent correspondence between the droplet phase of the BIB model and the CDT volume profile. Thus, we have compelling evidence that the effective dynamics of the CDT spatial slices is well captured by the BIB model (9)-(41), which in turn can be seen as a discretized path integral for a minusuperspace reduction of the Hořava-Lifshitz model (32).

具体而言，我们首先回顾了二维 CDT 中可精确得到空间长度的朗道自由能，且该自由能在连续极限下与二维 HL 引力模型一致。我们随后提出，为解释“体积数据”一节中综述的三维 CDT 时空凝聚现象，将爱因斯坦-希尔伯特作用量做超空间约化后离散化得到的朗道自由能并不充分，因为它会预测均匀分布占主导地位。转而研究由文献 [45] 提出、受 HL 引力启发得到的朗道自由能，我们发现连续半经典分析会得到凝聚现象，该现象由主导分布 (54) 捕捉，与 CDT 中观测到的结果一致。这种半经典分析得到了有效 BIB 模型的蒙特卡洛模拟 [46] 的证实，模拟的主要结果总结在图 7 和图 11 中。图 7 展示了文献 [45] 提出的 BIB 模型丰富的相图。特别需要注意液滴相的存在，若像广义相对论超空间约化对应的 BIB 模型那样设 $b_2 = 0$，液滴相就会消失。而图 11 则展示了 BIB 模型的液滴相与 CDT 体积分布之间极佳的对应关系。因此我们有充分证据表明，CDT 空间切片的有效动力学可以被 BIB 模型 (9)-(41) 很好地描述，而该模型本身可看作霍拉瓦-利夫希茨模型 (32) 超空间约化的离散路径积分。

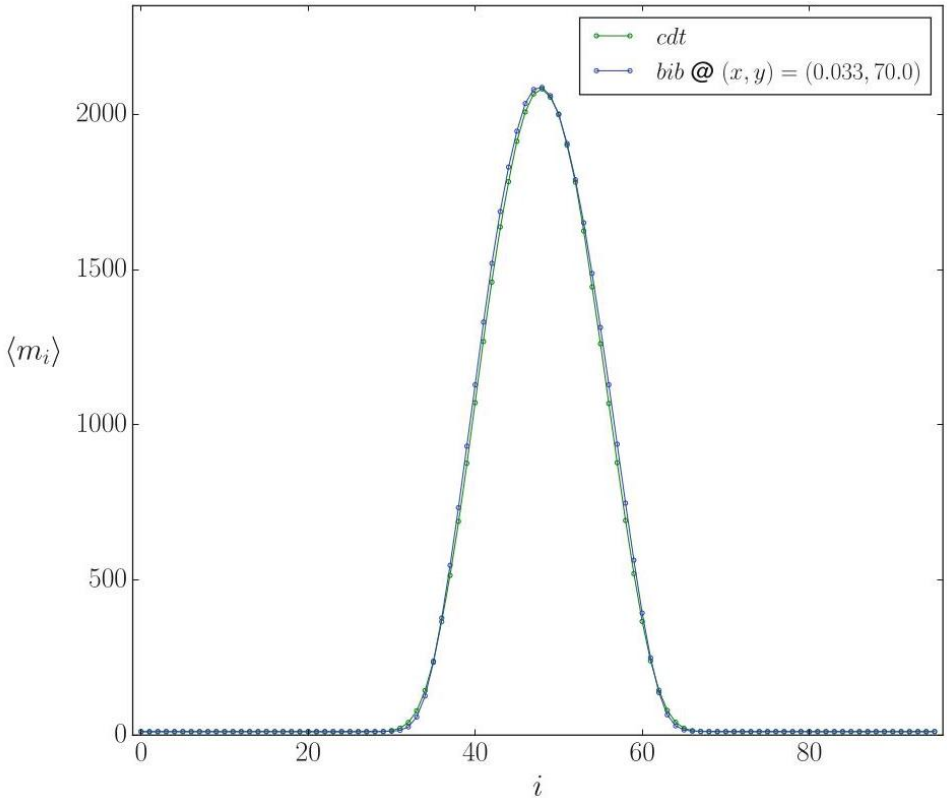

Fig. 11 Comparison of the mean volume profile from the BIB model and three-dimensional CDT

图 11 BIB 模型的平均体积分布与三维 CDT 的平均体积分布对比

As we mentioned along the course of this review, there are a number of other reasons in support of a link between CDT and HL gravity (or more generally, FPD-invariant effective field theories). It is worth to collect them here in order to summarize the status of this relation:

正如我们在本综述中提到的，有诸多其他理由支持 CDT 与 HL 引力 (或更广泛来说，FPD 不变有效场论) 之间存在关联。我们在此将这些理由汇总，以总结这一关联的研究现状:

- Presence of a foliation: This is on one hand a trivial observation, as it is a defining property of both CDT and HL gravity, and on the other a subtle one, as understanding the fate of the CDT foliation in the continuum limit is nontrivial. In particular, it is nontrivial because we have not yet identified a proper tuning toward the second-order phase transition that might lead to a continuum limit with propagating degrees of freedom (see [96, 97] for a first attempt). As a counter-argument to the importance of the foliation, a generalized CDT model with a local causality constraint but no built-in foliation was introduced in [98,99] and shown to also lead to a semiclassical droplet phase with similar properties to that of standard CDT. On the other hand, even if such generalized CDT model would turn out to be indeed in the same universality class of usual CDT, this would not tell us what is their continuum interpretation: it might well be that the FPD-invariant universality class is robust under small departures from the foliated structure at the discrete level. Moreover, as argued in the introduction, the very fact that observables that are local in time are available and are being studied in CDT is by itself a signal of a likely departure from a full-diffeomorphism invariant theory.

- 叶状结构的存在: 一方面，这是一个很直观的结论，因为叶状结构是 CDT 和 HL 引力共有的定义属性；另一方面，这一点也很微妙，因为理解连续极限下 CDT 叶状结构的最终状态并非易事。它之所以复杂，是因为我们尚未找到合适的方法调谐到可能得到带有传播自由度连续极限的二级相变 (相关初步尝试参见 [96, 97])。针对叶状结构重要性的一种反对观点指出，文献 [98, 99] 提出了一种带有局域因果约束、但不内置叶状结构的广义 CDT 模型，该模型也会得到性质与标准 CDT 相似的半经典液滴相。但另一方面，即使这种广义 CDT 模型确实和常规 CDT 属于同一个普适类，也无法说明它们的连续诠释:FPD 不变的普适类完全可以在离散层面偏离叶状结构微小变动后保持稳定性。此外，正如引言中所说，CDT 中可研究时间局域可观测量这一事实本身，就暗示它很可能偏离了完整微分同胚不变理论。

- Analogies in the phase diagram: This was discussed, for example, in [42], and it is based on the observation that a Lifshitz point is typically a tricritical point at the intersection of feromagnetic, paramagnetic, and modulated phases and that such phases, with their analog solutions in HL gravity, have a resemblance to the original three phases observed in four-dimensional CDT. While the comparison can be based on classical solutions and analogy to the Lifshitz scalar, the most concrete realization is in the kind of analysis we reviewed here: as reviewed in section "Three-Dimensional CDT," the BIB model based on HL gravity leads to the phase diagram of Fig. 7, which at $b_1 > 0$ matches the phase diagram of CDT. A similar result holds also in four dimensions [70]: in this case, no higher-order terms in the curvature are used; nevertheless, the fact that the coefficients of the kinetic and potential terms are tuned independently in order to reach the different phases suggests again a relation to HL gravity, as the ratio between the two would instead be fixed in the Einstein-Hilbert action. However, the four-dimensional picture was perturbed by the discovery of a new "bifurcation" phase in CDT [93, 94], which depends on peculiar properties of the three-dimensional slices. Such phase has no analogue in the BIB model, which is not surprising as it is due to a change in the internal structure of the three-dimensional slices, which cannot be captured by the spatial volume alone. In other words, it requires another order parameter in order to be identified. It has also been suggested that the appearance of the bifurcation phase might not be described by a conventional Landau-type phase transition [97]. This is one more reason why we have focused here on three-dimensional CDT, where no analogue of the bifurcation phase is found.

- 相图中的类比: 例如文献 [42] 已对此进行讨论，其基于以下观测: 利夫希茨点通常是铁磁相、顺磁相和调制相相交的三临界点，且这些相在 HL 引力中的类比解与四维 CDT 中观测到的原始三相位相似。虽然这种比较可以基于经典解与利夫希茨标量的类比，但最具体的实现正是本文回顾的这类分析: 正如“三维 CDT”一节所述，基于 HL 引力的 BIB 模型得到了图 7 的相图，该相图在 $b_1 > 0$ 与 CDT 的相图一致。类似结论也存在于四维情形 [70]: 该情形中没有使用曲率的高阶项；尽管如此，为得到不同相，动力学项和势能项的系数需要独立调谐，这一事实再次表明它与 HL 引力有关，因为二者的比值在爱因斯坦-希尔伯特作用量中是固定的。然而，四维图景因 CDT 中新发现的“分岔”相 [93, 94] 被改变，该相依于三维切片的特殊性质。这种相在 BIB 模型中没有对应，这并不奇怪，因为它源于三维切片内部结构的变化，仅靠空间体积无法捕捉。换句话说，识别它需要另一个序参量。也有观点认为分岔相的出现无法用常规朗道型相变描述 [97]。这是本文聚焦三维 CDT 的另一个原因，三维 CDT 中尚未发现分岔相的对应。

- Short-scale spectral dimension: The fact that in the droplet phase of CDT the spectral dimension matches the classical value at (not too) large scales and decreases at short scales [100] was shown to be repro-

duced by HL gravity in [40]. However, several other approaches to quantum gravity claimed a similar result (e.g., in asymptotic safety [101]), thus weakening this point of contact. On the other hand, in [41], it was pointed out that in three dimensions, asymptotic safety and HL gravity give different predictions, and numerical evidence was produced in CDT favoring the HL scenario over the asymptotic safety one.

- 小尺度谱维:CDT 液滴相中的谱维在 (不太小的) 大尺度上与经典值一致，在小尺度上减小 [100]，文献 [40] 已证明 HL 引力可以重现这一结果。但其他多个量子引力研究方法也得到了类似结论 (例如渐近安全情形 [101])，这削弱了该关联的说服力。另一方面，文献 [41] 指出，三维情形下渐近安全和 HL 引力给出的预测不同，且 CDT 中的数值证据更支持 HL 场景而非渐近安全场景。

- Large-scale geometry: In [41] it was also observed that the behavior of the spectral dimension at large scales, where it decays due to the compactness of spacetime, is better fitted by a stretched sphere geometry, rather than a round sphere. And the former is a solution to HL gravity.

- 大尺度几何: 文献 [41] 还观测到，由于时空的紧致性，谱维在大尺度上会衰减，其行为用拉伸球面几何比正圆形球面拟合效果更好，而前者正是 HL 引力的一个解。

- Absence of conformal factor problem: As we discussed in section "Effective Models," the effective actions controlling the dynamics of the spatial volumes in CDT in $d = 3$ and 4 have a kinetic term with the good sign, that is, there is no conformal sickness. While perhaps this could be interpreted as being due to non-perturbative contributions from the functional measure, as suggested in [35], it might also have the much simpler explanation that in HL gravity, the conformal factor problem can be avoided by an appropriate choice of the coupling t in (32). More investigations are probably needed in order to decide between the two scenarios, but one should keep in mind that if nonperturbative contributions could change the sign of the kinetic term for the conformal mode with respect to usual Euclidean quantum gravity [91], then either they would also spoil the good sign of the graviton term in the latter or they would be hard to reconcile with general covariance of the theory, as the relative sign between conformal and graviton terms is fixed by full-diffeomorphism invariance. Unfortunately no results are available in CDT about a possible graviton effective action, but the possibility that only the conformal factor's sign is changed with respect to usual Euclidean quantum gravity is corroborated by the results from three-dimensional CDT with toroidal slices [43], according to which both the conformal factor and the moduli have the good sign.

- 不存在共形因子问题: 正如我们在“有效模型”一节中讨论的，CDT 中 $d = 3$ 维和 4 维空间体积动力学所对应的有效作用量具有符号正确的动能项，也就是说不存在共形病态。这一点或许可以像文献 [35] 指出的那样，解释为泛函测度的非微扰贡献所致，但也存在更简单的解释: 在 Horava-Lifshitz 引力中，通过适当选取 (32) 式中的耦合常数 t 即可避开共形因子问题。要在两种解释间做出判断或许还需要更多研究，但我们需要记住: 如果说和常规欧几里得量子引力 [91] 相比，非微扰贡献能够改变共形模式动能项的符号，那么它们要么也会破坏常规欧几里得量子引力中引力子项的正确符号，要么就很难和理论的广义协变性相容——因为共形项和引力子项的相对符号是由完整微分同胚不变性固定的。遗憾的是，目前 CDT 中尚未得到关于可能存在的引力子有效作用量的相关结果，但带环面切片的三维 CDT 研究结果 [43] 确实支持了下述观点: 即仅共形因子的符号相对于常规欧几里得量子引力发生了改变，该结果表明共形因子和模空间的符号都是正确的。

- Potential versus higher-derivatives: Results from [89] indicate that in four-dimensional CDT, higher-order time derivatives in the effective action are sub-leading with respect to potential terms, which in a full action would correspond to higher-order spatial derivatives. This is suggestive again of an anisotropy.

  - 势能项与高阶导数: 文献 [89] 的结果表明，在四维 CDT 中，有效作用量的时间高阶导数相对于势能项是次导的，而在完整作用量中，势能项对应空间高阶导数。这再次暗示存在各向异性。

- Exact relation in two dimensions: Lastly, two-dimensional CDT is exactly solvable, and in the continuum limit, it reproduces HL gravity, as reviewed in section "Landau Theory of Two-Dimensional CDT" and more in detail in [77]. As there is currently no hint of a possible peculiarity of two dimensions when it comes to the CDT foliation (There is of course a difference in the HL action leading to a renormalizable theory, but this is irrelevant for an effective field theory argument.), this makes a strong plausibility argument for a relation between CDT and HL gravity also in higher dimensions.

  - 二维空间中的精确关系: 最后，二维 CDT 是可精确求解的，且在连续极限下它重现了 HL 引力，相关内容已在“二维 CDT 的朗道理论”一节中综述，文献 [77] 中有更详细的讨论。目前没有证据表明，在 CDT 分层中二维情况存在任何特殊性质 (当然，HL 作用量在二维存在差异，它能得到可重整化理论，但这对有效场论论证无关紧要)，这有力地表明，即使在更高维度，CDT 和 HL 引力之间也存在关联。

Clearly understanding the nonperturbative dynamics and continuum limit of a statistical model of higher-dimensional random geometries such as CDT is a very challenging task, which explains why many of the points above are still inconclusive and at a conjectural stage. However, we find that the while perhaps none of the arguments in support of a FPD-invariant effective field theory is conclusive in itself, the list of arguments is sufficiently long and varied, so that a different interpretation in terms of a fully diffeomorphism-invariant effective field theory would look as a lucky conspiracy.

要清晰理解 CDT 这类高维随机几何统计模型的非微扰动力学与连续极限是一项极具挑战性的任务，这也解释了为何上述许多观点至今尚无定论，仍处于猜想阶段。但我们发现，尽管支持 FPD 不变有效场论的每一个论证本身都不是结论性的，这些论证的数量足够多、覆盖范围足够广，若用完全微分同胚不变的有效场论来做另一种解释，反倒会显得是一种巧合。

It should be stressed that clearly CDT in its usual definition has less couplings than renormalizable HL gravity models in three or four dimensions. Therefore, such renormalizable models are probably not directly relevant for comparisons to CDT, unless one extends the latter with appropriate new terms in the action, as done in [47]. However, as we argued in the introduction and in section "Landau Theory of Two-Dimensional CDT," the fact that one starts in CDT with a discretization of the Einstein-Hilbert action (And moreover we remark again that in four dimensions the CDT action has one more coupling than the Einstein-Hilbert action.) does not imply that its symmetries will be preserved. The crucial point, on which we focused in this review by indirect means, is to assess in which theory space a renormalization group flow of CDT will lead us, or in other words what is the effective field theory of CDT. Once that is established, only in a second step we will be able to worry about how to take the continuum limit with propagating degrees of freedom corresponding to our desired target theory. It is at this step that the fact that CDT has only few tunable parameters might turn out to be a limitation. At present, the two competing scenarios that can serve as justification for a program

like CDT are asymptotic safety and HL gravity. While the latter is based on a Gaussian fixed point, and so it is straightforward to count the number of its relevant couplings (It is instead not so straightforward to study its renormalization group flow [102-105].), the former is based on a conjectural non-Gaussian fixed point, and we do not even know for sure if the number of relevant couplings is finite (except in special simple approximations [106,107]). However, all evidence so far suggests that if such a nontrivial fixed point exists, then it has at least three relevant perturbations, which include higher-order curvature terms [108-110]. Therefore, continuum scenarios and their results suggest that at some point one might need to introduce more couplings in CDT.

需要强调的是，通常定义下的 CDT，其耦合数量确实少于三维或四维可重整化 HL 引力模型。因此这类可重整化模型可能无法直接和 CDT 对比，除非人们像文献 [47] 所做的那样，通过在作用量中引入合适的新项来扩展 CDT。但正如我们在引言和“二维 CDT 的朗道理论”一节中所言，CDT 从爱因斯坦-希尔伯特作用量离散化出发 (此外我们再次指出，四维 CDT 的作用量比爱因斯坦-希尔伯特作用量多一个耦合)，这一事实并不意味着其对称性会得到保留。我们在本综述中通过间接方法重点讨论的核心问题是，判断 CDT 的重整化群流会将我们引向哪个理论空间，换句话说，CDT 的有效场论究竟是什么。确定这一点之后，我们才需要在第二步考虑如何得到带有符合我们目标理论的传播自由度的连续极限。恰恰是在这一步，CDT 仅含少量可调参数的特点可能会成为一种局限。目前，能够为 CDT 这类研究纲领提供支撑的两种竞争方案是渐近安全和 HL 引力。后者基于高斯不动点，因此其相关耦合的数量很容易计数 (但研究它的重整化群流却没那么简单 [102-105])，前者基于猜想中的非高斯不动点，我们甚至无法确定其相关耦合的数量是否有限 (特殊简单近似下除外 [106,107])。但迄今为止所有证据都表明，如果这种非平凡不动点确实存在，那么它至少有三个相关微扰，其中包含高阶曲率项 [108-110]。因此，连续场情形的各类方案和结果都表明，未来或许需要在 CDT 中引入更多耦合。

Lastly, we stress again that if indeed the effective field theory of CDT turns out to be a FPD-invariant one, this does not exclude the existence of a subspace of its theory space, which is invariant under full diffeomorphisms. In other words, one might hope to embed asymptotically safe Euclidean gravity in the HL theory space. Reaching such subspace would probably require again a very delicate fine-tuning of several breaking terms, yet perhaps in a less dramatic way than a full breaking of diffeomorphism invariance requires, as in the functional renormalization group approach to asymptotic safety.

最后，我们再次强调，如果 CDT 的有效场论确实是 FPD 不变的，这并不排除其理论空间中存在一个对完整微分同胚不变的子空间。换句话说，我们有望将渐近安全欧几里得引力嵌入 HL 理论空间。要到达这个子空间，可能仍然需要对多个破缺项进行非常精细的调参，但调参难度或许比渐近安全函数重整化群方法中完全破缺微分同胚不变性的要求要低。

Cross-References

交叉引用

CDT and Hořava-Lifshitz QG in Two Dimensions

二维中的因果动态三角剖分与霍拉瓦-里夫希茨量子引力

Hořava Models as Palladium of Unitarity and Renormalizability in Quantum Gravity

作为量子引力中幺正性与可重整性保障的霍拉瓦模型

- Lessons from the Mathematics of Two-Dimensional Euclidean Quantum Gravity

  - 二维欧几里得量子引力的数学启示

- The Causality Road from Dynamical Triangulations to Quantum Gravity That Describes Our Universe

  - 从动力学三角剖分到描述我们宇宙的量子引力的因果性之路

The Functional Renormalization Group in Quantum Gravity

量子引力中的函数重整化群

Acknowledgments I would like to thank Joe Henson and James Ryan for the precious collaboration on the work reviewed here. I also thank Jan Ambjorn and Renate Loll for the invitation to contribute a chapter to the CDT section of the Handbook of Quantum Gravity and in particular Jan Ambjorn for useful feedback on the draft.

致谢感谢 Joe Henson 与 James Ryan 对本文所评述工作的珍贵合作。感谢 Jan Ambjorn 与 Renate Loll 邀请我为《量子引力手册》的因果动态三角剖分部分撰稿，尤其感谢 Jan Ambjorn 对草稿给出的宝贵反馈。

References

参考文献

1. M. Aizenman, H. Duminil-Copin, Marginal triviality of the scaling limits of critical 4D Ising and ϕ^4_4 models. Ann. Math. 194(1), 163 (2021). http://arxiv.org/abs/1912.07973, arXiv:1912.07973

2. S. Weinberg, Ultraviolet divergences in quantum theories of gravitation, in General Relativity: An Einstein Centenary Survey, eds. by S.W. Hawking, W. Israel (Cambridge University Press, Cambridge, UK, 1979)

3. M. Niedermaier, M. Reuter, The asymptotic safety scenario in quantum gravity. Living Rev. Rel. 9, 5-173 (2006)

4. A. Bonanno, A. Eichhorn, H. Gies, J.M. Pawlowski, R. Percacci, M. Reuter, F. Saueressig, G.P. Vacca, Critical reflections on asymptotically safe gravity. Front. Phys. 8, 269 (2020). http://arxiv.org/abs/2004.06810, arXiv:2004.06810

5. J. Ambjørn, B. Durhuus, T. Jonsson, Quantum Geometry: A Statistical Field Theory Approach. Cambridge Monographs on Mathematical Physics (Cambridge University Press, Cambridge, UK, 2005), p. 12

6. T. Regge, General relativity without coordinates. Nuovo Cim. 19, 558-571 (1961)

7. F. David, Planar diagrams, two-dimensional lattice gravity and surface models. Nucl. Phys. B 257, 45 (1985)

8. J. Ambjorn, B. Durhuus, J. Frohlich, Diseases of triangulated random surface models, and possible cures. Nucl. Phys. B 257, 433-449 (1985)

9. V.A. Kazakov, A.A. Migdal, I.K. Kostov, Critical properties of randomly triangulated planar random surfaces. Phys. Lett. B 157, 295-300 (1985)

10. P. Di Francesco, P.H. Ginsparg, J. Zinn-Justin, 2 - D gravity and random matrices. Phys. Rept. 254, 1-133 (1995). http://arxiv.org/abs/hep-th/9306153, hep-th/9306153

11. T. Budd, Lessons from the mathematics of two-dimensional euclidean quantum gravity, in Handbook of Quantum Gravity, eds. by C. Bambi, L. Modesto, I. Shapiro (Springer, Singapore, 2024). http://arxiv.org/abs/2212.03031, arXiv:2212.03031

12. B.V. de Bakker, Further evidence that the transition of 4-D dynamical triangulation is first order. Phys. Lett. B 389, 238-242 (1996). http://arxiv.org/abs/hep-lat/9603024, hep-lat/9603024

13. P. Bialas, Z. Burda, A. Krzywicki, B. Petersson, Focusing on the fixed point of 4-D simplicial gravity. Nucl. Phys. B 472, 293-308 (1996). http://arxiv.org/abs/hep-lat/9601024, hep-lat/9601024

14. J. Ambjorn, J. Jurkiewicz, Scaling in four-dimensional quantum gravity. Nucl. Phys. B 451, 643-676 (1995). http://arxiv.org/abs/hep-th/9503006, hep-th/9503006

15. V. Bonzom, R. Gurau, A. Riello, V. Rivasseau, Critical behavior of colored tensor models in the large N limit. Nucl. Phys. B 853, 174-195 (2011). http://arxiv.org/abs/1105.3122, arXiv:1105.3122

16. R. Gurau, Random Tensors (Oxford University Press, Oxford, 2016)

17. J. Laiho, D. Coumbe, Evidence for asymptotic safety from lattice quantum gravity. Phys. Rev. Lett. 107, 161301 (2011). http://arxiv.org/abs/1104.5505, arXiv:1104.5505

18. D. Benedetti, R. Gurau, Phase transition in dually weighted colored tensor models. Nucl. Phys. B 855, 420-437 (2012). http://arxiv.org/abs/1108.5389, arXiv:1108.5389

19. R. Gurau, J.P. Ryan, Melons are branched polymers. Ann. Henri Poincare 15(11), 2085-2131 (2014). http://arxiv.org/abs/1302.4386, arXiv:1302.4386

20. V. Bonzom, Large N limits in tensor models: towards more universality classes of colored triangulations in dimension $d \geq 2$. SIGMA 12,073 (2016). http://arxiv.org/abs/1603.03570, arXiv:1603.03570

21. J. Ambjorn, L. Glaser, A. Goerlich, J. Jurkiewicz, Euclidian 4d quantum gravity with a nontrivial measure term. JHEP 10, 100 (2013). http://arxiv.org/abs/1307.2270, arXiv:1307.2270

22. D. Coumbe, J. Laiho, Exploring Euclidean dynamical triangulations with a non-trivial measure term. JHEP 04, 028 (2015). http://arxiv.org/abs/1401.3299, arXiv:1401.3299

23. J. Laiho, S. Bassler, D. Coumbe, D. Du, J.T. Neelakanta, Lattice quantum gravity and asymptotic safety. Phys. Rev. D 96(6), 064015 (2017). http://arxiv.org/abs/1604.02745, arXiv:1604.02745

24. J. Ambjorn, R. Loll, Nonperturbative Lorentzian quantum gravity, causality and topology change. Nucl. Phys. B 536, 407-434 (1998). http://arxiv.org/abs/hep-th/9805108, hep-th/9805108

25. J. Ambjorn, J. Jurkiewicz, R. Loll, Dynamically triangulating Lorentzian quantum gravity. Nucl. Phys. B 610, 347-382 (2001). http://arxiv.org/abs/hep-th/0105267, hep-th/0105267

26. J. Ambjorn, J. Jurkiewicz, R. Loll, Reconstructing the Universe. Phys. Rev. D 72, 064014 (2005). http://arxiv.org/abs/hep-th/0505154, hep-th/0505154

27. M. Visser, How to Wick rotate generic curved spacetime. http://arxiv.org/abs/1702.05572, arXiv:1702.05572

28. A. Baldazzi, R. Percacci, V. Skrinjar, Wicked metrics. Class. Quant. Grav. 36(10), 105008 (2019). http://arxiv.org/abs/1811.03369, arXiv:1811.03369

29. J. Ambjorn, S. Jordan, J. Jurkiewicz, R. Loll, Second- and first-order phase transitions in CDT. Phys. Rev. D 85, 124044 (2012). http://arxiv.org/abs/1205.1229, arXiv:1205.1229

30. J. Ambjorn, A. Goerlich, J. Jurkiewicz, R. Loll, Nonperturbative quantum gravity. Phys. Rept. 519, 127-210 (2012). http://arxiv.org/abs/1203.3591, arXiv:1203.3591

31. R. Loll, Quantum gravity from causal dynamical triangulations: a review. Class. Quant. Grav. 37(1), 013002 (2020). http://arxiv.org/abs/1905.08669, arXiv:1905.08669

32. C. Rovelli, What is observable in classical and quantum gravity?. Class. Quant. Grav. 8, 297- 316 (1991)

33. S.B. Giddings, D. Marolf, J.B. Hartle, Observables in effective gravity. Phys. Rev. D 74, 064018 (2006). http://arxiv.org/abs/hep-th/0512200, hep-th/0512200

34. J. Ambjorn, J. Jurkiewicz, R. Loll, Semiclassical universe from first principles. Phys. Lett. B 607, 205-213 (2005). http://arxiv.org/abs/hep-th/0411152, hep-th/0411152

35. A. Dasgupta, R. Loll, A proper time cure for the conformal sickness in quantum gravity. Nucl. Phys. B 606, 357-379 (2001). http://arxiv.org/abs/hep-th/0103186, hep-th/0103186

36. P. Horava, Membranes at quantum criticality. JHEP 03, 020 (2009). http://arxiv.org/abs/0812.4287, arXiv:0812.4287

37. P. Horava, Quantum gravity at a Lifshitz point. Phys. Rev. D 79, 084008 (2009). http://arxiv.org/abs/0901.3775, arXiv:0901.3775

38. A. Wang, Hořava gravity at a Lifshitz point: a progress report. Int. J. Mod. Phys. D 26(07), 1730014 (2017). http://arxiv.org/abs/1701.06087, arXiv:1701.06087

39. C.F. Steinwachs, Towards a unitary, renormalizable and ultraviolet-complete quantum theory of gravity. Front. Phys. 8, 4 (2020). http://arxiv.org/abs/2004.07842, arXiv:2004.07842

40. P. Horava, Spectral dimension of the Universe in quantum gravity at a Lifshitz point. Phys. Rev. Lett. 102, 161301 (2009). http://arxiv.org/abs/0902.3657, arXiv:0902.3657

41. D. Benedetti, J. Henson, Spectral geometry as a probe of quantum spacetime. Phys. Rev. D 80, 124036 (2009). http://arxiv.org/abs/0911.0401, arXiv:0911.0401

42. J. Ambjorn, A. Gorlich, S. Jordan, J. Jurkiewicz, R. Loll, CDT meets Horava-Lifshitz gravity. Phys. Lett. B 690, 413-419 (2010). http://arxiv.org/abs/1002.3298, arXiv:1002.3298

43. T.G. Budd, The effective kinetic term in CDT. J. Phys. Conf. Ser. 36, 012038 (2012). http:// arxiv.org/abs/1110.5158, arXiv:1110.5158

44. J. Ambjørn, L. Glaser, Y. Sato, Y. Watabiki, 2d CDT is 2d Hořava-Lifshitz quantum gravity. Phys. Lett. B 722, 172-175 (2013). http://arxiv.org/abs/1302.6359, arXiv:1302.6359

45. D. Benedetti, J. Henson, Spacetime condensation in (2+1)-dimensional CDT from a Hořava-Lifshitz minisuperspace model. Class. Quant. Grav. 32(21), 215007 (2015). http:// arxiv.org/abs/1410.0845, arXiv:1410.0845

46. D. Benedetti, J.P. Ryan, Capturing the phase diagram of (2 + 1)-dimensional CDT using a balls-in-boxes model. Class. Quant. Grav. 34(10), 105012 (2017). http://arxiv.org/abs/1612.09533, arXiv:1612.09533

47. C. Anderson, S.J. Carlip, J.H. Cooperman, P. Horava, R.K. Kommu, P.R. Zulkowski, Quantizing Horava-Lifshitz gravity via causal dynamical triangulations. Phys. Rev. D 85, 044027 (2012). http://arxiv.org/abs/1111.6634, arXiv:1111.6634

48. M. Borji, C. Kopper, Perturbative renormalization of the lattice regularized ϕ_4^4 with flow equations. J. Math. Phys. 61(11), 112304 (2020). http://arxiv.org/abs/2006.15943, arXiv:2006.15943

49. M. Testa, The Rome approach to chirality, in APCTP - ICTP Joint International Conference (AIJIC 97) on Recent Developments in Nonperturbative Quantum Field Theory, vol. 7 (1997), pp. 114-127. http://arxiv.org/abs/hep-lat/9707007, hep-lat/9707007

50. J. Magnen, V. Rivasseau, R. Seneor, Construction of Y M(4) with an infrared cutoff. Commun. Math. Phys. 155, 325-384 (1993)

51. U. Ellwanger, Flow equations and BRS invariance for Yang-Mills theories. Phys. Lett. B 335, 364-370 (1994). http://arxiv.org/abs/hep-th/9402077, hep-th/9402077

52. H. Gies, Introduction to the functional RG and applications to gauge theories. Lect. Notes Phys. 852, 287-348 (2012). http://arxiv.org/abs/hep-ph/0611146, hep-ph/0611146

53. N. Goldenfeld, Lectures on Phase Transitions and the Renormalization Group (CRC Press, Boca Raton, Florida, 1992)

54. D.A. Johnston, J.P. Kownacki, A. Krzywicki, Random geometries and real space renormalization group. Nucl. Phys. B Proc. Suppl. 42, 728-730 (1995). http://arxiv.org/abs/hep-lat/ 9407018, hep-lat/9407018

55. G. Thorleifsson, S. Catterall, A real space renormalization group for random surfaces. Nucl. Phys. B 461, 350-370 (1996). http://arxiv.org/abs/hep-lat/9510003, hep-lat/9510003

56. J. Ambjorn, P. Bialas, J. Jurkiewicz, RG flow in an exactly solvable model with fluctuating geometry. Phys. Lett. B 379, 93-98 (1996). http://arxiv.org/abs/hep-lat/9602021, hep-lat/9602021

57. R.L. Renken, A renormalization group for dynamical triangulations in arbitrary dimensions. Nucl. Phys. B 485, 503-516 (1997). http://arxiv.org/abs/hep-lat/9607074, hep-lat/9607074

58. J. Henson, Coarse graining dynamical triangulations: a new scheme. Class. Quant. Grav. 26, 175019 (2009). http://arxiv.org/abs/0907.5602, arXiv:0907.5602

59. F. Markopoulou, Coarse graining in spin foam models. Class. Quant. Grav. 20, 777-800 (2003). http://arxiv.org/abs/gr-qc/0203036, gr-qc/0203036

60. R. Oeckl, Renormalization of discrete models without background. Nucl. Phys. B 657, 107- 138 (2003). http://arxiv.org/abs/gr-qc/0212047, gr-qc/0212047

61. B. Bahr, B. Dittrich, F. Hellmann, W. Kaminski, Holonomy spin foam models: definition and coarse graining. Phys. Rev. D 87(4), 044048 (2013). http://arxiv.org/abs/1208.3388, arXiv:1208.3388

62. B. Dittrich, M. Martín-Benito, E. Schnetter, Coarse graining of spin net models: dynamics of intertwiners. New J. Phys. 15, 103004 (2013). http://arxiv.org/abs/1306.2987, arXiv:1306.2987

63. S. Steinhaus, Coarse graining spin foam quantum gravity - a review. Front. Phys. 8, 295 (2020). http://arxiv.org/abs/2007.01315, arXiv:2007.01315

64. R.L. Renken, S.M. Catterall, J.B. Kogut, Phase structure of dynamical triangulation models in three-dimensions. Nucl. Phys. B 523, 553-568 (1998). http://arxiv.org/abs/hep-lat/9712011, hep-lat/9712011

65. P. Bialas, Z. Burda, D. Johnston, Phase diagram of the mean field model of simplicial gravity. Nucl. Phys. B 542, 413-424 (1999). http://arxiv.org/abs/gr-qc/9808011, gr-qc/9808011

66. J. Ambjorn, J. Jurkiewicz, R. Loll, G. Vernizzi, Lorentzian 3-D gravity with wormholes via matrix models. JHEP 09, 022 (2001). http://arxiv.org/abs/hep-th/0106082, hep-th/0106082

67. M.R. Evans, T. Hanney, Nonequilibrium statistical mechanics of the zero-range process and related models. J. Phys. A: Math. and Gen. 38, R195 (2005)

68. P. Bialas, Z. Burda, B. Petersson, J. Tabaczek, Appearance of mother universe and singular vertices in random geometries. Nucl. Phys. B 495, 463-476 (1997). http://arxiv.org/abs/hep-lat/9608030, hep-lat/9608030

69. P. Bialas, Z. Burda, D. Johnston, Condensation in the backgammon model. Nucl. Phys. B 493, 505-516 (1997). http://arxiv.org/abs/cond-mat/9609264, cond-mat/9609264

70. L. Bogacz, Z. Burda, B. Waclaw, Quantum widening of CDT universe. Phys. Rev. D 86, 104015 (2012). http://arxiv.org/abs/1204.1356, arXiv:1204.1356

71. M.R. Evans, T. Hanney, S.N. Majumdar, Interaction-driven real-space condensation. Phys. Rev. Lett. 97, 010602 (2006)

72. B. Waclaw, J. Sopik, W. Janke, H. Meyer-Ortmanns, Tuning the shape of the condensate in spontaneous symmetry breaking. Phys. Rev. Lett. 103, 080602 (2009). http://arxiv.org/abs/ 0901.3664, arXiv:0901.3664

73. P. Di Francesco, E. Guitter, C. Kristjansen, Integrable 2-D Lorentzian gravity and random walks. Nucl. Phys. B 567, 515-553 (2000). http://arxiv.org/abs/hep-th/9907084, hep-th/9907084

74. P. Di Francesco, E. Guitter, C. Kristjansen, Generalized Lorentzian triangulations and the Calogero Hamiltonian. Nucl. Phys. B 608, 485-526, (2001). http://arxiv.org/abs/hep-th/ 0010259, hep-th/0010259

75. P. Di Francesco, E. Guitter, Critical and multicritical semirandom (1+d)-dimensional lattices and hard objects in d-dimensions. J. Phys. A 35, 897-928 (2002). http://arxiv.org/abs/cond-mat/0104383, cond-mat/0104383

76. A.K. Murtazaev, Z.G. Ibaev, On choosing the order parameter of modulated magnetic structures. J. Exp. Theor. Phys. 116, 266-271 (2013)

77. Y. Sato, CDT and Horava-Lifshitz QG in two dimensions, in Handbook of Quantum Gravity, eds. by C. Bambi, L. Modesto, I. Shapiro (Springer, Singapore, 2024), p. 12. http://arxiv.org/ abs/2212.03446, arXiv:2212.03446

78. F. Mattei, C. Rovelli, S. Speziale, M. Testa, From 3-geometry transition amplitudes to graviton states. Nucl. Phys. B 739, 234-253 (2006). http://arxiv.org/abs/gr-qc/0508007, gr-qc/0508007

79. J. Ambjorn, K.N. Anagnostopoulos, R. Loll, A new perspective on matter coupling in 2-D quantum gravity. Phys. Rev. D 60, 104035 (1999). http://arxiv.org/abs/hep-th/9904012, hep-th/9904012

80. J. Ambjørn, A. Görlich, J. Jurkiewicz, H. Zhang, The microscopic structure of 2D CDT coupled to matter. Phys. Lett. B 746, 359-364 (2015). http://arxiv.org/abs/1503.01636, arXiv:1503.01636

81. D. Benedetti, R. Loll, F. Zamponi, (2+1)-dimensional quantum gravity as the continuum limit of causal dynamical triangulations. Phys. Rev. D 76, 104022 (2007). http://arxiv.org/abs/0704.3214, arXiv:0704.3214

82. B. Durhuus, T. Jonsson, Exponential bounds on the number of causal triangulations. Com-mun. Math. Phys. 340(1), 105-124 (2015). http://arxiv.org/abs/1408.2101, arXiv:1408.2101

83. J. Ambjorn, J. Jurkiewicz, R. Loll, Nonperturbative 3-D Lorentzian quantum gravity. Phys. Rev. D 64, 044011 (2001). http://arxiv.org/abs/hep-th/0011276, hep-th/0011276

84. J.H. Cooperman, J. Miller, A first look at transition amplitudes in (2 + 1)-dimensional causal dynamical triangulations. Class. Quant. Grav. 31(3), 035012 (2014). http://arxiv.org/abs/1305.2932, arXiv:1305.2932

85. T.G. Budd, R. Loll, Exploring torus universes in causal dynamical triangulations. Phys. Rev. D 88(2), 024015 (2013). http://arxiv.org/abs/1305.4702, arXiv:1305.4702

86. J. Ambjorn, A. Gorlich, J. Jurkiewicz, R. Loll, The nonperturbative quantum de Sitter Universe. Phys. Rev. D 78, 063544 (2008). http://arxiv.org/abs/0807.4481, arXiv:0807.4481

87. A. Gorlich, Causal dynamical triangulations in four dimensions. Ph.D. thesis, Jagiellonian University, Astronomical Observatory, 2010. http://arxiv.org/abs/1111.6938, arXiv:1111.6938

88. J. Ambjorn, A. Gorlich, J. Jurkiewicz, R. Loll, Planckian birth of the quantum de Sitter universe. Phys. Rev. Lett. 100, 091304 (2008). http://arxiv.org/abs/0712.2485, arXiv:0712.2485

89. J. Ambjorn, A. Gorlich, J. Jurkiewicz, R. Loll, J. Gizbert-Studnicki, T. Trzesniewski, The semiclassical limit of causal dynamical triangulations. Nucl. Phys. B 849, 144-165 (2011). http://arxiv.org/abs/1102.3929, arXiv:1102.3929

90. J. Ambjorn, J. Gizbert-Studnicki, A. Gorlich, J. Jurkiewicz, The transfer matrix in four-dimensional CDT. JHEP 09, 017 (2012). http://arxiv.org/abs/1205.3791, arXiv:1205.3791

91. G.W. Gibbons, S.W. Hawking, M.J. Perry, Path integrals and the indefiniteness of the gravitational action. Nucl. Phys. B 138, 141-150 (1978)

92. J.B. Hartle, S.W. Hawking, Wave function of the universe. Phys. Rev. D 28, 2960-2975 (1983)

93. J. Ambjørn, J. Gizbert-Studnicki, A. Görlich, J. Jurkiewicz, The effective action in 4-dim CDT. The transfer matrix approach. JHEP 06, 034 (2014). http://arxiv.org/abs/1403.5940, arXiv:1403.5940

94. J. Ambjørn, J. Gizbert-Studnicki, A. Görlich, J. Jurkiewicz, N. Klitgaard, R. Loll, Characteristics of the new phase in CDT. Eur. Phys. J. C 77(3), 152 (2017). http://arxiv.org/abs/1610.05245, arXiv:1610.05245

95. J. Ambjorn, J. Jurkiewicz, R. Loll, 3-d Lorentzian, dynamically triangulated quantum gravity. Nucl. Phys. B Proc. Suppl. 106, 980-982 (2002). http://arxiv.org/abs/hep-lat/0201013, hep-lat/0201013

96. J. Ambjorn, A. Görlich, J. Jurkiewicz, A. Kreienbuehl, R. Loll, Renormalization group flow in CDT. Class. Quant. Grav. 31, 165003 (2014). http://arxiv.org/abs/1405.4585, arXiv:1405.4585

97. J. Ambjorn, J. Gizbert-Studnicki, A. Görlich, J. Jurkiewicz, R. Loll, Renormalization in quantum theories of geometry. Front. Phys. 8, 247 (2020). http://arxiv.org/abs/2002.01693, arXiv:2002.01693

98. S. Jordan, R. Loll, Causal dynamical triangulations without preferred foliation. Phys. Lett. B 724, 155-159 (2013). http://arxiv.org/abs/1305.4582, arXiv:1305.4582

99. S. Jordan, R. Loll, De Sitter universe from causal dynamical triangulations without preferred foliation. Phys. Rev. D 88, 044055 (2013). http://arxiv.org/abs/1307.5469, arXiv:1307.5469

100. J. Ambjorn, J. Jurkiewicz, R. Loll, Spectral dimension of the universe. Phys. Rev. Lett. 95, 171301 (2005). http://arxiv.org/abs/hep-th/0505113, hep-th/0505113

101. O. Lauscher, M. Reuter, Fractal spacetime structure in asymptotically safe gravity. JHEP 10, 050 (2005). http://arxiv.org/abs/hep-th/0508202, hep-th/0508202

102. D. Benedetti, F. Guarnieri, One-loop renormalization in a toy model of Hořava-Lifshitz gravity. JHEP 03, 078 (2014). http://arxiv.org/abs/1311.6253, arXiv:1311.6253

103. A.O. Barvinsky, D. Blas, M. Herrero-Valea, S.M. Sibiryakov, C.F. Steinwachs, Hořava gravity is asymptotically free in $2+1$ dimensions. Phys. Rev. Lett. 119(21), 211301 (2017). http:// arxiv.org/abs/1706.06809, arXiv:1706.06809

104. A.O. Barvinsky, M. Herrero-Valea, S.M. Sibiryakov, Towards the renormalization group flow of Horava gravity in $(3+1)$ dimensions. Phys. Rev. D 100(2), 026012 (2019). http://arxiv.org/abs/1905.03798, arXiv:1905.03798

105. A.O. Barvinsky, A.V. Kurov, S.M. Sibiryakov, Beta functions of (3+1)-dimensional projectable Hořava gravity. Phys. Rev. D 105(4), 044009 (2022). http://arxiv.org/abs/2110.14688, arXiv:2110.14688

106. D. Benedetti, On the number of relevant operators in asymptotically safe gravity. EPL 102(2), 20007 (2013). http://arxiv.org/abs/1301.4422, arXiv:1301.4422

107. A. Mitchell, T.R. Morris, D. Stulga, Provable properties of asymptotic safety in f(R) approximation. JHEP 01, 041 (2022). http://arxiv.org/abs/2111.05067, arXiv:2111.05067

108. A. Codello, R. Percacci, C. Rahmede, Investigating the ultraviolet properties of gravity with a Wilsonian renormalization group equation. Ann. Phys. 324, 414-469 (2009). http://arxiv.org/ abs/0805.2909, arXiv:0805.2909

109. D. Benedetti, P.F. Machado, F. Saueressig, Asymptotic safety in higher-derivative gravity. Mod. Phys. Lett. A 24, 2233-2241 (2009). http://arxiv.org/abs/0901.2984, arXiv:0901.2984

110. K. Falls, D.F. Litim, K. Nikolakopoulos, C. Rahmede, Further evidence for asymptotic safety of quantum gravity. Phys. Rev. D 93(10), 104022 (2016). http://arxiv.org/abs/1410.4815, arXiv:1410.4815